Fraunhofer
ITWM

Y. Efendiev, O. Iliev, V. Taralova

Upscaling of an isothermal Li-ion battery model via the Homogenization Theory

Berichte des Fraunhofer ITWM, Nr. 230 (2013)

ISSN 1434-9973

Bericht 230 (2013)

Die Veröffentlichungen in der Berichtsreihe des Fraunhofer ITWM können bezogen werden über:

Fraunhofer-Institut für Techno- und
Wirtschaftsmathematik ITWM
Fraunhofer-Platz 1

67663 Kaiserslautern
Germany

Telefon: +49(0)631/31600-4674
Telefax: +49(0)631/31600-5674
E-Mail: presse@itwm.fraunhofer.de
Internet: www.itwm.fraunhofer.de

Vorwort

Das Tätigkeitsfeld des Fraunhofer-Instituts für Techno- und Wirtschaftsmathematik ITWM umfasst anwendungsnahe Grundlagenforschung, angewandte Forschung sowie Beratung und kundenspezifische Lösungen auf allen Gebieten, die für Techno- und Wirtschaftsmathematik bedeutsam sind.

In der Reihe »Berichte des Fraunhofer ITWM« soll die Arbeit des Instituts kontinuierlich einer interessierten Öffentlichkeit in Industrie, Wirtschaft und Wissenschaft vorgestellt werden. Durch die enge Verzahnung mit dem Fachbereich Mathematik der Universität Kaiserslautern sowie durch zahlreiche Kooperationen mit internationalen Institutionen und Hochschulen in den Bereichen Ausbildung und Forschung ist ein großes Potenzial für Forschungsberichte vorhanden. In die Berichtreihe werden sowohl hervorragende Diplom- und Projektarbeiten und Dissertationen als auch Forschungsberichte der Institutsmitarbeiter und Institutsgäste zu aktuellen Fragen der Techno- und Wirtschaftsmathematik aufgenommen.

Darüber hinaus bietet die Reihe ein Forum für die Berichterstattung über die zahlreichen Kooperationsprojekte des Instituts mit Partnern aus Industrie und Wirtschaft.

Berichterstattung heißt hier Dokumentation des Transfers aktueller Ergebnisse aus mathematischer Forschungs- und Entwicklungsarbeit in industrielle Anwendungen und Softwareprodukte – und umgekehrt, denn Probleme der Praxis generieren neue interessante mathematische Fragestellungen.

Prof. Dr. Dieter Prätzel-Wolters
Institutsleiter

Kaiserslautern, im Juni 2001

Upscaling of an Isothermal Li-ion Battery Model via the Homogenization Theory

Y. Efendiev[*], O. Iliev[†], V. Taralova[†‡]

Abstract

Li-ion batteries are one of the most popular types of rechargeable batteries for portable electronics. They are multiscale systems with processes occuring at different scales. The aim of the mathematical modelling is better understanding of the electrochemical processes in Li-ion batteries as well as prolonging the batteries' lifetime and improving their performance. A broad range of scientific and engineering problems involve multiple scales. Direct numerical simulations lead to a huge number of degrees of freedom difficult to handle even with supercomputers. From an application perspective it is often sufficient to predict the macroscopic properties of the multiscale systems. The goal of the upscaling techniques for Lithium-ion battery models is to develop a method that captures the small-scale effects on the large scales, but does not require resolving all the small-scale features.

Keywords: Li-ion Batteries, Homogenization

[*]Texas A&M University, Mailstop 3368, College Station, TX 77843-3368
[†]Fraunhofer ITWM, Fraunhofer-Platz-1, 67663 Kaiserslautern, Germany
[‡]Corresponding author: vasilena.taralova@itwm.fraunhofer.de

Contents

List of Tables

List of Figures

List of Symbols

c^e - concentration of lithium ions in the electrolyte

c^s - concentration of lithium ions in the active particles

ϕ^e - potential in the electrolyte

ϕ^s - potential in the solid

T - temperature

D^e - interdiffusion coefficient in the electrolyte; strictly posivite

D^s - interdiffusion coefficient in the active particles; strictly posivite

t_+ - transference number of Li ions

κ^s - electric condictivity; strictly positive

$\mathbf{N}$ - ionic flux

$\mathbf{j}$ - electrical current

F - Faraday constant

R - Universal gas constant

η_s - overpotential

U_0 - half cell open circuit potential

$c_{s,max}$ - maximum concentration of ions in the active particle

k - reaction rate

soc - state of charge, i.e. $\frac{c_s}{c_{s,max}}$

1 Introduction

In this work we derive rigorously upscaled Li-ion battery model via the homogenization theory. We start from the microscopic model developed in [8]. Here we describe briefly the main components and processes in the battery. A more detailed description of the battery and the electrochemical processes involved is given in [12].

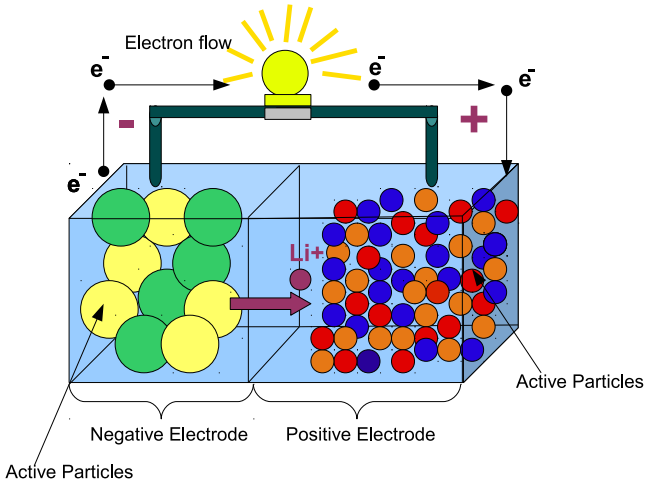

Figure 1: Battery Cell

A typical Li-ion battery consists of many electrically connected electrochemical cells. Each cell has two electrodes- anode and cathode, separator and electrolyte. The anode and the cathode have porous structure consisting of an active particle skeleton filled with liquid electrolyte (see Figure 1). During charge and discharge of the battery the lithium ions move from one electrode to the other. The model [8] is based on nonlinear diffusion equations for the transport of Lithium ions and charges in the electrolyte and in the active particles as well as their coupling due to electrochemical reactions on the interface boundary between the particles and the electrolyte. Usually in Li-ion batteries the number of particles in each electrode is very large. Resolving such a big number of particles in the microscale simulations would be very computationally expensive. The aim of the homogenization of the model is to derive equations on the macroscale which correctly capture the macroscopic behaviour of the battery cell without fully resolving all the microscopic features. This reduces significantly the computational cost. We consider periodically arranged active particles and we derive coupled micro-macroscopic model.
Another paper where homogenization of microscale Li-ion battery model is considered is [6]. However our approach differs in several aspects. First of all, they start from a different microscopic model [7]. Nevertheless, the two models are similar enough so that the approaches can be compared. In [6] it is stated that the current density is of the order of the small parameter but there is no justification. In the current work we derive this estimate mathematically. Another point is that the final homogenized model in [7] does not depend explicitly on the small parameter although it is present in the derivation. Furthermore it is not clear what boundary conditions are used in their model. In our case the boundary conditions are specified beforehand in the microscale setting of the model and they are homogenized along with the other equations. Finally we perform detailed numerical simulations in order to verify the proposed homogenization approach.
In the paper [9] the authors also apply the homogenization theory to derive macroscopic battery model. Their approach is very similar to ours. The differences are that they start

from a different microscopic model and do not provide a detailed numerical investigation in order to test their homogenized model against full microscopic simulations. In our work we run a series of numerical experiments varying the particles' size and we show a very good agreement between the solution of the homogenized model and that of the full microscopic model.
One of the most used models for Li-ion batteries on the scale of our homogenized problem is the model proposed by Newman et. al [5]. This model, however, is derived directly on the macroscale and is restricted only to spherical active particles, whereas our method allows for randomly shaped particles.
Our homogenization approach is also similar in some aspects to the one used by Arbogast et. al in[1, 2].

2 The Homogenization Method

The homogenization method [3], [10], [4] deals with partial differential equations with periodically oscillating coefficients. These type of equations model various physical problems arising in media with periodic structure. The aim of the method is to derive macroscale "homogenized" equations which adequately describe the macroscopic behaviour of the solution and in the same time significantly decrease the degrees of freedom of the considered problem. In these problems the size l of the periodic micro structure is small compared to the size L of a sample of the medium. We start from the microscopic description of the problem and we seek a macroscopic, or averaged, description.
Let us consider the following equation

$$\mathcal{L}u = f, \quad x \in \Omega \tag{2.1}$$

where $\mathcal{L}$ is some partial differential operator and u and f are functions of x. We want to investigate the behaviour of the partial differential equation as $\varepsilon = \dfrac{l}{L} \to 0$, i.e. as the size of the periodicities l goes to zero which is equivalent to their number becoming infinitely large. Therefore an asymptotic analysis is required as $\varepsilon \to 0$. We obtain a family of partial differential operators $\mathcal{L}_\varepsilon$ (with coefficients oscillating with period εL), and a family of solutions u_ε, which satisfy

$$\mathcal{L}_\varepsilon u_\varepsilon = f, \quad x \in \Omega \tag{2.2}$$

complemented by appropriate boundary conditions. Assuming that the sequence u_ε converges, in some sense, to a limit u^h, we look for a so-called homogenized operator $\mathcal{L}^h$ such that u^h is a solution of

$$\mathcal{L}^h u^h = f, \quad x \in \Omega \tag{2.3}$$

We use the well-klnown two-scale asymptotic expansion method in order to find the precise form of the homogenized operator $\mathcal{L}^h$. We postulate the following ansatz for u_ε

$$u_\varepsilon(x) = u_0\left(x, \frac{x}{\varepsilon}\right) + \varepsilon u_1\left(x, \frac{x}{\varepsilon}\right) + \varepsilon^2 u_2\left(x, \frac{x}{\varepsilon}\right) + \dots \tag{2.4}$$

where we denote

$$y = \frac{x}{\varepsilon} \tag{2.5}$$

and each term $u_i(x,y)$ is periodic in y. Inserting the asymptotic expansion (2.4) in (2.2) and identifying equal powers of ε leads to a cascade of equations for each term u_i. Averaging with respect to y the equation for u_0 gives the homogenized equation

$$\mathcal{L}^h u_0 = f \tag{2.6}$$

The precise form of the operator $\mathcal{L}^h$ is computed with the help of a so-called auxiliary cell problem in the unit period. It is proved (see [3], [10], [4]) for linear elliptic problems that $u_\varepsilon \rightarrow u_0$ in $H^1(\Omega)$ weakly.

2.1 One Example: Two-Dimensional Linear Elliptic Problem

We consider the following linear elliptic equation with oscillating coefficient $a_\varepsilon(x)$ ($a_\varepsilon(x) > 0$ for $\forall x \in \Omega$, ellipticity condition), with period of the oscillations εL:

$$-\nabla \cdot (a_\varepsilon(x) \nabla u_\varepsilon) = f(x), \quad x \in \Omega \subset \mathbb{R}^2 \tag{2.7a}$$

$$u_\varepsilon(x) = 0, \quad x \in \partial\Omega \tag{2.7b}$$

We assume that we have a regular periodic microstructure of the domain Ω with $\varepsilon L = l << L$ being the size of the periodicities. The medium varies rapidly on the small scale l and may also vary slowly on the large scale L. Here x is the so called global variable and $y = \dfrac{x}{\varepsilon}$ is its respective local variable. Let us denote with εY_i the microscopic periodicity cells. Then after the change of variables $y = \dfrac{x}{\varepsilon}$, each microscopic periodicity cell εY_i with characteristic length l transforms into the upscaled periodicity cell Y_i with characteristic length L. Then we translate each cell Y_i into a reference periodicty cell Y via the translation τ_i:

$$\tau_i : y' = y + \xi_i \tag{2.8}$$

where ξ_i is a given constant vector for each cell Y_i. It is clear that the characteristic length of the reference periodicity cell Y is also L. From now on, unless specified otherwise, we will say that a function $g(x,y)$ is Y-periodic in the y variable if $g(x, y+L) = g(x,y)$, i.e. if $g(x,y)$ is periodic in y with a period equal to L (the characteristic length of the reference periodicity cell Y). Therefore we have that $a_\varepsilon(x) = a\left(\dfrac{x}{\varepsilon}\right) = a(y)$ is Y-periodic function in y. We look for the solution of (2.7) in the form of the following two-scale asymptotic expansion:

$$u_\varepsilon(x) = u_0\left(x, \frac{x}{\varepsilon}\right) + \varepsilon u_1\left(x, \frac{x}{\varepsilon}\right) + \varepsilon^2 u_2\left(x, \frac{x}{\varepsilon}\right) \tag{2.9}$$

wher all the terms u_0, u_1 and u_2 are Y-periodic in $y = \dfrac{x}{\varepsilon}$. We want to investigate the behaviour of the PDE (2.7a) when $\varepsilon \rightarrow 0$. Now we plug the asymptotic expansion (2.9) in (2.7a) and taking into account that $\nabla = \nabla_x + \dfrac{1}{\varepsilon}\nabla_y$, we obtain

$$\begin{aligned} &-\left(\nabla_x + \frac{1}{\varepsilon}\nabla_y\right) \cdot \left(a(y)\left(\nabla_x + \frac{1}{\varepsilon}\nabla_y\right)\left(u_0(x,y) + \varepsilon u_1(x,y) + \varepsilon^2 u_2(x,y)\right)\right) = f(x) \iff \\ &-\left(\nabla_x + \frac{1}{\varepsilon}\nabla_y\right) \cdot \left(a(y)\left(\frac{1}{\varepsilon}\nabla_y u_0 + \nabla_x u_0 + \nabla_y u_1 + \varepsilon \nabla_x u_1 + \varepsilon \nabla_y u_2 + \varepsilon^2 \nabla_x u_2\right)\right) = f(x) \end{aligned} \tag{2.10}$$

which is equivalent to

$$
\begin{aligned}
&-\frac{1}{\varepsilon^2}\nabla_y\cdot(a(y)\nabla_y u_0)-\frac{1}{\varepsilon}\nabla_y\cdot(a(y)\nabla_x u_0+a(y)\nabla_y u_1)-\\
&-\nabla_y\cdot(a(y)\nabla_x u_1+a(y)\nabla_y u_2)-\varepsilon\nabla_y\cdot(a(y)\nabla_x u_2)-\frac{1}{\varepsilon}\nabla_x\cdot(a(y)\nabla_y u_0)-\\
&-\nabla_x\cdot(a(y)\nabla_x u_0+a(y)\nabla_y u_1)-\varepsilon\nabla_x\cdot(a(y)\nabla_x u_1+a(y)\nabla_y u_2)+O(\varepsilon^2)=f(x) \qquad (2.11)
\end{aligned}
$$

Finally we obtain

$$
\begin{aligned}
&-\frac{1}{\varepsilon^2}\nabla_y\cdot(a(y)\nabla_y u_0)-\\
&-\frac{1}{\varepsilon}\left[\nabla_y\cdot(a(y)\nabla_x u_0+a(y)\nabla_y u_1)+\nabla_x\cdot(a(y)\nabla_y u_0)\right]-\\
&-\varepsilon^0\left[\nabla_y\cdot(a(y)\nabla_x u_1+a(y)\nabla_y u_2)+\nabla_x\cdot(a(y)\nabla_x u_0+a(y)\nabla_y u_1)\right]+\\
&+O(\varepsilon)=f(x) \qquad (2.12)
\end{aligned}
$$

Since the latter equality must be true for each $x\in\Omega$, we equal like powers of ε. This way we obtain the following equations for $u_0(x,y)$ and the first and second order correctors $u_1(x,y)$ and $u_2(x,y)$ respectively:

$$
\begin{aligned}
&\varepsilon^{-2}: -\nabla_y\cdot(a(y)\nabla_y u_0)=0 && (2.13a)\\
&\varepsilon^{-1}: -\left[\nabla_y\cdot(a(y)\nabla_x u_0+a(y)\nabla_y u_1)+\nabla_x\cdot(a(y)\nabla_y u_0)\right]=0 && (2.13b)\\
&\varepsilon^{0}: -\left[\nabla_y\cdot(a(y)\nabla_x u_1+a(y)\nabla_y u_2)+\nabla_x\cdot(a(y)\nabla_x u_0+a(y)\nabla_y u_1)\right]=f(x) && (2.13c)
\end{aligned}
$$

2.1.1 Order ε^{-2}

We obtain the following equation for $u_0(x,y)$:

$$
-\nabla_y\cdot(a(y)\nabla_y u_0)=0,\quad (x,y)\in[\Omega\times Y] \qquad (2.14)
$$

and we will show that u_0 is a function only of x.
We want to solve equation (2.14) with respect to the y variable, assuming that x is a given constant. Therefore we write the weak formulation of equation (2.14) and after applying the divergence theorem we obtain

$$
\begin{aligned}
&-\int_Y \nabla_y\cdot(a(y)\nabla_y u_0)\,v(y)\,dy=0,\quad \forall v(y)\in H^1_{per}(Y)\Longleftrightarrow\\
&\int_Y \nabla_y\cdot(v(y)a(y)\nabla_y u_0)\,dy-\int_Y a(y)\nabla_y u_0\cdot\nabla_y v\,dy=0,\quad \forall v(y)\in H^1_{per}(Y)\Longleftrightarrow\\
&\underbrace{\int_{\partial Y} v(y)a(y)\nabla_y u_0\cdot\mathbf{n}\,ds}_{=0}-\int_Y a(y)\nabla_y u_0\cdot\nabla_y v\,dy=0,\quad \forall v(y)\in H^1_{per}(Y)\Longleftrightarrow\\
&-\int_Y a(y)\nabla_y u_0\cdot\nabla_y v\,dy=0,\quad \forall v(y)\in H^1_{per}(Y) \qquad (2.15)
\end{aligned}
$$

In the latter equality we have that $\int_{\partial Y} v(y)a(y)\nabla_y u_0 \cdot \mathbf{n}\, ds = 0$ due to symmetry (we assume that the reference periodicity cell is symmetric, see Figure 2) and periodicity (we have periodic microstructure, i.e. all the functions $v(y)$, $a(y)$ and $u_0(x,y)$ are Y-periodic with respect to the y variable which means that these functions take equal values on the opposite sides of the periodicity cell Y and the unit normal vectors $\mathbf{n}$ are collinear but pointing in opposite directions). Therefore for the weak formulation we obtain

$$\int_Y a(y)\nabla_y u_0 \cdot \nabla_y v\, dy = 0, \quad \forall v(y) \in H^1_{per}(Y) \tag{2.16}$$

Since (2.16) is true for each Y-periodic test function in $H^1(Y)$, we can take as test function $v(y) = u_0(x,y)$ (assuming x is constant) and thus we obtain

$$\int_Y a(y)\nabla_y u_0 \cdot \nabla_y u_0\, dy = 0 \Longleftrightarrow \tag{2.17}$$

$$0 \leq \int_Y a(y) \sum_i \left(\frac{\partial u_0}{\partial y_i}\right)^2 dy = 0 \quad (a(y) > 0, \forall y \in Y) \Longleftrightarrow$$

$$\left(\frac{\partial u_0}{\partial y_i}\right)^2 = 0, \quad \forall i \Longleftrightarrow$$

$$\frac{\partial u_0}{\partial y_i} = 0, \quad \forall i \Longleftrightarrow$$

$$u_0 = u_0(x) \tag{2.18}$$

which means that u_0 does not depend on the y variable.

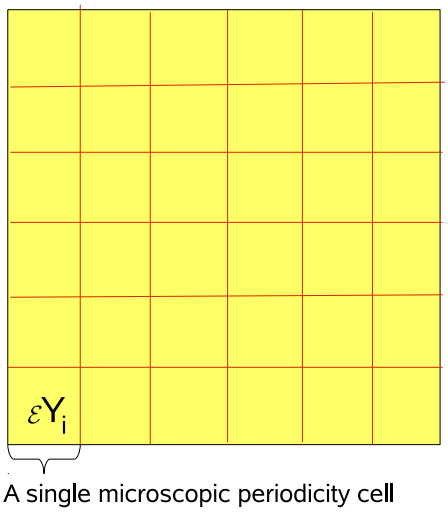

Figure 2: Periodic media

2.1.2 Order ε^{-1}

We have the following equation for the first order corrector $u_1(x,y)$:

$$-\left[\nabla_y \cdot (a(y)\nabla_x u_0 + a(y)\nabla_y u_1) + \nabla_x \cdot (a(y)\nabla_y u_0)\right] = 0 \tag{2.19}$$

where $\nabla_y u_0(x) = 0$ and therefore the latter equation becomes

$$\nabla_y \cdot (a(y)\nabla_x u_0 + a(y)\nabla_y u_1) = 0 \tag{2.20}$$

which is equivalent to

$$\nabla_y \cdot (a(y)\nabla_y u_1) = -\nabla_y \cdot (a(y)\nabla_x u_0) \tag{2.21}$$

Now we seek the solution u_1 in the following form

$$u_1(x, y) = \nabla_x u_0 \cdot \varphi \tag{2.22}$$

where $\varphi(y) = (\varphi_1(y), \varphi_2(y))$ is a vector function. Thus

$$u_1(x, y) = \sum_{i=1}^{2} \frac{\partial u_0}{\partial x_i}(x)\varphi_i(y) \tag{2.23}$$

And we obtain that $u_1 = \nabla_x u_0 \cdot \varphi$ is a solution of (2.21) if and only if the Y-periodic functions $\varphi_i(y)$ satisfy the following auxiliary cell problems

$$-\nabla_y \cdot (a(y)\nabla_y \varphi_i) = \frac{\partial a}{\partial y_i}, \quad i = 1, 2, y \in Y \tag{2.24}$$

2.1.3 Order ε^0

From (2.13c) we have

$$-\nabla_y \cdot (a(y)\nabla_x u_1 + a(y)\nabla_y u_2) - \nabla_x \cdot (a(y)\nabla_x u_0 + a(y)\nabla_y u_1) = f(x) \tag{2.25}$$

Now we integrate both sides of the equality over the periodicity cell Y and we divide by the measure of Y

$$\begin{aligned}
&-\frac{1}{|Y|}\int_Y \nabla_y \cdot (a(y)\nabla_x u_1 + a(y)\nabla_y u_2)\, dy - \\
&-\frac{1}{|Y|}\int_Y \nabla_x \cdot (a(y)\nabla_x u_0 + a(y)\nabla_y u_1)\, dy = f(x) \Longleftrightarrow \\
&-\frac{1}{|Y|}\underbrace{\int_{\partial Y} (a(y)\nabla_x u_1 + a(y)\nabla_y u_2) \cdot \mathbf{n}\, ds}_{=0} - \\
&-\frac{1}{|Y|}\int_Y \nabla_x \cdot (a(y)\nabla_x u_0 + a(y)\nabla_y u_1)\, dy = f(x) \Longleftrightarrow \\
&-\frac{1}{|Y|}\int_Y \nabla_x \cdot (a(y)\nabla_x u_0 + a(y)\nabla_y u_1)\, dy = f(x)
\end{aligned} \tag{2.26}$$

We substitute $u_1 = \sum_{i=1}^{2} \frac{\partial u_0}{\partial x_i}(x)\varphi_i(y)$ and $\nabla_x u_0 = \sum_{i=1}^{2} \frac{\partial u_0}{\partial x_i}\vec{\mathbf{e}}_i$, and we obtain

$$
\begin{aligned}
&-\frac{1}{|Y|}\int_Y \nabla_x \cdot \left(a(y)\nabla_x u_0 + a(y)\sum_{i=1}^{2}\frac{\partial u_0}{\partial x_i}(x)\nabla_y\varphi_i \right) dy = f(x) \iff \\
&-\frac{1}{|Y|}\nabla_x \cdot \left(\int_Y \left(a(y)\nabla_x u_0 + a(y)\sum_{i=1}^{2}\frac{\partial u_0}{\partial x_i}(x)\nabla_y\varphi_i \right) dy \right) = f(x) \iff \\
&-\frac{1}{|Y|}\nabla_x \cdot \left(\left(\int_Y a(y)\,dy \right)\nabla_x u_0 + \sum_{i=1}^{2}\frac{\partial u_0}{\partial x_i}(x)\left(\int_Y a(y)\nabla_y\varphi_i\,dy \right) \right) = f(x) \iff \\
&-\frac{1}{|Y|}\nabla_x \cdot \left(\left(\int_Y a(y)\,dy \right)\sum_{i=1}^{2}\frac{\partial u_0}{\partial x_i}\vec{\mathbf{e}}_i + \sum_{i=1}^{2}\frac{\partial u_0}{\partial x_i}(x)\left(\int_Y a(y)\nabla_y\varphi_i\,dy \right) \right) = f(x) \iff \\
&-\frac{1}{|Y|}\nabla_x \cdot \left(\sum_{i=1}^{2}\frac{\partial u_0}{\partial x_i}\left(\int_Y a(y)\,dy \right)\vec{\mathbf{e}}_i + \sum_{i=1}^{2}\frac{\partial u_0}{\partial x_i}\left(\int_Y a(y)\nabla_y\varphi_i\,dy \right) \right) = f(x) \iff \\
&-\frac{1}{|Y|}\nabla_x \cdot \left(\sum_{i=1}^{2}\frac{\partial u_0}{\partial x_i}\left(\int_Y a(y)\vec{\mathbf{e}}_i\,dy + \int_Y a(y)\nabla_y\varphi_i\,dy \right) \right) = f(x) \iff \\
&-\nabla_x \cdot \left(\sum_{i=1}^{2}\frac{\partial u_0}{\partial x_i}\left(\frac{1}{|Y|}\int_Y a(y)\left(\vec{\mathbf{e}}_i + \nabla_y\varphi_i\right)\,dy \right) \right) = f(x) \qquad (2.27)
\end{aligned}
$$

where

$$\vec{\mathbf{e}_1} + \nabla_y\varphi_1 = \left(1 + \frac{\partial\varphi_1}{\partial y_1}, \frac{\partial\varphi_1}{\partial y_2}\right) \qquad (2.28)$$

$$\vec{\mathbf{e}_2} + \nabla_y\varphi_2 = \left(\frac{\partial\varphi_2}{\partial y_1}, 1 + \frac{\partial\varphi_2}{\partial y_2}\right) \qquad (2.29)$$

$$
\begin{aligned}
&\sum_{i=1}^{2}\frac{\partial u_0}{\partial x_i}\left(\frac{1}{|Y|}\int_Y a(y)\left(\vec{\mathbf{e}}_i + \nabla_y\varphi_i\right)\,dy \right) = \\
&= \begin{pmatrix} \frac{1}{|Y|}\int_Y a(y)\left(1 + \frac{\partial\varphi_1}{\partial y_1}\right)dy & \frac{1}{|Y|}\int_Y a(y)\frac{\partial\varphi_2}{\partial y_1}\,dy \\ \frac{1}{|Y|}\int_Y a(y)\frac{\partial\varphi_1}{\partial y_2}\,dy & \frac{1}{|Y|}\int_Y a(y)\left(1 + \frac{\partial\varphi_2}{\partial y_2}\right)dy \end{pmatrix} \begin{pmatrix} \frac{\partial u_0}{\partial x_1} \\ \frac{\partial u_0}{\partial x_2} \end{pmatrix} \qquad (2.30)
\end{aligned}
$$

Thus we obtain the homogenized problem

$$-\nabla_x \cdot (a_H \nabla_x u_0) = f(x), \quad x \in \Omega, \qquad (2.31a)$$

$$u_0(x) = 0, \quad x \in \partial\Omega \qquad (2.31b)$$

where the homogenized coefficient a_H (constant) is the following tensor

$$(a_H)_{i,j=1}^{2} = \frac{1}{|Y|}\int_Y a(y)\left(\delta_{ij} + \frac{\partial\varphi_j}{\partial y_i}(y)\right)dy \qquad (2.32)$$

2.1.4 Numerical Experiment

- $\Omega = [0,1] \times [0,1]$
- $Y = [0,1] \times [0,1]$
- We take $a(x) = \cos(32\pi x_1)\cos(32\pi x_2) + 1.1 > 0$ and $f(x) = 16$
- $\varepsilon = \frac{1}{16}$

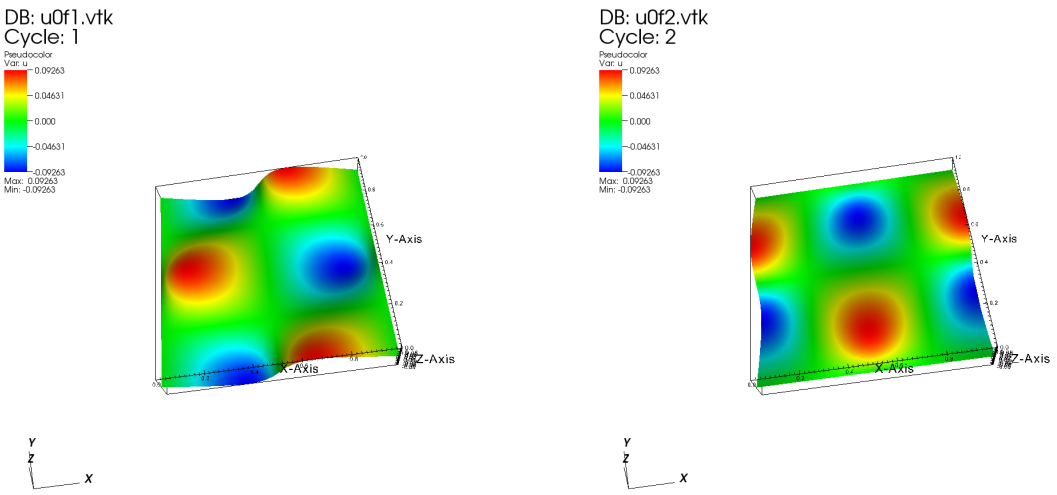

Figure 3: Solutions of the Cell Problems

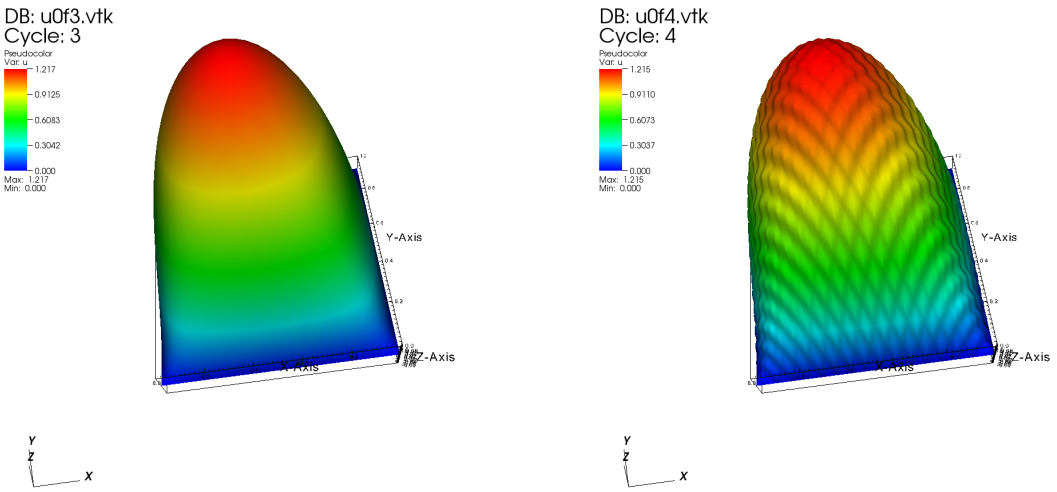

(a) Homogenized Solution (b) Exact Solution

Figure 4: Homogenized Solution and Exact Solution

3 Some Test Problems

3.1 Nonlinear Elliptic Problem: Straightforward Approach

We consider the following nonlinear equation with periodic coefficient:

$$-\nabla \cdot (a_\varepsilon(x, u_\varepsilon)\nabla u_\varepsilon) = f(x), \quad x \in \Omega = [0,1] \times [0,1] \tag{3.1a}$$

$$u_\varepsilon(x) = 0, \quad x \in \partial\Omega \tag{3.1b}$$

where

- $a_\varepsilon(x, u_\varepsilon) > 0, \forall x \in \Omega$ (ellipticity condition), and we assume that $a_\varepsilon(x, u_\varepsilon)$ is a smooth function $\forall x \in \Omega$
- $\varepsilon = l/L$
- L - characteristic length of the macrodomain Ω
- l - characteristic length of the periodic microscale structures
- $a_\varepsilon(x, u_\varepsilon(x)) = a\left(\frac{x}{\varepsilon}, u_\varepsilon\right)$ is an oscillating coefficient with period εL
- We assume the following asymptotic expansion for the function u_ε:
  $u_\varepsilon(x) = u_0(x) + \varepsilon u_1\left(x, \frac{x}{\varepsilon}\right) + \varepsilon^2 u_2\left(x, \frac{x}{\varepsilon}\right), \quad y = \frac{x}{\varepsilon}$
- $a(y, u_\varepsilon) = a(y, u_0) + O(\varepsilon)$ for smooth functions $a(y, u_\varepsilon)$ (Taylor series)
- We also have that the functions $a(y, u_\varepsilon)$, $u_1(x, y)$ and $u_2(x, y)$ are Y-periodic in the y variable

3.1.1 Homogenization: Order ε^{-1}

After we plug the asymptotic expansion of u_ε in (3.1a) and we identify equal powers of ε, for order ε^{-1} we obtain the following equation

$$\nabla_y \cdot (a(y, u_0)\nabla_y u_1) = -\nabla_y \cdot (a(y, u_0)\nabla_x u_0) \tag{3.2}$$

From (3.2) where we obtain that

$$u_1(x, y) = \sum_{l=1}^{2} \chi_l(y) \frac{\partial u_0}{\partial x_l}(x) \tag{3.3}$$

where the Y-periodic functions $\chi_l(y)$ are the solution of the following auxuliary cell problems:

$$\nabla \cdot (a(y, u_0(x))\nabla_y \chi_l) = -\frac{\partial a}{\partial y_l}(y, u_0(x)), \quad y \in Y, \quad l = 1, 2 \tag{3.4}$$

Therefore we have to solve the cell problems for each integration point $x \in \Omega$.
We apply periodic boundary conditions on ∂Y (see Figure 5)

$$\nabla_y \chi_l \cdot \mathbf{n}|_{AD} = \nabla_y \chi_l \cdot \mathbf{n}|_{BC}$$
$$\nabla_y \chi_l \cdot \mathbf{n}|_{AB} = \nabla_y \chi_l \cdot \mathbf{n}|_{CD}$$

and in order to fix the solution we impose

$$\int_Y \chi_l(y)\, dy = 0$$

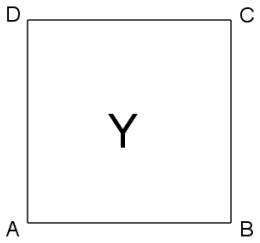

Figure 5: Solution Domain of the Auxiliary Cell Problems

3.1.2 Homogenization: Order ε^0

From the order ε^0 equation we obtain the homogenized problem

$$-\nabla \cdot (a^*(u_0)\nabla u_0) = f(x), \quad x \in \Omega \tag{3.5a}$$

$$u_0(x) = 0, \quad x \in \partial\Omega \tag{3.5b}$$

where $a^*(u_0)$ is the following tensor:

$$a^* = (a^*)_{i,j=1}^2 = \frac{1}{|Y|}\int_Y a(y, u_0)\left(\delta_{ij} + \frac{\partial \chi_j}{\partial y_i}(y)\right) dy \tag{3.6}$$

3.1.3 Numerical Experiment

We solve the following test problem:

- $-\nabla \cdot (a_\varepsilon(x, u_\varepsilon)\nabla u_\varepsilon) = f(x), \quad x \in \Omega = [0,1] \times [0,1]$
- $u_\varepsilon(x) = 0, \quad x \in \partial\Omega$
- $a_\varepsilon(x, u_\varepsilon) = k_\varepsilon(x)u_\varepsilon^2 + 1 > 0$- ellipticity condition, where
- $k_\varepsilon(x) = \cos(32\pi x_1)\cos(32\pi x_2) + 1.1$
- $f(x) = 5$
- We have $L = 32\pi$ and $l = 2\pi$, and therefore $\varepsilon = \frac{1}{16} = 0.0625$, and we have 256 periodicity cells
- Since the auxiliary cell problem depends on the macrosolution $u_0(x)$, we have to solve the cell problem for each integration point x in the macrodomain and at each Newton iteration

Note: From now on in all the numerical experiments we will refer to the numerical solution of the full microscale model as to the "exact solution".

	Nodes	Periodicity Cells	Time	Max	Min
Homogenized Problem	289	256	681s	1.163	1
Cell Problem	2113				
Exact Solution	65536	256	74s	1.173	1

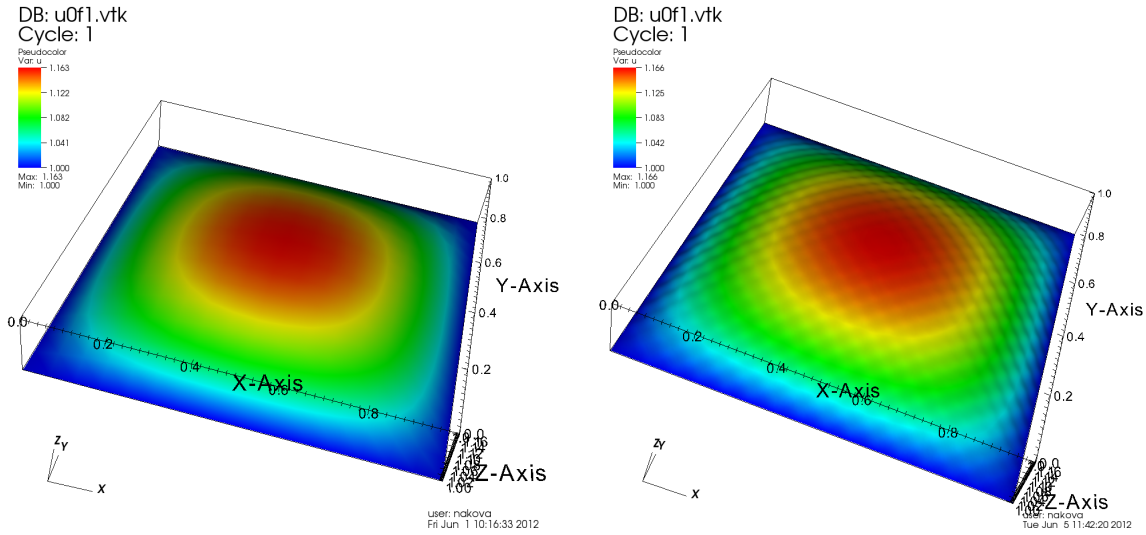

(a) Homogenized Solution (b) Exact Solution

Figure 6: 289 Nodes for the Homogenized Problem and 2113 Nodes for the Cell Problems

	Nodes	Periodicity Cells	Time	Max	Min
Homogenized Problem	289	256	125s	1.163	1
Cell Problem	545				
Exact Solution	65536	256	74s	1.173	1

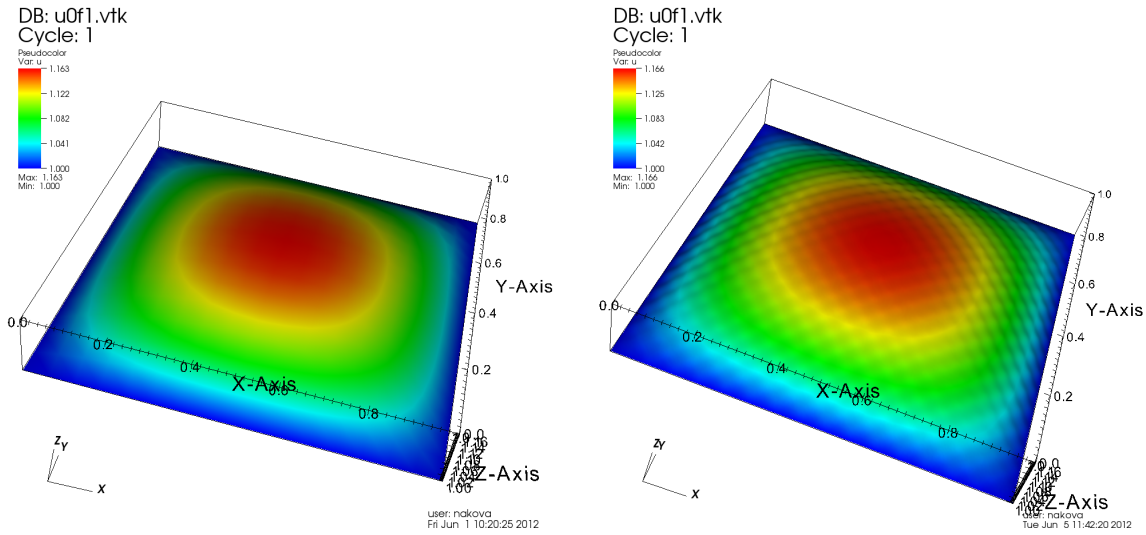

(a) Homogenized Solution (b) Exact Solution

Figure 7: 289 Nodes for the Homogenized Problem and 545 Nodes for the Cell Problems

	Nodes	Periodicity Cells	Time	Max	Min
Homogenized Problem	289	256	36s	1.163	1
Cell Problem	145				
Exact Solution	65536	256	74s	1.173	1

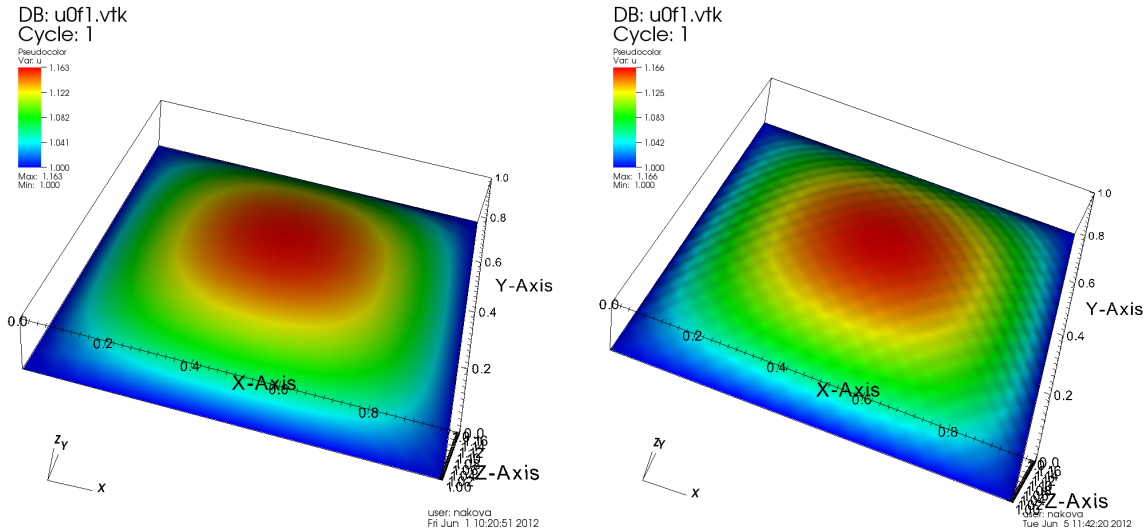

(a) Homogenized Solution (b) Exact Solution

Figure 8: 289 Nodes for the Homogenized Problem and 145 Nodes for the Cell Problems

	Nodes	Periodicity Cells	Time	Max	Min
Homogenized Problem	81	256	31s	1.155	1
Cell Problem	545				
Exact Solution	65536	256	74s	1.173	1

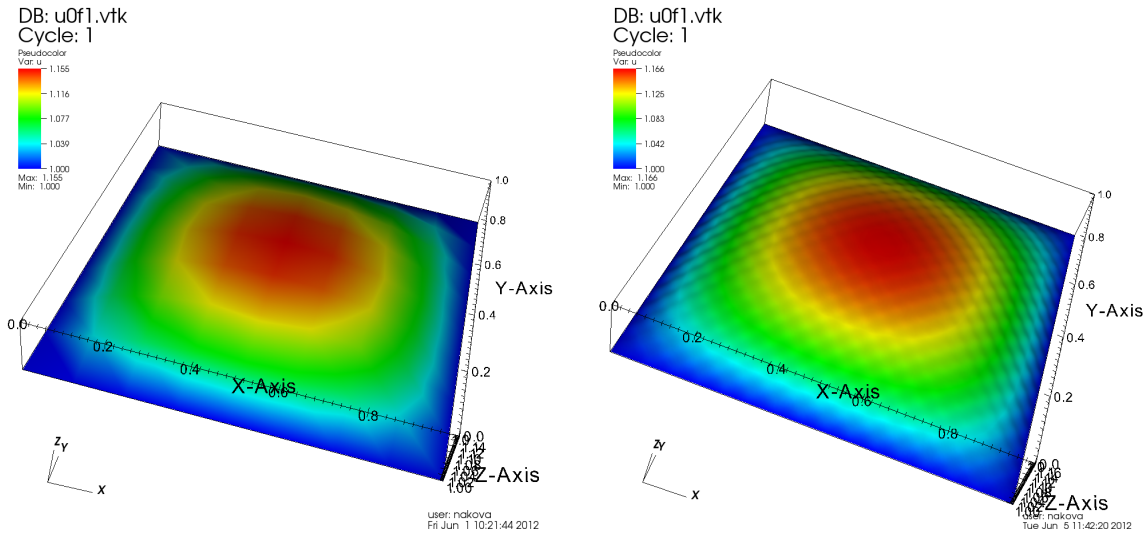

(a) Homogenized Solution (b) Exact Solution

Figure 9: 81 Nodes for the Homogenized Problem and 545 Nodes for the Cell Problems

As we can see from the numerical results above, the computational time needed for solving the homogenized problem is larger than that needed for the full microscale

simulation. This is due to the fact that the considered problem is nonlinear and we have to solve a cell problem for each integration point $x \in \Omega$. In the case of nonlinear problems different optimizations and simplifications can be done in order to reduce the computational time. We will not discuss here this topic.

3.2 Nonlinear Elliptic Problem: Case Specific Optimization

We solve the following problem:

$$-\nabla \cdot (a_\varepsilon(x, u_\varepsilon(x))\nabla u_\varepsilon) = f(x), \quad x \in \Omega = [0,1] \times [0,1] \tag{3.7a}$$

$$u_\varepsilon(x) = 1, \quad x \in \partial\Omega \tag{3.7b}$$

3.2.1 Cell Problem

The Y-periodic function $\chi_l(y)$ is the solution of the following auxuliary cell problem:

$$\nabla_y \cdot (a(y, u_0)\nabla_y \chi_l) = -\frac{\partial a(y, u_0)}{\partial y_l}, \quad l = 1, 2 \tag{3.8}$$

which is equivalent to

$$\nabla_y \cdot \left(k(y)u_0^2(x)\nabla_y \chi_l\right) = -\frac{\partial}{\partial y_l}\left(k(y)u_0^2(x)\right), \quad l = 1, 2 \Longleftrightarrow$$

$$u_0^2(x)\nabla_y \cdot (k(y)\nabla_y \chi_l) = -u_0^2(x)\frac{\partial k}{\partial y_l}(y), \quad l = 1, 2 \tag{3.9}$$

Thus for the cell problem we obtain (since $u_0(x) \neq 0$)

$$\nabla_y \cdot (k(y)\nabla_y \chi_l) = -\frac{\partial k}{\partial y_l}(y), \quad l = 1, 2 \tag{3.10}$$

This means that we do not have to solve the cell problems for each point $x \in \Omega$ of the macrodomain, but only once. Thus, due to the specific form of the coefficient $a_\varepsilon(x, u_\varepsilon)$ we are able to entirely decouple the macro and the micro scales and to reduce significantly the computational time.

3.2.2 Homogenized Problem

We obtain the following homogenized problem:

$$-\nabla \cdot (a^*(u_0)\nabla u_0) = f(x), \quad x \in \Omega \tag{3.11a}$$

$$u_0(x) = 1, \quad x \in \partial\Omega \tag{3.11b}$$

where the homogenized coefficient a^* is given by

$$a^* = (a^*)_{i,j=1}^2 = \frac{1}{|Y|}\int_Y a(y,u_0)\left(\delta_{ij} + \frac{\partial \chi_j}{\partial y_i}(y)\right) dy =$$

$$= \frac{1}{|Y|}\int_Y k(y)u_0^2\left(\delta_{ij} + \frac{\partial \chi_j}{\partial y_i}(y)\right) dy =$$

$$= u_0^2(x) \underbrace{\frac{1}{|Y|}\int_Y k(y)\left(\delta_{ij} + \frac{\partial \chi_j}{\partial y_i}(y)\right) dy}_{we\ \ calculate\ \ this\ \ integral\ \ only\ \ once} \tag{3.12}$$

3.2.3 Numerical Experiment

We have the following setting for our test problem:

- $\Omega = [0,1] \times [0,1]$
- $a_\varepsilon(x, u_\varepsilon) = k_\varepsilon(x)u_\varepsilon^2$
- $k_\varepsilon(x) = \cos(32\pi x_1)\cos(32\pi x_2) + 1.1$
- $f(x) = 5$
- $\varepsilon = 0.0625$

	Nodes	Periodicity Cells	Time	Max	Min
Homogenized Problem	289	256	0.27s	1.282	1
Cell Problem	145				
Exact Solution	16384	256	22s	1.284	1

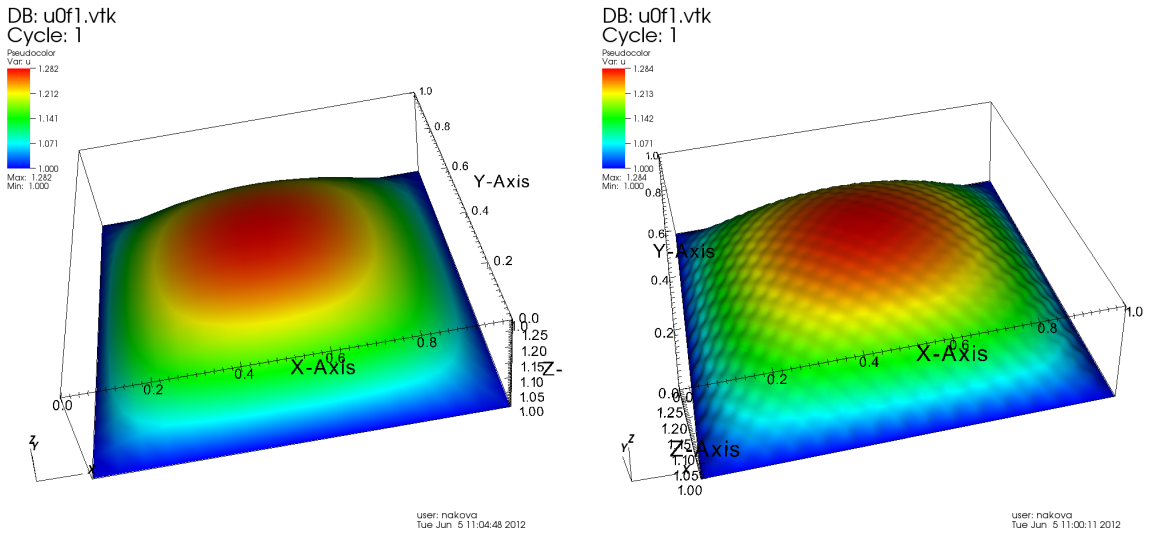

(a) Homogenized Solution (b) Exact Solution

Figure 10: 289 Nodes for Solving the Homogenized Problem and 145 Nodes for the Cell Problems

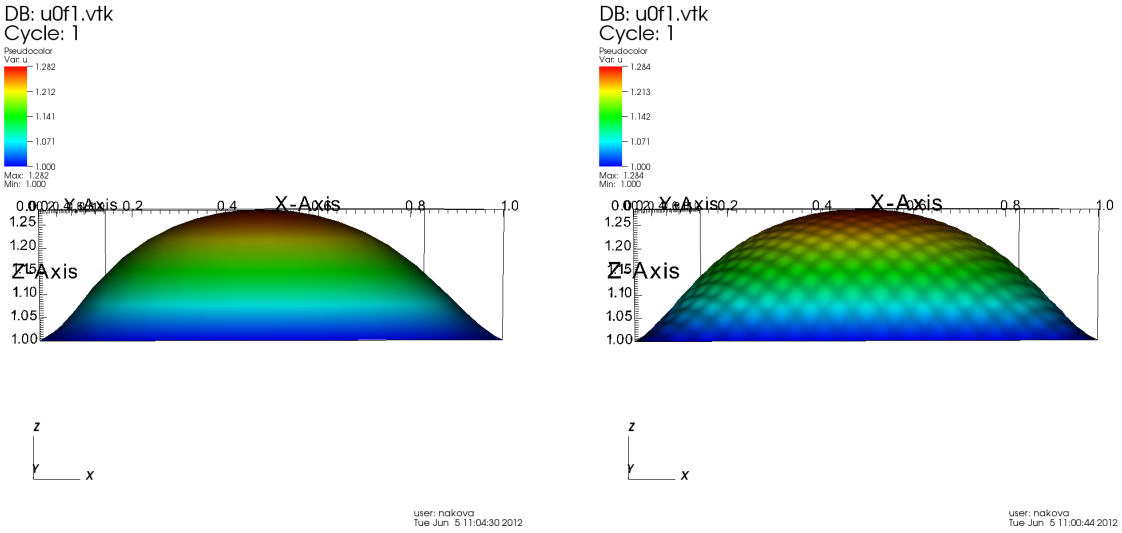

(a) Homogenized Solution (b) Exact Solution

Figure 11: 289 Nodes for Solving the Homogenized Problem and 145 Nodes for the Cell Problems: Side View

	Nodes	Periodicity Cells	Time	Max	Min
Homogenized Problem	1089	256	0.98s	1.286	1
Cell Problem	145				
Exact Solution	16384	256	22s	1.284	1

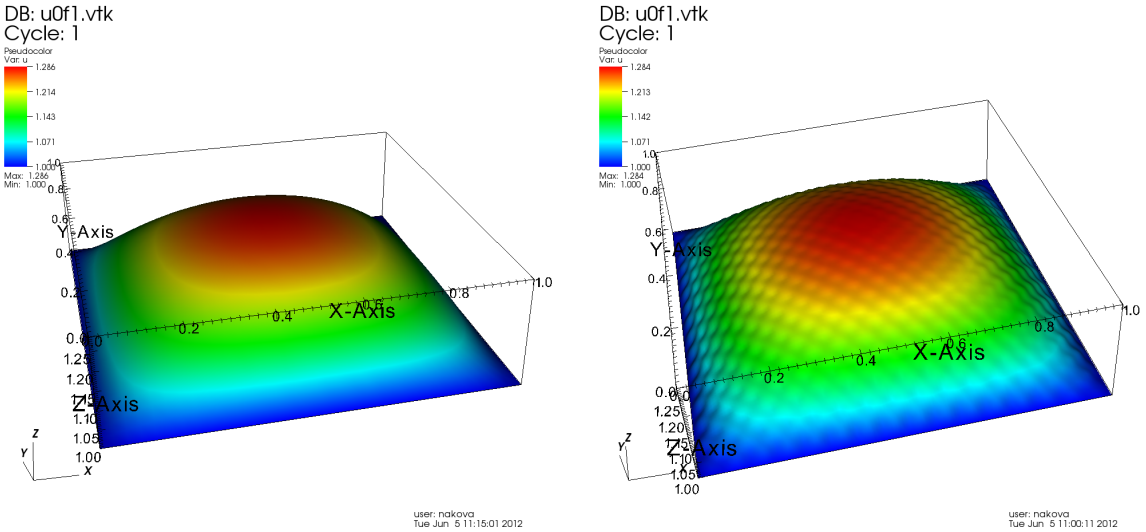

(a) Homogenized Solution (b) Exact Solution

Figure 12: 1089 Nodes for Solving the Homogenized Problem and 145 Nodes for the Cell Problems

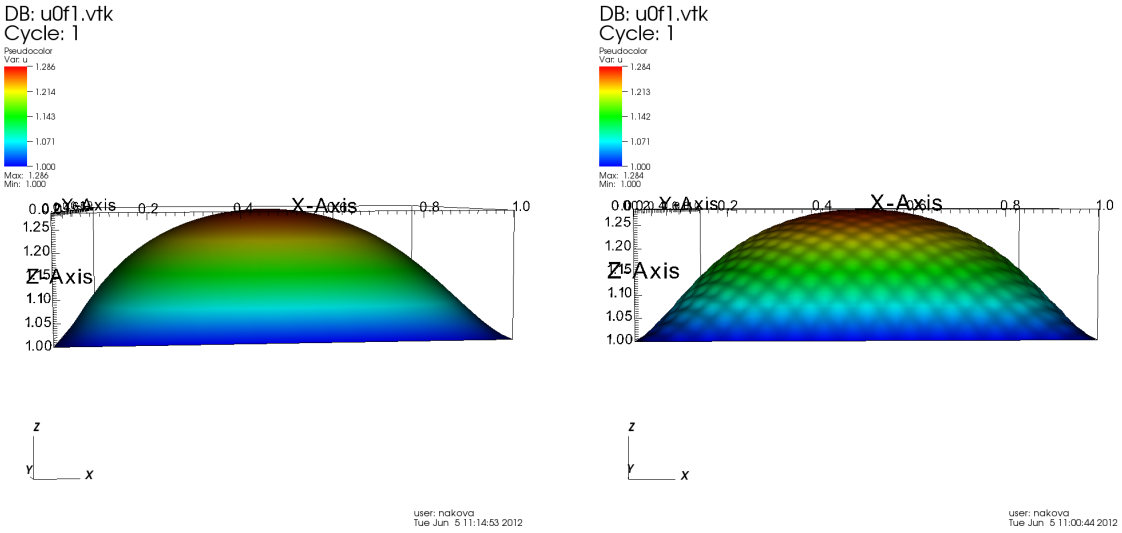

(a) Homogenized Solution (b) Exact Solution

Figure 13: 1089 Nodes for Solving the Homogenized Problem and 145 Nodes for the Cell Problems: Side View

	Nodes	Periodicity Cells	Time	Max	Min
Homogenized Problem	1089	256	1.05s	1.287	1
Cell Problem	545				
Exact Solution	16384	256	22s	1.284	1

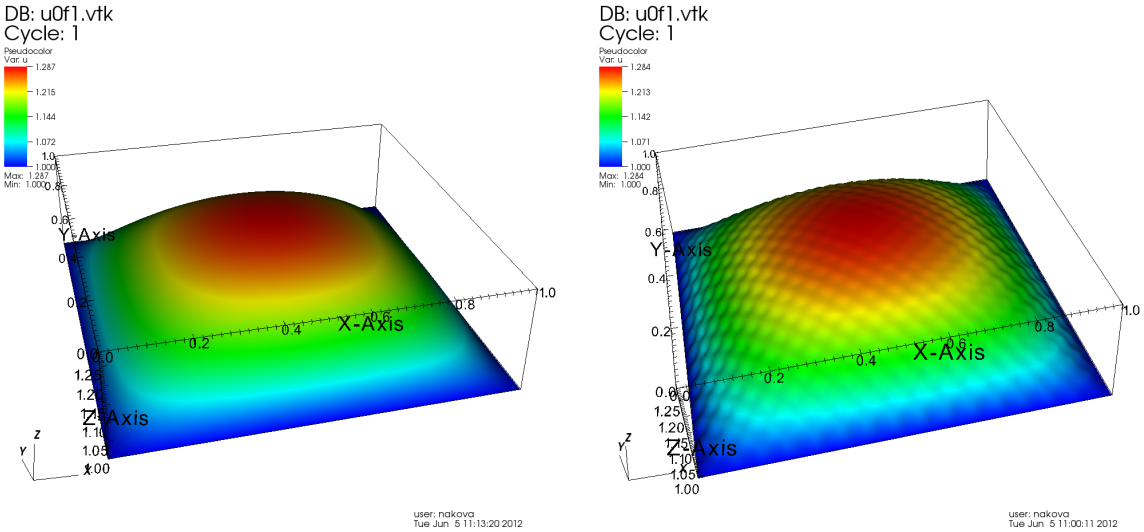

(a) Homogenized Solution (b) Exact Solution

Figure 14: 1089 Nodes for Solving the Homogenized Problem and 545 Nodes for the Cell Problems

4 Lithium-ion Batteries: Mathematical Model

We consider the microscale mathematical model derived in [8].
We use the following notation:

- Ω - domain of the whole battery cell
- $\partial\Omega$ - boundary of Ω
- Ω_e - domain of the electrolyte
- Ω_a - domain of the anode active particles
- $\partial\Omega_a$ - boundary of Ω_a
- Ω_c - domain of the cathode active particles
- $\partial\Omega_c$ - boundary of Ω_c
- $\Omega_s = \Omega_a \cup \Omega_c$ - domain of the solid active particles

4.1 Equations of the Electrolyte

The equations of the electrolyte phase couple the concentration c^e of lithium ions and the potential ϕ^e in the electrolyte and they have the following form

$$\frac{\partial c^e}{\partial t} - \nabla \cdot (k^e_{11}(c^e)\nabla c^e + k^e_{12}\nabla \phi^e) = 0, \quad x \in \Omega_e \tag{4.1a}$$

$$-\nabla \cdot (k^e_{21}(c^e)\nabla c^e + k^e_{22}\nabla \phi^e) = 0, \quad x \in \Omega_e \tag{4.1b}$$

where for the coefficients we have

$$k^e_{11}(c^e) = D^e + \frac{RT}{F^2}\frac{(t_+)^2\kappa^e}{c^e} \tag{4.2a}$$

$$k^e_{12} = \kappa^e \frac{t_+}{F} \tag{4.2b}$$

$$k^e_{21}(c^e) = \frac{RT}{F}\frac{\kappa^e t_+}{c^e} \tag{4.2c}$$

$$k^e_{22} = \kappa^e \tag{4.2d}$$

with

- c^e - concentration of Li+ in the electrolyte
- ϕ^e - potential in the electrolyte
- κ^e-ion conductivity
- D^e-interdiffusion coefficient

4.2 Equations of the Solid

The equations describing the transport of Lithium ions and charge in the solid active particles are

$$\frac{\partial c^s}{\partial t} - \nabla \cdot (D^s \nabla c^s) = 0, \quad x \in \Omega_s \tag{4.3a}$$

$$-\nabla \cdot (\kappa^s \nabla \phi^s) = 0, \quad x \in \Omega_s \tag{4.3b}$$

where

- c^s - concentration of Li+ in the active particles
- ϕ^s - potential in the active particles
- D^s-ion diffusion
- κ^s-electronic conductivity

We make no distinction between anode and cathode active particles since the equations describing the electrochemical processes in both type of particles are identical. We only have different values for the diffusion coefficient D^s and the electronic conductivity κ^s.

4.3 Interface Conditions

The ion flux and the electrical current in the electrolyte are respectively:

$$\mathbf{N}^e = -\left(k^e_{11}(c^e)\nabla c^e + k^e_{12}\nabla \phi^e\right) \tag{4.4a}$$

$$\mathbf{J}^e = -\left(k^e_{21}(c^e)\nabla c^e + k^e_{22}\nabla \phi^e\right) \tag{4.4b}$$

The ion flux and the electrical current in the active particles are respectively:

$$\mathbf{N}^s = -D^s \nabla c^s \tag{4.5a}$$

$$\mathbf{J}^s = -\kappa^s \nabla \phi^s \tag{4.5b}$$

We have the following interface conditions, which are imposed on the boundary between the active particles and the electrolyte:

$$\mathbf{N}^s \cdot \mathbf{n_s} = \mathbf{N}^e \cdot \mathbf{n_s} = \mathcal{N}(c^e, c^s, \phi^e, \phi^s), \quad x \in \gamma \tag{4.6}$$

$$\mathbf{J}^s \cdot \mathbf{n_s} = \mathbf{J}^e \cdot \mathbf{n_s} = \mathcal{J}(c^e, c^s, \phi^e, \phi^s), \quad x \in \gamma \tag{4.7}$$

The unit normal vector $\mathbf{n_s}$ points in the direction from the solid particles to the electrolyte. where γ is the interface boundary between the solid and the electrolyte and the current densities $\mathcal{N}$ and $\mathcal{J}$ are given by:

$$\mathcal{N} = \frac{k}{F}\sqrt{c^e c^s \left(c^s_{max} - c^s\right)}\left[\exp^{\frac{F\eta}{2RT}} - \exp^{\frac{-F\eta}{2RT}}\right] \tag{4.8}$$

$$\mathcal{J} = F\mathcal{N} \tag{4.9}$$

- $\eta = \phi^s - \phi^e - U_0(c^s)$, where $U_0(c^s)$ is the open circuit potential

4.4 Boundary Conditions

With ω_1 and ω_2 we denote the outer anode and cathode boundary walls as shown in Figure 15. On the anode particles boundary $\omega_1 \cap \partial\Omega_a$ we impose constant potential ϕ^s and on the cathode particles boundary $\omega_2 \cap \partial\Omega_c$ - constant applied current.

- Dirichlet boundary conditions: $\phi^s(x) = E_1^s = const, \quad x \in \omega_1 \cap \partial\Omega_a$
- Neumann boundary conditions:

$$(\kappa^s \nabla \phi^s) \cdot \mathbf{n} = E_2^s = const, \quad x \in \omega_2 \cap \partial\Omega_c \tag{4.10}$$

$$\nabla c^s \cdot \mathbf{n} = 0, \quad x \in \{\omega_1 \cap \partial\Omega_a\} \cup \{\omega_2 \cap \partial\Omega_c\} \tag{4.11}$$

$$\mathbf{N}^e \cdot \mathbf{n} = \mathbf{J}^e \cdot \mathbf{n} = 0, \quad x \in \partial\Omega \tag{4.12}$$

$$\mathbf{N}^s \cdot \mathbf{n} = \mathbf{J}^s \cdot \mathbf{n} = 0, \quad x \in \partial\Omega \backslash \{\omega_1 \cup \omega_2\} \tag{4.13}$$

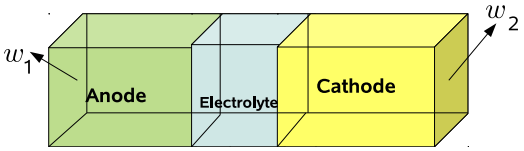

Figure 15: Battery Cell

5 Homogenization of the Li-ion Battery Model

We consider periodic arrangement of the active particles as shown in Figure 16 ([11]). As a single periodic cell we consider a cubic block consisting of one active particle surrounded by electrolyte as shown in Figure 17.

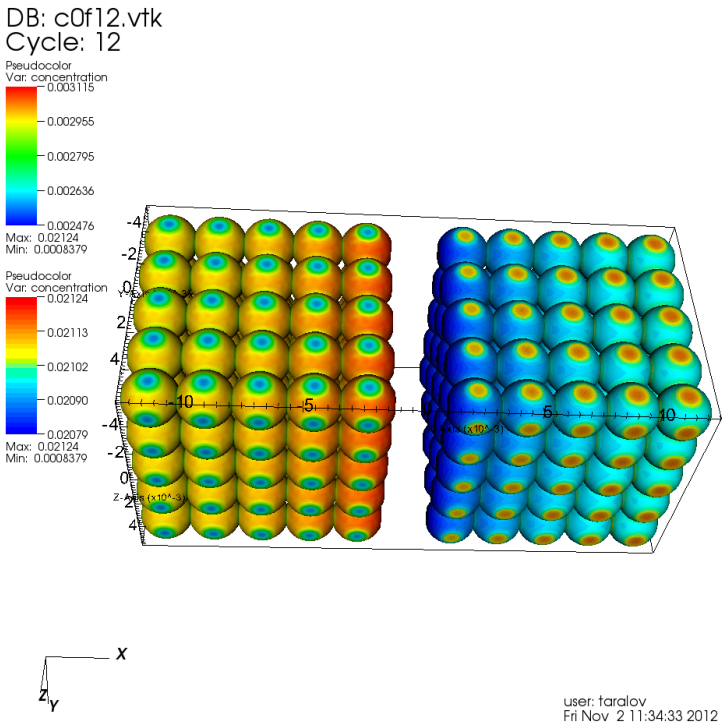

Figure 16: Battery Cell

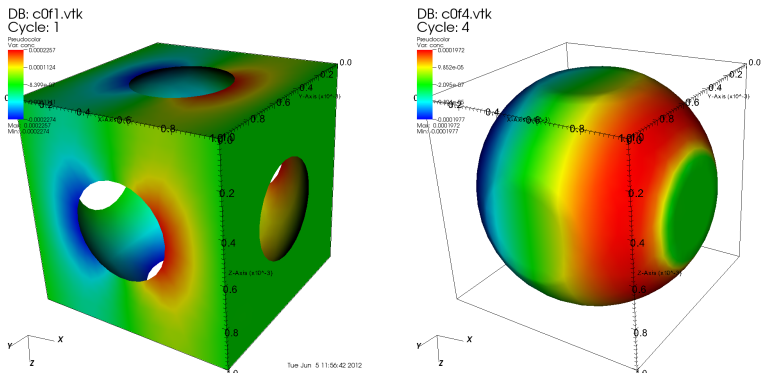

(a) Electrolyte (b) Solid

Figure 17: Geometry of the Periodicity Cell

We start by defining the model equations in the whole domain $\Omega = \Omega_s \cup \Omega_e$, $\Omega \in \mathbb{R}^3$

$$\frac{\partial\left(\chi^e(x)c^e\right)}{\partial t} - \nabla \cdot \left(k_{11}(x, c^e)\nabla c^e + k_{12}(x)\nabla\phi^e\right) = 0, \quad x \in \Omega \tag{5.1a}$$

$$-\nabla \cdot \left(k_{21}(x, c^e)\nabla c^e + k_{22}(x)\nabla\phi^e\right) = 0, \quad x \in \Omega \tag{5.1b}$$

$$\frac{\partial\left(\chi^s(x)c^s\right)}{\partial t} - \nabla \cdot \left(D(x)\nabla c^s\right) = 0, \quad x \in \Omega \tag{5.1c}$$

$$-\nabla \cdot \left(\kappa(x)\nabla\phi^s\right) = 0, \quad x \in \Omega \tag{5.1d}$$

with the boundary conditions:

- Dirichlet BC: $\phi^s(x) = E_1^s = const, \quad x \in \omega_1$
- Neumann BC:

$$\left(\kappa(x)\nabla\phi^s\right) \cdot \mathbf{n} = E_2(x) = \chi^s(x)E_2^s, \quad x \in \omega_2 \tag{5.2}$$

$$\nabla c^s \cdot \mathbf{n} = 0, \quad x \in \omega_1 \cup \omega_2 \tag{5.3}$$

$$\mathbf{N}^e \cdot \mathbf{n} = \mathbf{J}^e \cdot \mathbf{n} = 0, \quad x \in \partial\Omega \tag{5.4}$$

where

$$k_{11}(x, c^e) = \chi^e(x)k_{11}^e(c^e) = \begin{cases} k_{11}^e(c^e), & x \in \Omega_e \\ 0, & x \in \Omega_s \end{cases}$$

$$k_{12}(x) = \chi^e(x)k_{12}^e = \begin{cases} k_{12}^e, & x \in \Omega_e \\ 0, & x \in \Omega_s \end{cases}$$

$$k_{21}(x, c^e) = \chi^e(x)k_{21}^e(c^e) = \begin{cases} k_{21}^e(c^e), & x \in \Omega_e \\ 0, & x \in \Omega_s \end{cases}$$

$$k_{22}(x) = \chi^e(x)k_{22}^e = \begin{cases} k_{22}^e, & x \in \Omega_e \\ 0, & x \in \Omega_s \end{cases}$$

$$D(x) = \chi^s(x)D^s = \begin{cases} 0, & x \in \Omega_e \\ D^s, & x \in \Omega_s \end{cases}$$

$$\kappa(x) = \chi^s(x)\kappa^s = \begin{cases} 0, & x \in \Omega_e \\ \kappa^s, & x \in \Omega_s \end{cases}$$

and

$$\chi^e(x) = \begin{cases} 1, & x \in \Omega_e \\ 0, & x \in \Omega_s \end{cases}$$

$$\chi^s(x) = \begin{cases} 0, & x \in \Omega_e \\ 1, & x \in \Omega_s \end{cases}$$

5.1 Asymptotic Analysis

We use the following notation

- L - characteristic length of the electrodes
- l - characteristic length of the active particles which in our case we consider to be the diameter of the "spherical-like" particle shown on Figure 17
- $\varepsilon = \dfrac{l}{L} \to 0, \quad y = \dfrac{x}{\varepsilon}$, periodic structure with a reference periodicity cell $Y = E \cup S$, where
- $Y \sim L$, i.e. the characteristic length of the reference periodicity cell is L
- E - electrolyte domain in the reference periodicity cell
- S - solid particle domain in the reference periodicity cell
- Γ - interface between the electrolyte and the particle in the reference periodicity cell

Now we write the problem in terms of a dependence on the small parameter ε and then we want to investigate the behaviour of the partial differential equations when ε goes to zero.

$$\frac{\partial\left(\chi^e_\varepsilon(x)c^e_\varepsilon\right)}{\partial t} - \nabla\cdot\left((k_{11})_\varepsilon(x,c^e_\varepsilon)\nabla c^e_\varepsilon + (k_{12})_\varepsilon(x)\nabla\phi^e_\varepsilon\right) = 0, \quad x\in\Omega \tag{5.5a}$$

$$-\nabla\cdot\left((k_{21})_\varepsilon(x,c^e_\varepsilon)\nabla c^e_\varepsilon + (k_{22})_\varepsilon(x)\nabla\phi^e_\varepsilon\right) = 0, \quad x\in\Omega \tag{5.5b}$$

$$\frac{\partial\left(\chi^s_\varepsilon(x)c^s_\varepsilon\right)}{\partial t} - \nabla\cdot\left(D_\varepsilon(x)\nabla c^s_\varepsilon\right) = 0, \quad x\in\Omega \tag{5.5c}$$

$$-\nabla\cdot\left(\kappa_\varepsilon(x)\nabla\phi^s_\varepsilon\right) = 0, \quad x\in\Omega \tag{5.5d}$$

with the following boundary conditions

- Dirichlet BC: $\phi^s_\varepsilon(x) = E^s_1 = const, \quad x\in\omega_1$
- Neumann BC:

$$\left(\kappa_\varepsilon(x)\nabla\phi^s_\varepsilon\right)\cdot\mathbf{n} = E^\varepsilon_2(x) = \chi^s_\varepsilon(x)E^s_2 = \chi^s\left(\frac{x}{\varepsilon}\right)E^s_2, \quad x\in\omega_2 \tag{5.6}$$

$$\nabla c^s_\varepsilon\cdot\mathbf{n} = 0, \quad x\in\omega_1\cup\omega_2 \tag{5.7}$$

$$\mathbf{N}^e_\varepsilon\cdot\mathbf{n} = \mathbf{J}^e_\varepsilon\cdot\mathbf{n} = 0, \quad x\in\partial\Omega \tag{5.8}$$

and interface conditions

$$-\left((k_{11})_\varepsilon\nabla c^e_\varepsilon + (k_{12})_\varepsilon\nabla\phi^e_\varepsilon\right)\cdot\mathbf{n_s} = \mathcal{N}_\varepsilon, \quad x\in\gamma_\varepsilon \tag{5.9}$$

$$-\left((k_{21})_\varepsilon\nabla c^e_\varepsilon + (k_{22})_\varepsilon\nabla\phi^e_\varepsilon\right)\cdot\mathbf{n_s} = \mathcal{J}_\varepsilon, \quad x\in\gamma_\varepsilon \tag{5.10}$$

$$-\left(D_\varepsilon\nabla c^s_\varepsilon\right)\cdot\mathbf{n_s} = \mathcal{N}_\varepsilon, \quad x\in\gamma_\varepsilon \tag{5.11}$$

$$-\left(\kappa_\varepsilon\nabla\phi^s_\varepsilon\right)\cdot\mathbf{n_s} = \mathcal{J}_\varepsilon, \quad x\in\gamma_\varepsilon \tag{5.12}$$

where

- $\mathcal{N}_\varepsilon = \mathcal{N}\left(c_\varepsilon^e, \phi_\varepsilon^e, \phi_\varepsilon^s, c_\varepsilon^s\right)$ and
- $\mathcal{J}_\varepsilon = \mathcal{J}\left(c_\varepsilon^e, \phi_\varepsilon^e, \phi_\varepsilon^s, c_\varepsilon^s\right)$ and
- $(k_{11})_\varepsilon(x, c_\varepsilon^e) = k_{11}\left(\frac{x}{\varepsilon}, c_\varepsilon^e\right) = k_{11}(y, c_\varepsilon^e) = \chi^e(y) k_{11}^e(c_\varepsilon^e)$, where $\chi^e(y)$ is Y-periodic in y and therefore $k_{11}(y, c_\varepsilon^e)$ is also Y-periodic
- $$\chi^e(y) = \begin{cases} 1, & y \in E \\ 0, & y \in S \end{cases}, \tag{5.13}$$
$$\chi^s(y) = 1 - \chi^e(y) \tag{5.14}$$
- $(k_{12})_\varepsilon(x) = k_{12}\left(\frac{x}{\varepsilon}\right) = k_{12}(y) = \chi^e(y) k_{12}^e$, Y-periodic in y
- $(k_{21})_\varepsilon(x, c_\varepsilon^e) = k_{21}\left(\frac{x}{\varepsilon}, c_\varepsilon^e\right) = k_{21}(y, c_\varepsilon^e) = \chi^e(y) k_{21}^e(c_\varepsilon^e)$, Y-periodic in y
- $(k_{22})_\varepsilon(x) = k_{22}\left(\frac{x}{\varepsilon}\right) = k_{22}(y) = \chi^e(y) k_{22}^e$, Y-periodic in y
- $D_\varepsilon(x) = D\left(\frac{x}{\varepsilon}\right) = D(y) = \chi^s(y) D^s$, Y-periodic in the y variable
- $\kappa_\varepsilon(x) = \kappa\left(\frac{x}{\varepsilon}\right) = \kappa(y) = \chi^s(y)\kappa^s$, Y-periodic in the y variable

5.2 Microscale Solid Equation for the Concentration c^s

The diffusion of Lithium ions in the active particles is much slower than the diffusion of ions in the electrolyte. Therefore we do not upscale the equation for the concentration c^s of Lithium ions in the active particles since the behaviour of the function c^s can be captured adequately only on the microscale. Thus on the microscale we solve the original microscopic equation for the concentration c^s of Lithium ions in the active particles given in scale invariant form in terms of the variable $y \in S$:

$$\frac{\partial c^s}{\partial t} - \nabla_y \cdot \left(\frac{D^s}{\varepsilon^2} \nabla_y c^s\right) = 0, \quad y \in S \tag{5.15a}$$

$$-\frac{D^s}{\varepsilon^2} \nabla_y c^s \cdot \mathbf{n_s} = \frac{1}{\varepsilon} \mathcal{N}(c_0^e, c^s, \phi_0^e, \phi_0^s), \quad y \in \Gamma \tag{5.15b}$$

, where we have

- Γ - the interface boundary between the electrolyte and the particle in the reference periodicity cell Y
- Periodic boundary conditions on $\partial S \backslash \Gamma$, i.e. on the boundary of the solid particle where the particles are connected

5.3 Asymptotic expansion of the functions c^e, ϕ^e and ϕ^s

We suppose the following asymptotic expansions for the functions c^e_ε, ϕ^e_ε and ϕ^s_ε:

- $c^e_\varepsilon(x,t) = c^e_0(x,t) + \varepsilon c^e_1\left(x, \frac{x}{\varepsilon}, t\right) + \varepsilon^2 c^e_2\left(x, \frac{x}{\varepsilon}, t\right)$
- $\phi^e_\varepsilon(x,t) = \phi^e_0(x,t) + \varepsilon \phi^e_1\left(x, \frac{x}{\varepsilon}, t\right) + \varepsilon^2 \phi^e_2\left(x, \frac{x}{\varepsilon}, t\right)$
- $\phi^s_\varepsilon(x,t) = \phi^s_0(x,t) + \varepsilon \phi^s_1\left(x, \frac{x}{\varepsilon}, t\right) + \varepsilon^2 \phi^s_2\left(x, \frac{x}{\varepsilon}, t\right)$
- $y = \frac{x}{\varepsilon}$
- $\nabla = \nabla_x + \frac{1}{\varepsilon}\nabla_y$

where we assume that the functions c^e_0, ϕ^e_0 and ϕ^s_0 depend only on the macroscopic (slow) variable x and the functions $c^e_1, c^e_2, \phi^e_1, \phi^e_2, \phi^s_1, \phi^s_2$ are Y-periodic in the $y = \frac{x}{\varepsilon}$ variable, where Y is the reference periodicity cell.
For $y \in Y$, provided that k^e_{11} is a smooth function of c^e in E, and using Taylor series, for the nonlinear coefficient $k_{11}(y, c^e_\varepsilon)$ for $\varepsilon \to 0$ we obtain:

$$\begin{aligned} k_{11}(y, c^e_\varepsilon) &= k_{11}\left(y, c^e_0(x,t) + \varepsilon c^e_1(x,y,t)\right) = \\ &= k_{11}(y, c^e_0) + \varepsilon c^e_1 \frac{\partial k_{11}}{\partial c^e}(y, c^e_0) + \varepsilon^2 (c^e_1)^2 \frac{\partial^2 k_{11}}{\partial (c^e)^2}(y, c^e_0) = \\ &= k_{11}(y, c^e_0) + O(\varepsilon) \end{aligned}$$

where

$$\frac{\partial k_{11}}{\partial c^e} = \frac{\partial(\chi^e(y) k^e_{11}(c^e))}{\partial c^e} = \chi^e(y)\frac{\partial k^e_{11}}{\partial c^e} = \begin{cases} \dfrac{\partial k^e_{11}}{\partial c^e}, & y \in E \\ 0, & y \in S \end{cases}$$

Therefore

$$k_{11}(y, c^e_\varepsilon) = k_{11}(y, c^e_0) + O(\varepsilon)$$

By analogy for the current density $\mathcal{N}_\varepsilon$ we obtain:

$$\begin{aligned} \mathcal{N}_\varepsilon = \mathcal{N}\left(c^e_\varepsilon, c^s, \phi^e_\varepsilon, \phi^s_\varepsilon\right) &= \mathcal{N}\left(c^e_0 + \varepsilon c^e_1, c^s, \phi^e_0 + \varepsilon \phi^e_1, \phi^s_0 + \varepsilon \phi^s_1\right) = \\ &= \mathcal{N}\left(c^e_0, c^s, \phi^e_0, \phi^s_0\right) + \varepsilon c^e_1 \frac{\partial \mathcal{N}}{\partial c^e}\left(c^e_0, c^s, \phi^e_0, \phi^s_0\right) + \\ &+ \varepsilon \phi^e_1 \frac{\partial \mathcal{N}}{\partial \phi^e}\left(c^e_0, c^s, \phi^e_0, \phi^s_0\right) + \varepsilon \phi^s_1 \frac{\partial \mathcal{N}}{\partial \phi^s}\left(c^e_0, c^s, \phi^e_0, \phi^s_0\right) = \\ &= \mathcal{N}\left(c^e_0, c^s, \phi^e_0, \phi^s_0\right) + O(\varepsilon^\alpha) \end{aligned} \tag{5.16}$$

with $\alpha \geq 1$.
Finally, we obtain

$$k_{11}(y, c_\varepsilon^e) = k_{11}(y, c_0^e) + O(\varepsilon) \tag{5.17}$$
$$k_{21}(y, c_\varepsilon^e) = k_{21}(y, c_0^e) + O(\varepsilon) \tag{5.18}$$
$$\mathcal{N}_\varepsilon = \mathcal{N}\left(c_\varepsilon^e, c^s, \phi_\varepsilon^e, \phi_\varepsilon^s\right) = \mathcal{N}\left(c_0^e, c^s, \phi_0^e, \phi_0^s\right) + O(\varepsilon^\alpha) \tag{5.19}$$
$$\mathcal{J}_\varepsilon = \mathcal{J}\left(c_\varepsilon^e, c^s, \phi_\varepsilon^e, \phi_\varepsilon^s\right) = \mathcal{J}\left(c_0^e, c^s, \phi_0^e, \phi_0^s\right) + O(\varepsilon^\alpha) \tag{5.20}$$

We denote

$$\mathcal{N}_0 = \mathcal{N}\left(c_0^e, c^s, \phi_0^e, \phi_0^s\right) \tag{5.21}$$
$$\mathcal{J}_0 = \mathcal{J}\left(c_0^e, c^s, \phi_0^e, \phi_0^s\right) \tag{5.22}$$

5.4 Homogenization of the Interface Conditions

First we show that the total flux over the interfaces is preserved over a change of the total interface surface. A similar idea is applied in [1] and [2] in order for the total flux across the interfaces to be properly scaled.
We use the following notation:

- $\gamma = \gamma_a \cup \gamma_c$ -the interface boundary, where
- γ_a - the interface boundary between the anode active particles and the electrolyte
- γ_c - the interface boundary between the cathode active particles and the electrolyte

Let us consider the equation for ϕ^s in the cathode where we apply constant current.

$$-\nabla \cdot (\kappa^s \nabla \phi^s) = 0, \quad x \in \Omega_c \tag{5.23}$$

We now integrate both sides of this equation over the domain of the cathode particles and we use the divergence theorem:

$$\int_{\Omega_c} -\nabla \cdot (\kappa^s \nabla \phi^s)\, dx = 0 \Leftrightarrow$$
$$\int_{\partial\Omega_c} -\kappa^s \nabla \phi^s \cdot \mathbf{n}\, ds = 0 \Leftrightarrow$$
$$\int_{\gamma_c} \mathcal{J}\, ds + \int_{\omega_2 \cap \partial\Omega_c} E_2^s\, ds = 0 \Leftrightarrow$$
$$\int_{\gamma_c} \mathcal{J}\, ds = -\int_{\omega_2 \cap \partial\Omega_c} E_2^s\, ds \Leftrightarrow$$
$$\int_{\gamma_c} \mathcal{J}\, ds = -|\omega_2 \cap \partial\Omega_c| E_2^s \tag{5.24}$$

Since E_2^s is constant, if we keep the measure of $\omega_2 \cap \partial\Omega_c$ constant, regardless of the interface surface, the total flux in the cathode $I = \int_{\gamma_c} \mathcal{J}\, ds$ is a constant and does not depend on ε.
We will show that, indeed, the measure of $\omega_2 \cap \partial\Omega_c$ is constant with respect to ε. In the

case $\varepsilon = 1$ we have only one particle in each electrode and thus only one periodicity cell which concides with the whole electrode. Taking into account the type of particles we consider (see Figure 17), it is clear that the intersection of a single particle with the outer battery cell boundary ω_1 or ω_2, is a circle. Let us denote the radius of this circle for $\varepsilon = 1$ with R_1. Therefore for the measure $|\omega_2 \cap \partial\Omega_c|$ we obtain (see Figure 18)

$$S_1 = |\omega_2 \cap \partial\Omega_c| = \pi R_1^2 \tag{5.25}$$

With L we denote the length of the electrode. Now let us decrease ε in such a way that we decrease the length of the periodicity cell twice. This means that in each electrode we have 8 periodicity cells and thus 8 active particles. The side length of each periodicity cell is then $\dfrac{L}{2}$. Let us denote with R_2 the radius of the circle obtained from the intersection of the cathode particle with the outer boundary ω_2 (see Figure 18). Then the total surface area $|\omega_2 \cap \partial\Omega_c|$ is

$$S_2 = |\omega_2 \cap \partial\Omega_c| = 4\pi R_2^2 \tag{5.26}$$

Now taking into account that

$$\frac{R_2}{\frac{L}{2}} = \frac{R_1}{L} \tag{5.27}$$

we obtain that

$$R_2 = \frac{R_1}{2} \tag{5.28}$$

and

$$S_2 = 4\pi \frac{R_1^2}{4} = \pi R_1^2 = S_1 \tag{5.29}$$

Consequently we obtain that the measure $|\omega_2 \cap \partial\Omega_c|$ does not change when we uniformly decrease ε.

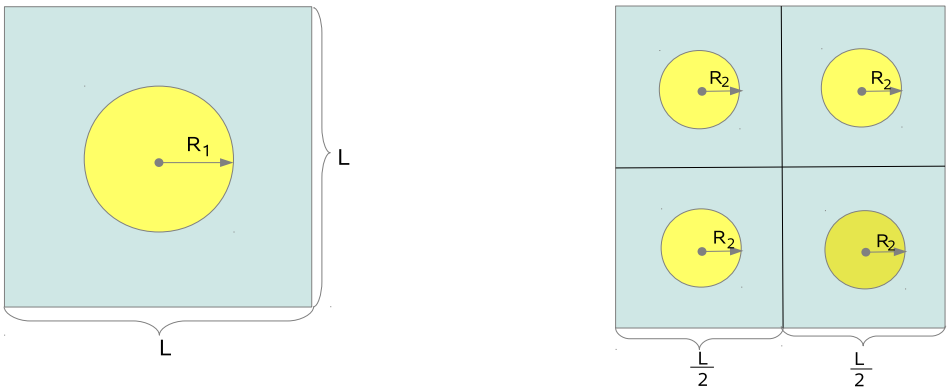

(a) $\varepsilon = 1$ (b) $\varepsilon = 0.5$

Figure 18: Cathode outer boundary

From equation (4.1b) we obtain

$$\begin{aligned}
\int_{\Omega_e} \nabla \cdot \mathbf{J}^e \, dx = 0 \Leftrightarrow \\
\int_{\partial\Omega_e} \mathbf{J}^e \cdot \mathbf{n} \, ds = 0 \Leftrightarrow \\
\underbrace{\int_{\partial\Omega} \mathbf{J}^e \cdot \mathbf{n} \, ds}_{=0} + \int_{\gamma} \mathbf{J}^e \cdot \mathbf{n} \, ds = 0 \Leftrightarrow \\
-\int_{\gamma} \mathbf{J}^e \cdot \mathbf{n}_s \, ds = 0 \Leftrightarrow \\
\int_{\gamma} \mathcal{J} \, ds = 0 \Leftrightarrow \\
\int_{\gamma_a} \mathcal{J} \, ds + \int_{\gamma_c} \mathcal{J} \, ds = 0 \Leftrightarrow \\
\int_{\gamma_a} \mathcal{J} \, ds = -\int_{\gamma_c} \mathcal{J} \, ds
\end{aligned} \tag{5.30}$$

From here it follows that since the total flux in the cathode is equal to the total flux in the anode, then the total flux in the anode is also constant with respect to ε. We also

have from (4.9) that $\mathcal{J} = F\mathcal{N}$ and consequently we obtain that

$$\int\limits_{\gamma_a} \mathcal{N}\, ds = \frac{1}{F} \int\limits_{\gamma_a} \mathcal{J}\, ds \tag{5.31}$$

$$\int\limits_{\gamma_c} \mathcal{N}\, ds = \frac{1}{F} \int\limits_{\gamma_c} \mathcal{J}\, ds \tag{5.32}$$

which means that also the total ion flux in each electrode is a constant.

Let $\varepsilon\Gamma$ be a parametrically defined surface in 3D (the three dimensionsional Euclidean space). Then we have the following formula for the change of variables: $x = \varepsilon y$

$$\int\limits_{\varepsilon\Gamma} f(x)\, ds_x = \varepsilon^2 \int\limits_{\Gamma} g(y)\, ds_y \tag{5.33}$$

where

$$f(x) = f(x(y)) = f(\varepsilon y) = g(y) \tag{5.34}$$

and the surface $\varepsilon\Gamma$ transforms into the surface Γ after the change of variables.
Let us denote with εY_i, $i = 1, 2, \ldots, M$ the periodic microscale cells where $\varepsilon Y_i = \varepsilon E_i \cup \varepsilon S_i \cup \varepsilon\Gamma_i$ with εE_i being the electrolyte part of the periodicity cell, εS_i-the solid part, and $\varepsilon\Gamma_i$-the interface boundary between the solid and the electrolyte. Then with Y_i we denote the upscaled periodic cells after the transformation of coordinates $y = \dfrac{x}{\varepsilon}$. Consequently we have that $Y_i = E_i \cup S_i \cup \Gamma_i$. For each upscaled periodic cell Y_i we make the translation τ_i:

$$\tau_i : \quad y' = y + \xi_i \tag{5.35}$$

so that

$$Y_i \xrightarrow{\tau_i} Y \tag{5.36}$$

where Y is the reference periodicity cell, which consists of electrolyte domain E, active particle domain S and interface boundary Γ, i.e. $Y = E \cup S \cup \Gamma$. We also note that ξ_i is a constant vector for each periodicity cell Y_i. Therefore we have that

$$\int\limits_{\Gamma_i} g(y)\, ds_y = \int\limits_{\Gamma} h(y')\, ds_{y'} \tag{5.37}$$

where

$$g(y) = g(y(y')) = g(y' - \xi_i) = h(y') \tag{5.38}$$

Let us consider the asymptotic expansion of the function c_ε^e:

$$c_\varepsilon^e(x) = c_0^e(x) + \varepsilon c_1^e\left(x, \frac{x}{\varepsilon}\right) + \varepsilon^2 c_2^e\left(x, \frac{x}{\varepsilon}\right) =$$

$$= c_0^e(\varepsilon y) + \varepsilon c_1^e\left(\varepsilon y, y\right) + \varepsilon^2 c_2^e\left(\varepsilon y, y\right) =$$

$$= C_0^e(y) + \varepsilon C_1^e(y) + \varepsilon^2 C_2^e(y) = C_\varepsilon^e(y) \tag{5.39}$$

where we denoted

$$C_0^e(y) = c_0^e(\varepsilon y) \tag{5.40}$$
$$C_1^e(y) = c_1^e(\varepsilon y, y) \tag{5.41}$$
$$C_2^e(y) = c_2^e(\varepsilon y, y) \tag{5.42}$$

By analogy, we obtain similar expressions as (5.39) for the functions ϕ_ε^e and ϕ_ε^s.
After the change of variables $y' = y + \xi_i$ which is equivalent to $y = y' - \xi_i$, we denote

$$\hat{C}_0^e(y') = C_0^e(y) \tag{5.43}$$
$$\hat{C}_1^e(y') = C_1^e(y) \tag{5.44}$$
$$\hat{C}_2^s(y') = C_2^s(y) \tag{5.45}$$

and we obtain

$$c_\varepsilon^e(x) = \underbrace{C_\varepsilon^e(y) = C_0^e(y) + \varepsilon C_1^e(y) + \varepsilon^2 C_2^e(y)} = \underbrace{\hat{C}_0^e(y') + \varepsilon \hat{C}_1^e(y') + \varepsilon^2 \hat{C}_2^e(y') = \hat{C}_\varepsilon^e(y')} \tag{5.46}$$

or equivalently

$$c_\varepsilon^e(x) = C_\varepsilon^e(y) = \hat{C}_\varepsilon^e(y') \tag{5.47}$$

By analogy, for the functions $\phi_\varepsilon^e(x)$ and $\phi_\varepsilon^s(x)$ we obtain

$$\phi_\varepsilon^e(x) = \Phi_\varepsilon^e(y) = \hat{\Phi}_\varepsilon^e(y') \tag{5.48}$$
$$\phi_\varepsilon^s(x) = \Phi_\varepsilon^s(y) = \hat{\Phi}_\varepsilon^s(y') \tag{5.49}$$

For the concentration c^s of ions in the particles we have

$$c^s(x) = C^s(y) = \hat{C}^s(y') \tag{5.50}$$

For the current density we use the following notation:

$$\mathcal{N}_\varepsilon = \mathcal{N}\left(c_\varepsilon^e(x), c^s(x), \phi_\varepsilon^e(x), \phi_\varepsilon^s(x)\right) = f_\varepsilon(x) \tag{5.51}$$
$$\tag{5.52}$$

Therefore after the subsequent changes of variables $x = \varepsilon y$ and $y' = y + \xi_i$ we obtain

$$\begin{aligned} \mathcal{N}_\varepsilon &= \mathcal{N}\left(c_\varepsilon^e(x), c^s(x), \phi_\varepsilon^e(x), \phi_\varepsilon^s(x)\right) = f_\varepsilon(x) = \\ &= \underbrace{\mathcal{N}\left(C_\varepsilon^e(y), C^s(y), \Phi_\varepsilon^e(y), \Phi_\varepsilon^s(y)\right) = g_\varepsilon(y)} \\ &= \underbrace{\mathcal{N}\left(\hat{C}_\varepsilon^e(y'), \hat{C}^s(y'), \hat{\Phi}_\varepsilon^e(y'), \hat{\Phi}_\varepsilon^s(y')\right) = h_\varepsilon(y')} \end{aligned} \tag{5.53}$$

where we denoted

$$\begin{aligned} g_\varepsilon(y) &= \mathcal{N}\left(C_\varepsilon^e(y), C^s(y), \Phi_\varepsilon^e(y), \Phi_\varepsilon^s(y)\right) \\ h_\varepsilon(y') &= \mathcal{N}\left(\hat{C}_\varepsilon^e(y'), \hat{C}^s(y'), \hat{\Phi}_\varepsilon^e(y'), \hat{\Phi}_\varepsilon^s(y')\right) \end{aligned} \tag{5.54}$$

We denote with $\varepsilon\Gamma_i$ the interface boundary for each periodicity cell εY_i and with $\varepsilon\Gamma = \sum_{i=1}^{M} \varepsilon\Gamma_i$ the whole interface boundary in the electrode (if we follow the already

introduced notation for the interface boundary, namely $\gamma = \gamma_a \cup \gamma_c$, and taking into account the dependence on ε, we should use here γ_a^ε and γ_c^ε, but we use instead the $\varepsilon\Gamma$ notation for simplicity). The number of all the microscopic periodicity cells in the electrode (which is a cube with length of the side L, or a parallelepiped with a charcteristic length of the sides L, then the total number of periodicity cells is of order $\frac{1}{\varepsilon^3} = \left(\frac{L}{l}\right)^3$) is $M \sim \left(\frac{L}{l}\right)^3 = \frac{1}{\varepsilon^3}$. This means that $M \sim O\left(\frac{1}{\varepsilon^3}\right)$.
We showed that the total flux I across the whole interface boundary must be preserved, i.e. must be the same, no matter how many active particles we have in the electrode (provided that we impose the same Neumann and Dirichlet boundary conditions on the outer cathode and anode boundaries). This is due to the fact that all the outer boundaries of the battery cell are insulated except for the cathode and anode boundaries ω_1 and ω_2 where we apply constant potential and constant current respectively. Therefore the total flux across the interface must be the same constant if we have one, two, or thousands of particles, i.e the total flux must not depend on ε.
Then for the total flux across the whole interface boundary $\varepsilon\Gamma$ in the case of multiple active particles, we obtain

$$\begin{aligned}
I &= \int\limits_{\varepsilon\Gamma} -\left((k_{11})_\varepsilon \nabla c_\varepsilon^e + (k_{12})_\varepsilon \nabla \phi_\varepsilon^e\right) \cdot \mathbf{n_s}\, ds_x = \int\limits_{\varepsilon\Gamma} \mathcal{N}_\varepsilon\, ds_x = \\
&= \sum_{i=1}^{M} \int\limits_{\varepsilon\Gamma_i} \mathcal{N}_\varepsilon\, ds_x = \sum_{i=1}^{M} \int\limits_{\varepsilon\Gamma_i} \mathcal{N}\left(c_\varepsilon^e(x), c^s(x), \phi_\varepsilon^e(x), \phi_\varepsilon^s(x)\right)\, ds_x = \\
&= \sum_{i=1}^{M} \int\limits_{\varepsilon\Gamma_i} f_\varepsilon(x)\, ds_x = \sum_{i=1}^{M} \varepsilon^2 \int\limits_{\Gamma_i} g_\varepsilon(y)\, ds_y = \\
&= \sum_{i=1}^{M} \varepsilon^2 \left(\int\limits_{\Gamma_i} g_\varepsilon(y)\, ds_y\right) = \sum_{i=1}^{M} \varepsilon^2 \left(\int\limits_{\Gamma} h_\varepsilon(y')\, ds_{y'}\right) = \\
&= \sum_{i=1}^{M} \left(\varepsilon^2 \int\limits_{\Gamma} h_\varepsilon(y')\, ds_{y'}\right) = \frac{1}{\varepsilon^3} \left(\varepsilon^2 \int\limits_{\Gamma} h_\varepsilon(y')\, ds_{y'}\right) = \\
&= \varepsilon^{-1} \int\limits_{\Gamma} h_\varepsilon(y')\, ds_{y'}
\end{aligned} \tag{5.55}$$

From the latter it follows that the total flux I does not depend on ε if and only if

$$h_\varepsilon(y') = O(\varepsilon) \tag{5.56}$$

But we have that

$$\mathcal{N}_\varepsilon = \mathcal{N}\left(c_\varepsilon^e(x), c^s(x), \phi_\varepsilon^e(x), \phi_\varepsilon^s(x)\right) = f_\varepsilon(x) = g_\varepsilon(y) = h_\varepsilon(y')$$

and consequently

$$\mathcal{N}_\varepsilon = O(\varepsilon) \tag{5.57}$$

From (5.19) it follows that

$$\mathcal{N}_0 = O(\varepsilon) \tag{5.58}$$

(we have $\mathcal{N}_\varepsilon = \mathcal{N}\left(c_0^e, c^s, \phi_0^e, \phi_0^s\right) + O(\varepsilon^\alpha) = O(\varepsilon)(1 + O(\varepsilon^{\alpha-1})) = O(\varepsilon)$) Thus we obtained that the current densities $\mathcal{N}_\varepsilon$ and $\mathcal{J}_\varepsilon$ must be of order ε. On the other hand, from physical considerations and from the numerical results from the full microscopic simulations [11] we also show experimentally that $\mathcal{N}_\varepsilon$ and $\mathcal{J}_\varepsilon$ are of order ε implicitly, i.e. the current density decreases with rate ε when we increase the number of particles.

Finally, for the interface conditions in each electrode we obtain:

$$-\left((k_{11})_\varepsilon \nabla c_\varepsilon^e + (k_{12})_\varepsilon \nabla \phi_\varepsilon^e\right) \cdot \mathbf{n_s} = \mathcal{N}_\varepsilon, \quad x \in \varepsilon\Gamma \tag{5.59}$$

$$-\left((k_{21})_\varepsilon \nabla c_\varepsilon^e + (k_{22})_\varepsilon \nabla \phi_\varepsilon^e\right) \cdot \mathbf{n_s} = \mathcal{J}_\varepsilon, \quad x \in \varepsilon\Gamma \tag{5.60}$$

$$-\left(D^s \nabla c^s\right) \cdot \mathbf{n_s} = \mathcal{N}_0, \quad x \in \Gamma \tag{5.61}$$

$$-\left(\kappa_\varepsilon \nabla \phi_\varepsilon^s\right) \cdot \mathbf{n_s} = \mathcal{J}_\varepsilon, \quad x \in \varepsilon\Gamma \tag{5.62}$$

Thus for the homogenization of the interface conditions we obtain

$$\begin{aligned}
\mathcal{N}_\varepsilon =& \mathbf{N}_\varepsilon^{\mathbf{e}} \cdot \mathbf{n_s} = -\left\{k_{11}\left(y, c_\varepsilon^e\right) \nabla c_\varepsilon^e + k_{12}(y) \nabla \phi_\varepsilon^e\right\} \cdot \mathbf{n_s} = \\
=& -\left\{k_{11}\left(y, c_0^e\right)\left(\nabla_x + \frac{1}{\varepsilon}\nabla_y\right)\left(c_0^e + \varepsilon c_1^e + \varepsilon^2 c_2^e\right) + \right. \\
& \left. + k_{12}(y)\left(\nabla_x + \frac{1}{\varepsilon}\nabla_y\right)\left(\phi_0^e + \varepsilon\phi_1^e + \varepsilon^2\phi_2^e\right)\right\} \cdot \mathbf{n_s} = \\
=& -\left\{\frac{1}{\varepsilon}\left[k_{11}\left(y, c_0^e\right) \nabla_y c_0^e + k_{12}(y) \nabla_y \phi_0^e\right] + \right. \\
& + \varepsilon^0\left[k_{11}\left(y, c_0^e\right)\left(\nabla_x c_0^e + \nabla_y c_1^e\right) + k_{12}(y)\left(\nabla_x \phi_0^e + \nabla_y \phi_1^e\right)\right] + \\
& + \varepsilon\left[k_{11}\left(y, c_0^e\right)\left(\nabla_x c_1^e + \nabla_y c_2^e\right) + k_{12}(y)\left(\nabla_x \phi_1^e + \nabla_y \phi_2^e\right)\right] + \\
& \left. + \varepsilon^2[\ldots]\right]\right\} \cdot \mathbf{n_s}
\end{aligned} \tag{5.63}$$

which is equivalent to

$$\begin{aligned}
\frac{1}{\varepsilon}\mathcal{N}_\varepsilon = -\Bigg[& \frac{1}{\varepsilon^2}\left(k_{11}\left(y, c_0^e\right) \nabla_y c_0^e + k_{12}(y) \nabla_y \phi_0^e\right) + \\
& + \frac{1}{\varepsilon}\left(k_{11}\left(y, c_0^e\right)\left(\nabla_x c_0^e + \nabla_y c_1^e\right) + k_{12}(y)\left(\nabla_x \phi_0^e + \nabla_y \phi_1^e\right)\right) + \\
& + \varepsilon^0\left(k_{11}\left(y, c_0^e\right)\left(\nabla_x c_1^e + \nabla_y c_2^e\right) + k_{12}(y)\left(\nabla_x \phi_1^e + \nabla_y \phi_2^e\right)\right) + \\
& + \varepsilon(\ldots)\Bigg] \cdot \mathbf{n_s}
\end{aligned} \tag{5.64}$$

Now taking into account that $\mathcal{N}_\varepsilon = O(\varepsilon) = \mathcal{N}\left(c_0^e, c^s, \phi_0^e, \phi_0^s\right) + O(\varepsilon^2)$, and consequently $\mathcal{N}\left(c_0^e, c^s, \phi_0^e, \phi_0^s\right) = O(\varepsilon)$, it follows that $\frac{1}{\varepsilon}\mathcal{N}_0 = O(1)$. Then, by grouping equal powers of

ε, we obtain

$$\varepsilon^{-2}: \quad 0 = \left[k_{11}\left(y, c_0^e\right) \underbrace{\nabla_y c_0^e}_{=0} + k_{12}(y) \underbrace{\nabla_y \phi_0^e}_{=0} \right] \cdot \mathbf{n_s} \Longleftrightarrow 0 = 0$$

$$\varepsilon^{-1}: \quad 0 = \left[k_{11}\left(y, c_0^e\right) \left(\nabla_x c_0^e + \nabla_y c_1^e\right) + k_{12}(y) \left(\nabla_x \phi_0^e + \nabla_y \phi_1^e\right) \right] \cdot \mathbf{n_s}$$

$$\begin{aligned} &\varepsilon^{0}: \quad \frac{1}{\varepsilon} \mathcal{N}\left(c_0^e, c^s, \phi_0^e, \phi_0^s\right) = \\ &= -\left[k_{11}\left(y, c_0^e\right) \nabla_x c_1^e + k_{11}\left(y, c_0^e\right) \nabla_y c_2^e + k_{12}(y) \nabla_x \phi_1^e + k_{12}(y) \nabla_y \phi_2^e \right] \cdot \mathbf{n_s} \end{aligned} \tag{5.65}$$

where we account for the fact that the functions c_0^e and ϕ_0^e depend only on x and do not depend on y. By analogy, from $\mathbf{J}_\varepsilon^{\mathbf{e}} \cdot \mathbf{n_s} = \mathcal{J}_\varepsilon$ we obtain:

$$\varepsilon^{-2}: \quad 0 = \left[k_{21}\left(y, c_0^e\right) \underbrace{\nabla_y c_0^e}_{=0} + k_{22}(y) \underbrace{\nabla_y \phi_0^e}_{=0} \right] \cdot \mathbf{n_s} \Longleftrightarrow 0 = 0$$

$$\varepsilon^{-1}: \quad 0 = \left[k_{21}\left(y, c_0^e\right) \left(\nabla_x c_0^e + \nabla_y c_1^e\right) + k_{22}(y) \left(\nabla_x \phi_0^e + \nabla_y \phi_1^e\right) \right] \cdot \mathbf{n_s}$$

$$\begin{aligned} &\varepsilon^{0}: \quad \frac{1}{\varepsilon} \mathcal{J}\left(c_0^e, c^s, \phi_0^e, \phi_0^s\right) = \\ &= -\left[k_{21}\left(y, c_0^e\right) \nabla_x c_1^e + k_{21}\left(y, c_0^e\right) \nabla_y c_2^e + k_{22}(y) \nabla_x \phi_1^e + k_{22}(y) \nabla_y \phi_2^e \right] \cdot \mathbf{n_s} \end{aligned} \tag{5.66}$$

5.5 Homogenization of the Electrolyte Phase PDEs

For the time derivative $\dfrac{\partial\left(\chi_\varepsilon^e(x) c_\varepsilon^e\right)}{\partial t}$ we take the zero order approximation $\dfrac{\partial\left(\chi_\varepsilon^e(x) c_0\right)}{\partial t}$, i.e. $\dfrac{\partial\left(\chi_\varepsilon^e(x) c_\varepsilon^e\right)}{\partial t} = \dfrac{\partial\left(\chi^e(y) \partial c_0\right)}{\partial t} + O(\varepsilon)$. We have that $y \in Y = E \cup S$ and $x \in \Omega$.

Therefore for equation (5.5a) we obtain:

$$\frac{\partial\left(\chi^e(y)c_0\right)}{\partial t} = \nabla\cdot\left(\left(k_{11}\right)_\varepsilon\left(x,c_\varepsilon^e\right)\nabla c_\varepsilon^e + \left(k_{12}\right)_\varepsilon(x)\nabla\phi_\varepsilon^e\right) =$$

$$= \left(\nabla_x + \frac{1}{\varepsilon}\nabla_y\right)\cdot\left[k_{11}(y,c_0^e)\left(\nabla_x + \frac{1}{\varepsilon}\nabla_y\right)\left(c_0^e(x,t) + \varepsilon c_1^e(x,y,t) + \varepsilon^2 c_2^e(x,y,t)\right) +\right.$$

$$\left. + k_{12}(y)\left(\nabla_x + \frac{1}{\varepsilon}\nabla_y\right)\left(\phi_0^e(x,t) + \varepsilon\phi_1^e(x,y,t) + \varepsilon^2\phi_2^e(x,y,t)\right)\right] =$$

$$= \left(\nabla_x + \frac{1}{\varepsilon}\nabla_y\right)\cdot\left[k_{11}(y,c_0^e)\nabla_x c_0^e + \varepsilon k_{11}(y,c_0^e)\nabla_x c_1^e + \varepsilon^2 k_{11}(y,c_0^e)\nabla_x c_2^e + \frac{1}{\varepsilon}k_{11}(y,c_0^e)\nabla_y c_0^e +\right.$$

$$+ k_{11}(y,c_0^e)\nabla_y c_1^e + \varepsilon k_{11}(y,c_0^e)\nabla_y c_2^e + k_{12}(y)\nabla_x\phi_0^e + \varepsilon k_{12}(y)\nabla_x\phi_1^e + \varepsilon^2 k_{12}(y)\nabla_x\phi_2^e +$$

$$\left. + \frac{1}{\varepsilon}k_{12}(y)\nabla_y\phi_0^e + k_{12}(y)\nabla_y\phi_1^e + \varepsilon k_{12}(y)\nabla_y\phi_2^e\right] =$$

$$= \left(\nabla_x + \frac{1}{\varepsilon}\nabla_y\right)\cdot\left\{k_{11}(y,c_0^e)\left(\nabla_x c_0^e + \nabla_y c_1^e\right) + k_{12}(y)\left(\nabla_x\phi_0^e + \nabla_y\phi_1^e\right) +\right.$$

$$+ \varepsilon\left[k_{11}(y,c_0^e)\left(\nabla_x c_1^e + \nabla_y c_2^e\right) + k_{12}(y)\left(\nabla_x\phi_1^e + \nabla_y\phi_2^e\right)\right] +$$

$$\left. + \varepsilon^2\left(k_{11}(y,c_0^e)\nabla_x c_2^e + k_{12}(y)\nabla_x\phi_2^e\right) + \frac{1}{\varepsilon}\left(k_{11}(y,c_0^e)\nabla_y c_0^e + k_{12}(y)\nabla_y\phi_0^e\right)\right\} =$$

$$= \frac{1}{\varepsilon^2}\nabla_y\cdot\left\{k_{11}(y,c_0^e)\nabla_y c_0^e + k_{12}(y)\nabla_y\phi_0^e\right\} +$$

$$+ \frac{1}{\varepsilon}\left\{\nabla_x\cdot\left(k_{11}(y,c_0^e)\nabla_y c_0^e + k_{12}(y)\nabla_y\phi_0^e\right) +\right.$$

$$+ \quad \left.\nabla_y\cdot\left(k_{11}(y,c_0^e)\nabla_x c_0^e + k_{11}(y,c_0^e)\nabla_y c_1^e + k_{12}(y)\nabla_x\phi_0^e + k_{12}(y)\nabla_y\phi_1^e\right)\right\} +$$

$$+ \varepsilon^0\left\{\nabla_x\cdot\left[k_{11}(y,c_0^e)\nabla_x c_0^e + k_{11}(y,c_0^e)\nabla_y c_1^e + k_{12}(y)\nabla_x\phi_0^e + k_{12}(y)\nabla_y\phi_1^e\right] +\right.$$

$$+ \quad \left.\nabla_y\cdot\left[k_{11}(y,c_0^e)\nabla_x c_1^e + k_{11}(y,c_0^e)\nabla_y c_2^e + k_{12}(y)\nabla_x\phi_1^e + k_{12}(y)\nabla_y\phi_2^e\right]\right\} +$$

$$+ \varepsilon\left\{\nabla_x\cdot\left(k_{11}(y,c_0^e)\nabla_x c_1^e + k_{11}(y,c_0^e)\nabla_y c_2^e + k_{12}(y)\nabla_x\phi_1^e + k_{12}(y)\nabla_y\phi_2^e\right) +\right.$$

$$+ \quad \left.\nabla_y\cdot\left(k_{11}(y,c_0^e)\nabla_x c_2^e + k_{12}(y)\nabla_x\phi_2^e\right)\right\} +$$

$$+ \varepsilon^2\nabla_x\cdot\left\{k_{11}(y,c_0^e)\nabla_x c_2^e + k_{12}(y)\nabla_x\phi_2^e\right\} \tag{5.67}$$

Therefore from the equal powers of ε we obtain:

$$\varepsilon^{-2}: \quad \nabla_y \cdot \left(k_{11}(y, c_0^e) \underbrace{\nabla_y c_0^e}_{=0} + k_{12}(y) \underbrace{\nabla_y \phi_0^e}_{=0} \right) = 0 \Longleftrightarrow 0 = 0 \tag{5.68}$$

$$\varepsilon^{-1}: \quad \nabla_x \cdot \left(k_{11}(y, c_0^e) \underbrace{\nabla_y c_0^e}_{=0} + k_{12}(y) \underbrace{\nabla_y \phi_0^e}_{=0} \right) +$$

$$+ \nabla_y \cdot (k_{11}(y, c_0^e) \nabla_x c_0^e + k_{11}(y, c_0^e) \nabla_y c_1^e + k_{12}(y) \nabla_x \phi_0^e + k_{12}(y) \nabla_y \phi_1^e) = 0 \tag{5.69}$$

$$\varepsilon^{0}: \quad \chi^e(y) \frac{\partial c_0^e}{\partial t} = \nabla_x \cdot [k_{11}(y, c_0^e) \nabla_x c_0^e + k_{11}(y, c_0^e) \nabla_y c_1^e + k_{12}(y) \nabla_x \phi_0^e + k_{12}(y) \nabla_y \phi_1^e] +$$

$$+ \nabla_y \cdot [k_{11}(y, c_0^e) \nabla_x c_1^e + k_{11}(y, c_0^e) \nabla_y c_2^e + k_{12}(y) \nabla_x \phi_1^e + k_{12}(y) \nabla_y \phi_2^e] \tag{5.70}$$

We have analogous result for the second partial differential equation from the electrolyte system of equations:

$$\varepsilon^{-2}: \quad \nabla_y \cdot \left(k_{21}(y, c_0^e) \underbrace{\nabla_y c_0^e}_{=0} + k_{22}(y) \underbrace{\nabla_y \phi_0^e}_{=0} \right) = 0 \Longleftrightarrow 0 = 0 \tag{5.71}$$

$$\varepsilon^{-1}: \quad \nabla_x \cdot \left(k_{21}(y, c_0^e) \underbrace{\nabla_y c_0^e}_{=0} + k_{22}(y) \underbrace{\nabla_y \phi_0^e}_{=0} \right) +$$

$$+ \nabla_y \cdot (k_{21}(y, c_0^e) \nabla_x c_0^e + k_{21}(y, c_0^e) \nabla_y c_1^e + k_{22}(y) \nabla_x \phi_0^e + k_{22}(y) \nabla_y \phi_1^e) = 0 \tag{5.72}$$

$$\varepsilon^{0}: \quad 0 = \nabla_x \cdot [k_{21}(y, c_0^e) \nabla_x c_0^e + k_{21}(y, c_0^e) \nabla_y c_1^e + k_{22}(y) \nabla_x \phi_0^e + k_{22}(y) \nabla_y \phi_1^e] +$$

$$+ \nabla_y \cdot [k_{21}(y, c_0^e) \nabla_x c_1^e + k_{21}(y, c_0^e) \nabla_y c_2^e + k_{22}(y) \nabla_x \phi_1^e + k_{22}(y) \nabla_y \phi_2^e] \tag{5.73}$$

5.5.1 Order ε^{-1}: Derivation of the Auxiliary Cell Problems

We have the following system of equations for $y \in Y$ and $x \in \Omega$

$$\nabla_y \cdot (k_{11}(y, c_0^e) \nabla_x c_0^e + k_{11}(y, c_0^e) \nabla_y c_1^e + k_{12}(y) \nabla_x \phi_0^e + k_{12}(y) \nabla_y \phi_1^e) = 0 \tag{5.74a}$$

$$\nabla_y \cdot (k_{21}(y, c_0^e) \nabla_x c_0^e + k_{21}(y, c_0^e) \nabla_y c_1^e + k_{22}(y) \nabla_x \phi_0^e + k_{22}(y) \nabla_y \phi_1^e) = 0 \tag{5.74b}$$

which is equivalent to

$$\nabla_y \cdot (k_{11}(y, c_0^e) \nabla_y c_1^e + k_{12}(y) \nabla_y \phi_1^e) = -\nabla_y \cdot (k_{11}(y, c_0^e) \nabla_x c_0^e + k_{12}(y) \nabla_x \phi_0^e) \tag{5.75a}$$

$$\nabla_y \cdot (k_{21}(y, c_0^e) \nabla_y c_1^e + k_{22}(y) \nabla_y \phi_1^e) = -\nabla_y \cdot (k_{21}(y, c_0^e) \nabla_x c_0^e + k_{22}(y) \nabla_x \phi_0^e) \tag{5.75b}$$

with the following interface conditions:

$$(k_{11}(y, c_0^e)\nabla_y c_1^e + k_{12}(y)\nabla_y \phi_1^e) \cdot \mathbf{n}_s = -\left(k_{11}(y, c_0^e)\nabla_x c_0^e + k_{12}(y)\nabla_x \phi_0^e\right) \cdot \mathbf{n}_s \tag{5.76a}$$

$$(k_{21}(y, c_0^e)\nabla_y c_1^e + k_{22}(y)\nabla_y \phi_1^e) \cdot \mathbf{n}_s = -\left(k_{21}(y, c_0^e)\nabla_x c_0^e + k_{22}(y)\nabla_x \phi_0^e\right) \cdot \mathbf{n}_s \tag{5.76b}$$

We introduce the following notation for system (5.75) of PDEs:

$$\nabla_y \cdot (K(y,x)\nabla_y U_1) = -\nabla_y \cdot (K(y,x)\nabla_x U_0) \tag{5.77}$$

where we denote

$$K = \begin{pmatrix} k_{11} & k_{12} \\ k_{21} & k_{22} \end{pmatrix}, \quad U_1 = \begin{pmatrix} c_1^e(x,y) \\ \\ \phi_1^e(x,y) \end{pmatrix}, \quad U_0 = \begin{pmatrix} c_0^e(x) \\ \\ \phi_0^e(x) \end{pmatrix},$$

$$\nabla_y U_1 = \begin{pmatrix} \nabla_y c_1^e \\ \\ \nabla_y \phi_1^e \end{pmatrix}, \quad \nabla_x U_0 = \begin{pmatrix} \nabla_x c_0^e \\ \\ \nabla_x \phi_0^e \end{pmatrix}$$

- **Some Notations**
  - Divergence of a vector whose elements are vectors

$$\nabla_y \cdot \begin{pmatrix} v_1(y) \\ v_2(y) \end{pmatrix} = \begin{pmatrix} \nabla_y \cdot v_1 \\ \nabla_y \cdot v_2 \end{pmatrix}$$

  - Scalar product of matrix and vector

$$A \cdot \mathbf{v} = \begin{pmatrix} a_{11} & \dots & a_{1n} \\ \dots & \dots & \dots \\ a_{n1} & \dots & a_{nn} \end{pmatrix} \cdot \mathbf{v} = \begin{pmatrix} (a_{11}, \dots, a_{1n}) \cdot \mathbf{v} \\ \dots \\ (a_{n1}, \dots, a_{nn}) \cdot \mathbf{v} \end{pmatrix}$$

  - Divergence of a matrix

$$\nabla_y \cdot A = \nabla_y \cdot \begin{pmatrix} a_{11} & \dots & a_{1n} \\ \dots & \dots & \dots \\ a_{n1} & \dots & a_{nn} \end{pmatrix} = \begin{pmatrix} \nabla_y \cdot (a_{11}, \dots, a_{1n}) \\ \dots \\ \nabla_y \cdot (a_{n1}, \dots, a_{nn}) \end{pmatrix}$$

Let $w(y)$ be a matrix 2×3 whose elements are functions of y, i.e.

$$w(y) = \begin{pmatrix} w_1(y) \\ w_2(y) \end{pmatrix} = \begin{pmatrix} w_{11}(y) & w_{12}(y) & w_{13}(y) \\ \\ w_{21}(y) & w_{22}(y) & w_{23}(y) \end{pmatrix}$$

where

$$w_1(y) = (w_{11}(y), w_{12}(y), w_{13}(y))$$
$$w_2(y) = (w_{21}(y), w_{22}(y), w_{23}(y))$$

Then we define the scalar product

$$\nabla_x U_0 \cdot w(y) = \begin{pmatrix} \nabla_x c_0^e \\ \\ \nabla_x \phi_0^e \end{pmatrix} \cdot \begin{pmatrix} w_1(y) \\ \\ w_2(y) \end{pmatrix} = \begin{pmatrix} \nabla_x c_0^e \cdot w_1 \\ \\ \nabla_x \phi_0^e \cdot w_2 \end{pmatrix}$$

Now by analogy with the scalar case, from the equation $\nabla_y \cdot (K\nabla_y U_1) = -\nabla_y \cdot (K\nabla_x U_0)$ we look for the solution $U_1(x, y)$ of this equation in the following form

$$U_1(x, y) = \nabla_x U_0 \cdot w(y) \tag{5.78}$$

Now by definition we have that

$$\nabla_y U_1 = \begin{pmatrix} \nabla_y \left(\nabla_x c_0^e \cdot w_1\right) \\ \\ \nabla_y \left(\nabla_x \phi_0^e \cdot w_2\right) \end{pmatrix} = \begin{pmatrix} \sum\limits_{i=1}^{3} \dfrac{\partial c_0^e}{\partial x_i} \nabla_y w_{1i} \\ \\ \sum\limits_{i=1}^{3} \dfrac{\partial \phi_0^e}{\partial x_i} \nabla_y w_{2i} \end{pmatrix}$$

We denote

$$a_i = \frac{\partial c_0^e}{\partial x_i} \nabla_y w_{1i}$$

$$b_i = \frac{\partial \phi_0^e}{\partial x_i} \nabla_y w_{2i}$$

Therefore

$$\nabla_y U_1 = \begin{pmatrix} \sum\limits_{i=1}^{3} a_i \\ \sum\limits_{i=1}^{3} b_i \end{pmatrix}$$

Then we have that

$$K\nabla_y U_1 = K \begin{pmatrix} \sum\limits_{i=1}^{3} a_i \\ \sum\limits_{i=1}^{3} b_i \end{pmatrix} = \sum_{i=1}^{3} K \begin{pmatrix} a_i \\ b_i \end{pmatrix} = \sum_{i=1}^{3} \begin{pmatrix} k_{11} & k_{12} \\ k_{21} & k_{22} \end{pmatrix} \begin{pmatrix} a_i \\ b_i \end{pmatrix} =$$

$$= \sum_{i=1}^{3} \begin{pmatrix} k_{11} a_i + k_{12} b_i \\ k_{21} a_i + k_{22} b_i \end{pmatrix} = \sum_{i=1}^{3} K V_i$$

where

$$V_i = \begin{pmatrix} a_i \\ b_i \end{pmatrix}$$

Now, after we substitute $U_1(x, y)$ with $\nabla_x U_0 \cdot w(y)$ in the equation $\nabla_y \cdot (K(y, x)\nabla_y U_1) = -\nabla_y \cdot (K(y, x)\nabla_x U_0)$ we obtain the following equality which must be satisfied for each $x \in \Omega$:

$$\sum_{i=1}^{3} \nabla_y \cdot (K(y, x) V_i) = -\nabla_y \cdot (K(y, x)\nabla_x U_0)$$

Since

$$k_{11}(y,c_0) = \chi^e(y)k^e_{11}(c^e_0), \quad k_{12}(y) = \chi^e(y)k^e_{12}$$
$$k_{21}(y,c_0) = \chi^e(y)k^e_{21}(c^e_0), \quad k_{22}(y) = \chi^e(y)k^e_{22}$$

we have that $K(y,x) = \chi^e(y)K^e(x)$, and for $y \in S$ we have that $\chi^e(y) = 0$, and $\chi^e(y) = 1$ for $y \in E$. Hence for $y \in E$ we have that $K(y,x) = K^e(x)$ and consequently $-\nabla_y \cdot (K^e(x)\nabla_x U_0(x)) = 0$. Therefore the equality

$$\sum_{i=1}^{3} \nabla_y \cdot (K(y,x)V_i) = -\nabla_y \cdot (K(y,x)\nabla_x U_0)$$

which must be true for each $x \in \Omega$, for $y \in E$ is equivalent to

$$\sum_{i=1}^{3} \nabla_y \cdot (K^e(x)V_i) = -\nabla_y \cdot (K^e(x)\nabla_x U_0), \quad y \in E$$

is equivalent to

$$\sum_{i=1}^{3} \nabla_y \cdot (K^e(x)V_i) = 0, \quad y \in E$$

$$V_i = \begin{pmatrix} a_i \\ b_i \end{pmatrix} = \begin{pmatrix} \dfrac{\partial c^e_0}{\partial x_i}\nabla_y w_{1i} \\ \\ \dfrac{\partial \phi^e_0}{\partial x_i}\nabla_y w_{2i} \end{pmatrix} =$$

$$= \underbrace{\begin{pmatrix} \dfrac{\partial c^e_0}{\partial x_i}(x) & 0 \\ \\ 0 & \dfrac{\partial \phi^e_0}{\partial x_i}(x) \end{pmatrix}}_{=C_i} \begin{pmatrix} \nabla_y w_{1i} \\ \\ \nabla_y w_{2i} \end{pmatrix} = C_i \begin{pmatrix} \nabla_y w_{1i} \\ \\ \nabla_y w_{2i} \end{pmatrix}$$

From here it follows that for the equality $\sum_{i=1}^{3} \nabla_y \cdot (K^e(x)V_i) = 0, \quad y \in E$ we obtain:

$$\sum_{i=1}^{3} \nabla_y \cdot \left(K^e(x)C_i(x) \begin{pmatrix} \nabla_y w_{1i} \\ \\ \nabla_y w_{2i} \end{pmatrix} \right) = 0, \quad y \in E$$

We denote

$$A(x) = (a_{ij})^2_{i,j=1} = K^e(x)C_i(x)$$

Then

$$A(x) \begin{pmatrix} \nabla_y w_{1i} \\ \nabla_y w_{2i} \end{pmatrix} = \begin{pmatrix} a_{11}\nabla_y w_{1i} + a_{12}\nabla_y w_{2i} \\ a_{21}\nabla_y w_{1i} + a_{22}\nabla_y w_{2i} \end{pmatrix}$$

Therefore by definition we have that

$$\nabla_y \cdot \begin{pmatrix} a_{11}\nabla_y w_{1i} + a_{12}\nabla_y w_{2i} \\ a_{21}\nabla_y w_{1i} + a_{22}\nabla_y w_{2i} \end{pmatrix} = \begin{pmatrix} \nabla_y \cdot (a_{11}\nabla_y w_{1i} + a_{12}\nabla_y w_{2i}) \\ \nabla_y \cdot (a_{21}\nabla_y w_{1i} + a_{22}\nabla_y w_{2i}) \end{pmatrix}$$

Hence the equality

$$\sum_{i=1}^{3} \nabla_y \cdot \left(K^e(x) C_i(x) \begin{pmatrix} \nabla_y w_{1i} \\ \\ \nabla_y w_{2i} \end{pmatrix} \right) = \vec{0}, \quad y \in E$$

which is equivalent to

$$\sum_{i=1}^{3} \nabla_y \cdot \left(A(x) \begin{pmatrix} \nabla_y w_{1i} \\ \\ \nabla_y w_{2i} \end{pmatrix} \right) = \vec{0}, \quad y \in E$$

becomes

$$\sum_{i=1}^{3} \begin{pmatrix} \nabla_y \cdot (a_{11}\nabla_y w_{1i} + a_{12}\nabla_y w_{2i}) \\ \nabla_y \cdot (a_{21}\nabla_y w_{1i} + a_{22}\nabla_y w_{2i}) \end{pmatrix} = \vec{0}, \quad y \in E$$

By definiton, the latter is equivalent to

$$\left| \begin{array}{l} \displaystyle\sum_{i=1}^{3} \nabla_y \cdot (a_{11}(x)\nabla_y w_{1i} + a_{12}(x)\nabla_y w_{2i}) = 0, \quad y \in E \\ \displaystyle\sum_{i=1}^{3} \nabla_y \cdot (a_{21}(x)\nabla_y w_{1i} + a_{22}(x)\nabla_y w_{2i}) = 0, \quad y \in E \end{array} \right.$$

which is equivalent to

$$\left| \begin{array}{l} \displaystyle\sum_{i=1}^{3} \{a_{11}(x)\nabla_y \cdot (\nabla_y w_{1i}) + a_{12}(x)\nabla_y \cdot (\nabla_y w_{2i})\} = 0, \quad y \in E \\ \displaystyle\sum_{i=1}^{3} \{a_{21}(x)\nabla_y \cdot (\nabla_y w_{1i}) + a_{22}(x)\nabla_y \cdot (\nabla_y w_{2i})\} = 0, \quad y \in E \end{array} \right.$$

Since the latter equality must be satisfied for each $x \in \Omega$ it follows that each term must be equal to zero, i.e.

$$\left| \begin{array}{l} \nabla_y \cdot (\nabla_y w_{1i}) = 0, \quad y \in E \\ \nabla_y \cdot (\nabla_y w_{2i}) = 0, \quad y \in E \end{array} \right.$$

and from here (as well as from the interface conditions) it follows that $w_{1i}(y) \equiv w_{2i}(y)$ for each $i = 1, 2, 3$.

For the functions c_1^e and ϕ_1^e we have the following interface conditions:

$$\begin{aligned} (k_{11}\nabla_y c_1^e + k_{12}\nabla_y \phi_1^e) \cdot \mathbf{n_s} &= -(k_{11}\nabla_x c_0^e + k_{12}\nabla_x \phi_0^e) \cdot \mathbf{n_s}, \quad y \in \Gamma \\ (k_{21}\nabla_y c_1^e + k_{22}\nabla_y \phi_1^e) \cdot \mathbf{n_s} &= -(k_{21}\nabla_x c_0^e + k_{22}\nabla_x \phi_0^e) \cdot \mathbf{n_s}, \quad y \in \Gamma \end{aligned}$$

which according to our notation is equivalent to

$$(K\nabla_y U_1) \cdot \mathbf{n_s} = -(K\nabla_x U_0) \cdot \mathbf{n_s}$$

For $y \in E$ we have the following system of PDEs and corresponding interface conditions:

$$\sum_{i=1}^{3} \nabla_y \cdot (K^e V_i) = 0, \quad y \in E$$
$$\sum_{i=1}^{3} (K^e V_i) \cdot \mathbf{n_s} = -(K^e \nabla_x U_0) \cdot \mathbf{n_s}, \quad y \in \Gamma$$

where

$$V_i = C_i \begin{pmatrix} \nabla_y w_{1i} \\ \nabla_y w_{2i} \end{pmatrix}$$

$$K^e(x) C_i(x) = \begin{pmatrix} k_{11}^e & k_{12}^e \\ k_{21}^e & k_{22}^e \end{pmatrix} \begin{pmatrix} \frac{\partial c_0^e}{\partial x_i} & 0 \\ 0 & \frac{\partial \phi_0^e}{\partial x_i} \end{pmatrix} = \begin{pmatrix} k_{11}^e \frac{\partial c_0^e}{\partial x_i} & k_{12}^e \frac{\partial \phi_0^e}{\partial x_i} \\ k_{21}^e \frac{\partial c_0^e}{\partial x_i} & k_{22}^e \frac{\partial \phi_0^e}{\partial x_i} \end{pmatrix}$$

Therefore for the interface conditions we obtain

$$\sum_{i=1}^{3} \left[\begin{pmatrix} k_{11}^e \frac{\partial c_0^e}{\partial x_i} & k_{12}^e \frac{\partial \phi_0^e}{\partial x_i} \\ k_{21}^e \frac{\partial c_0^e}{\partial x_i} & k_{22}^e \frac{\partial \phi_0^e}{\partial x_i} \end{pmatrix} \begin{pmatrix} \nabla_y w_{1i} \\ \nabla_y w_{2i} \end{pmatrix} \right] \cdot \mathbf{n_s} = - \begin{pmatrix} k_{11}^e \nabla_x c_0^e + k_{12}^e \nabla_x \phi_0^e \\ k_{21}^e \nabla_x c_0^e + k_{22}^e \nabla_x \phi_0^e \end{pmatrix} \cdot \mathbf{n_s}$$

which is equivalent to

$$\sum_{i=1}^{3} \left[\begin{pmatrix} k_{11}^e \frac{\partial c_0^e}{\partial x_i} \nabla_y w_{1i} + k_{12}^e \frac{\partial \phi_0^e}{\partial x_i} \nabla_y w_{2i} \\ k_{21}^e \frac{\partial c_0^e}{\partial x_i} \nabla_y w_{1i} + k_{22}^e \frac{\partial \phi_0^e}{\partial x_i} \nabla_y w_{2i} \end{pmatrix} \right] \cdot \mathbf{n_s} = - \begin{pmatrix} k_{11}^e \nabla_x c_0^e + k_{12}^e \nabla_x \phi_0^e \\ k_{21}^e \nabla_x c_0^e + k_{22}^e \nabla_x \phi_0^e \end{pmatrix} \cdot \mathbf{n_s}$$

The latter is equivalent to (according to the previously defined operations)

$$\sum_{i=1}^{3} \left(k_{11}^e \frac{\partial c_0^e}{\partial x_i} \nabla_y w_{1i} + k_{12}^e \frac{\partial \phi_0^e}{\partial x_i} \nabla_y w_{2i} \right) \cdot \mathbf{n_s} = - \left(k_{11}^e \sum_{i=1}^{3} \frac{\partial c_0^e}{\partial x_i} \mathbf{e_i} + k_{12}^e \sum_{i=1}^{3} \frac{\partial \phi_0^e}{\partial x_i} \mathbf{e_i} \right) \cdot \mathbf{n_s}$$

$$\sum_{i=1}^{3} \left(k_{21}^e \frac{\partial c_0^e}{\partial x_i} \nabla_y w_{1i} + k_{22}^e \frac{\partial \phi_0^e}{\partial x_i} \nabla_y w_{2i} \right) \cdot \mathbf{n_s} = - \left(k_{21}^e \sum_{i=1}^{3} \frac{\partial c_0^e}{\partial x_i} \mathbf{e_i} + k_{22}^e \sum_{i=1}^{3} \frac{\partial \phi_0^e}{\partial x_i} \mathbf{e_i} \right) \cdot \mathbf{n_s}$$

which is equivalent to

$$\sum_{i=1}^{3} \left\{ k_{11}^e(x) \frac{\partial c_0^e}{\partial x_i}(x) (\nabla_y w_{1i} + \mathbf{e_i}) + k_{12}^e(x) \frac{\partial \phi_0^e}{\partial x_i}(x) (\nabla_y w_{2i} + \mathbf{e_i}) \right\} \cdot \mathbf{n_s} = 0$$

$$\sum_{i=1}^{3} \left\{ k_{21}^e(x) \frac{\partial c_0^e}{\partial x_i}(x) (\nabla_y w_{1i} + \mathbf{e_i}) + k_{22}^e(x) \frac{\partial \phi_0^e}{\partial x_i}(x) (\nabla_y w_{2i} + \mathbf{e_i}) \right\} \cdot \mathbf{n_s} = 0$$

Since the latter equalities must be satisfied for each $x \in \Omega$, it follows that

$$\left| \begin{array}{l} (\nabla_y w_{1i} + \mathbf{e_i}) \cdot \mathbf{n_s} = 0 \\ \\ (\nabla_y w_{2i} + \mathbf{e_i}) \cdot \mathbf{n_s} = 0 \end{array} \right.$$

which is equivalent to

$$\left| \begin{array}{l} \nabla_y w_{1i} \cdot \mathbf{n_s} = -\mathbf{e_i} \cdot \mathbf{n_s} \\ \\ \nabla_y w_{2i} \cdot \mathbf{n_s} = -\mathbf{e_i} \cdot \mathbf{n_s} \end{array} \right.$$

And since we obtained identical PDEs for w_{1i} and w_{2i}, for $i = 1, 2, 3$, we obtained that $w_{1i}(y) \equiv w_{2i}(y)$ and the interface conditions are:

$$\nabla_y w_{1i} \cdot \mathbf{n_s} = -\mathbf{e_i} \cdot \mathbf{n_s}, \quad y \in \Gamma \tag{5.79}$$

- After we obtained that $w_{1i}(y) \equiv w_{2i}(y)$ for $i = 1, 2, 3$, we introduce a new notation: we remove the first index "1" from the notation of the function w.
- Thus we obtain cell problems which turned out to depend only on the geometry of the domain but not on the nonlinear model coefficients k_{ij}^e.
- Therefore we do not have to solve the cell problems for each $x \in \Omega$, but only once for each time step and this will reduce significantly the computational time.
- **Auxiliary Cell Problems:** $i = 1, 2, 3$

$$\nabla_y \cdot (\nabla_y w_i) = 0, \quad y \in E \tag{5.80a}$$
$$\nabla_y w_i \cdot \mathbf{n_s} = -\mathbf{e_i} \cdot \mathbf{n_s}, \quad y \in \Gamma \tag{5.80b}$$

- Periodic boundary conditions on $\partial E \backslash \Gamma$, i.e. on the outer boundary of the electrolyte domain which is not part of the interface
- $\int_E w_i(y)\, dy = 0, \quad i = 1, 2, 3$ in order to fix the solution

Finally we obtain that

$$c_1^e(x, y, t) = \sum_{i=1}^{3} w_i(y, t) \frac{\partial c_0^e}{\partial x_i}(x, t) \tag{5.81}$$

$$\phi_1^e(x, y, t) = \sum_{i=1}^{3} w_i(y, t) \frac{\partial \phi_0^e}{\partial x_i}(x, t) \tag{5.82}$$

where $w_i(y, t)$ and $\psi_i(y, t)$ are Y-periodic functions in the y variable.

5.5.2 Order ε^0: Derivation of the Homogenized Equations

We have the following system of equations for $y \in Y$ and $x \in \Omega$

$$\chi^e(y)\frac{\partial}{\partial t}(c_0^e) = \nabla_x \cdot [k_{11}(y, c_0^e)\left(\nabla_x c_0^e + \nabla_y c_1^e\right) + k_{12}(y)\left(\nabla_x \phi_0^e + \nabla_y \phi_1^e\right)] + \\ + \nabla_y \cdot [k_{11}(y, c_0^e)\nabla_x c_1^e + k_{11}(y, c_0^e)\nabla_y c_2^e + k_{12}(y)\nabla_x \phi_1^e + k_{12}(y)\nabla_y \phi_2^e] \tag{5.83a}$$

$$\nabla_x \cdot [k_{21}(y, c_0^e)\left(\nabla_x c_0^e + \nabla_y c_1^e\right) + k_{22}(y)\left(\nabla_x \phi_0^e + \nabla_y \phi_1^e\right)] + \\ + \nabla_y \cdot [k_{21}(y, c_0^e)\nabla_x c_1^e + k_{21}(y, c_0^e)\nabla_y c_2^e + k_{22}(y)\nabla_x \phi_1^e + k_{22}(y)\nabla_y \phi_2^e] = 0 \tag{5.83b}$$

with periodic boundary conditions on ∂Y and with the following interface conditions on Γ:

$$-[k_{11}(y, c_0^e)\nabla_x c_1^e + k_{11}(y, c_0^e)\nabla_y c_2^e + k_{12}(y)\nabla_x \phi_1^e + k_{12}(y)\nabla_y \phi_2^e] \cdot \mathbf{n_s} = \frac{1}{\varepsilon}\mathcal{N}(c_0^e, c_0^s, \phi_0^e, \phi_0^s) \tag{5.84a}$$

$$-[k_{21}(y, c_0^e)\nabla_x c_1^e + k_{21}(y, c_0^e)\nabla_y c_2^e + k_{22}(y)\nabla_x \phi_1^e + k_{22}(y)\nabla_y \phi_2^e] \cdot \mathbf{n_s} = \frac{1}{\varepsilon}\mathcal{J}(c_0^e, c_0^s, \phi_0^e, \phi_0^s) \tag{5.84b}$$

Now we integrate both sides of equations (5.83) over the reference periodicity cell Y and we divide by the measure of Y, and then we obtain

$$\frac{|E|}{|Y|}\frac{\partial c_0^e}{\partial t} = \frac{1}{|Y|}\int_Y \nabla_x \cdot [k_{11}(y, c_0^e)\left(\nabla_x c_0^e + \nabla_y c_1^e\right) + k_{12}(y)\left(\nabla_x \phi_0^e + \nabla_y \phi_1^e\right)]\, dy + \\ + \frac{1}{|Y|}\int_Y \nabla_y \cdot [k_{11}(y, c_0^e)\nabla_x c_1^e + k_{11}(y, c_0^e)\nabla_y c_2^e + k_{12}(y)\nabla_x \phi_1^e + k_{12}(y)\nabla_y \phi_2^e]\, dy \tag{5.85a}$$

$$\frac{1}{|Y|}\int_Y \nabla_x \cdot [k_{21}(y, c_0^e)\left(\nabla_x c_0^e + \nabla_y c_1^e\right) + k_{22}(y)\left(\nabla_x \phi_0^e + \nabla_y \phi_1^e\right)]\, dy + \\ + \frac{1}{|Y|}\int_Y \nabla_y \cdot [k_{21}(y, c_0^e)\nabla_x c_1^e + k_{21}(y)\nabla_y c_2^e + k_{22}(y)\nabla_x \phi_1^e + k_{22}(y)\nabla_y \phi_2^e]\, dy = 0 \tag{5.85b}$$

In equation (5.85a) for the left hand side we have

$$\frac{1}{|Y|}\int_Y \chi^e(y)\frac{\partial c_0^e}{\partial t}(x,t)\, dy = \frac{1}{|Y|}\frac{\partial c_0^e}{\partial t}\int_Y \chi^e(y)\, dy = \frac{1}{|Y|}\frac{\partial c_0^e}{\partial t}\left(\int_E 1\, dy + \int_S 0\, dy\right) = \frac{|E|}{|Y|}\frac{\partial c_0^e}{\partial t} \tag{5.86}$$

Since $Y = E \cup S$ and

$$k_{ij}(y, c_0^e) = \chi^e(y)k_{ij}^e = \begin{cases} k_{ij}^e, & y \in E \\ 0, & y \in S \end{cases}$$

then it follows that

$$\frac{1}{|Y|}\int\limits_{Y} k_{ij}(y,c_0^e)(\ldots)\,dy = \frac{1}{|Y|}\left(\int\limits_{E} k_{ij}^e(\ldots)\,dy + \underbrace{\int\limits_{S} 0(\ldots)\,dy}_{=0}\right) = \frac{1}{|Y|}\int\limits_{E} k_{ij}^e(\ldots)\,dy$$

Now we consider the second integral of the right hand side of equation (5.85a):

$$\begin{aligned}
&\frac{1}{|Y|}\int\limits_{E} \nabla_y\cdot[k_{11}^e(c_0^e)\nabla_x c_1^e + k_{11}^e(c_0^e)\nabla_y c_2^e + k_{12}^e\nabla_x\phi_1^e + k_{12}^e\nabla_y\phi_2^e]\;dy = \\
&= \frac{1}{|Y|}\int\limits_{\partial E} [k_{11}^e(c_0^e)\nabla_x c_1^e + k_{11}^e(c_0^e)\nabla_y c_2^e + k_{12}^e\nabla_x\phi_1^e + (k_{12}^e)_0\,\nabla_y\phi_2^e]\cdot\mathbf{n}\,ds = \\
&= \frac{1}{|Y|}\underbrace{\int\limits_{\partial E\cap\partial Y} [k_{11}^e(c_0^e)\nabla_x c_1^e + k_{11}^e(c_0^e)\nabla_y c_2^e + k_{12}^e\nabla_x\phi_1^e + k_{12}^e\nabla_y\phi_2^e]\cdot\mathbf{n}\,ds}_{=0} + \\
&+ \frac{1}{|Y|}\int\limits_{\Gamma} [k_{11}^e(c_0^e)\nabla_x c_1^e + k_{11}^e(c_0^e)\nabla_y c_2^e + k_{12}^e\nabla_x\phi_1^e + k_{12}^e\nabla_y\phi_2^e]\cdot\mathbf{n_e}\,ds = \\
&= 0 - \frac{1}{|Y|}\int\limits_{\Gamma} [k_{11}^e(c_0^e)\nabla_x c_1^e + k_{11}^e(c_0^e)\nabla_y c_2^e + k_{12}^e\nabla_x\phi_1^e + k_{12}^e\nabla_y\phi_2^e]\cdot\mathbf{n_s}\,ds = \\
&= \frac{1}{\varepsilon\,|Y|}\int\limits_{\Gamma} \mathcal{N}(c_0^e, c_0^s, \phi_0^e, \phi_0^s)\,ds
\end{aligned}$$

For the first integral in the right hand side of equation (5.85a) we obtain:

$$\frac{1}{|Y|}\int\limits_{E} \nabla_x\cdot[k_{11}^e\nabla_y c_1^e + k_{12}^e\nabla_y\phi_1^e + k_{11}^e\nabla_x c_0^e + k_{12}^e\nabla_x\phi_0^e]\;dy =$$

$$= \frac{1}{|Y|}\int\limits_{E} \nabla_x\cdot\left[k_{11}^e\sum_{i=1}^{3}\frac{\partial c_0^e}{\partial x_i}\nabla_y w_i + k_{12}^e\sum_{i=1}^{3}\frac{\partial\phi_0^e}{\partial x_i}\nabla_y w_i + k_{11}^e\nabla_x c_0^e + k_{12}^e\nabla_x\phi_0^e\right]\;dy =$$

$$= \nabla_x\cdot\left\{\frac{1}{|Y|}\int\limits_{E}\left[k_{11}^e\sum_{i=1}^{3}\frac{\partial c_0^e}{\partial x_i}\nabla_y w_i + k_{12}^e\sum_{i=1}^{3}\frac{\partial\phi_0^e}{\partial x_i}\nabla_y w_i + k_{11}^e\nabla_x c_0^e + k_{12}^e\nabla_x\phi_0^e\right]\;dy\right\} =$$

$$\begin{aligned}
= \nabla_x\cdot\Bigg\{&\sum_{i=1}^{3}\frac{1}{|Y|}\int\limits_{E} k_{11}^e\frac{\partial c_0^e}{\partial x_i}(x)\nabla_y w_i\,dy + \sum_{i=1}^{3}\frac{1}{|Y|}\int\limits_{E} k_{12}^e\frac{\partial\phi_0^e}{\partial x_i}(x)\nabla_y w_i\,dy + \\
&+\frac{1}{|Y|}\int\limits_{E} k_{11}^e\nabla_x c_0^e\,dy + \frac{1}{|Y|}\int\limits_{E} k_{12}^e\nabla_x\phi_0^e\,dy\Bigg\} =
\end{aligned}$$

$$= \nabla_x \cdot \left\{ \sum_{i=1}^{3} \left(\frac{1}{|Y|} \int\limits_E k_{11}^e \nabla_y w_i \, dy \right) \frac{\partial c_0^e}{\partial x_i}(x) + \sum_{i=1}^{3} \left(\frac{1}{|Y|} \int\limits_E k_{12}^e \nabla_y w_i \, dy \right) \frac{\partial \phi_0^e}{\partial x_i}(x) + \right.$$

$$\left. + \left(\frac{1}{|Y|} \int\limits_E k_{11}^e \, dy \right) \nabla_x c_0^e + \left(\frac{1}{|Y|} \int\limits_E k_{12}^e \, dy \right) \nabla_x \phi_0^e \right\} =$$

$$= \nabla_x \cdot \left\{ A \nabla_x c_0^e + B \nabla_x \phi_0^e + k_{11}^e \frac{|E|}{|Y|} I \nabla_x c_0^e + k_{12}^e \frac{|E|}{|Y|} I \nabla_x \phi_0^e \right\} =$$

$$= \nabla_x \cdot \left\{ \left(A + k_{11}^e \frac{|E|}{|Y|} I \right) \nabla_x c_0^e + \left(B + k_{12}^e \frac{|E|}{|Y|} I \right) \nabla_x \phi_0^e \right\}$$

where I is the identity matrix and

$$A = (a_{ij})_{i,j=1}^3 = \frac{1}{|Y|} \int\limits_E k_{11}^e \frac{\partial w_j}{\partial y_i}(y) \, dy$$

$$B = (b_{ij})_{i,j=1}^3 = \frac{1}{|Y|} \int\limits_E k_{12}^e \frac{\partial w_j}{\partial y_i}(y) \, dy$$

Now we denote

$$\mathbf{K_{11}} = A + k_{11}^e \frac{|E|}{|Y|} I$$

$$\mathbf{K_{12}} = B + k_{12}^e \frac{|E|}{|Y|} I$$

Then

$$(\mathbf{K_{11}})_{ij} = \frac{1}{|Y|} \int\limits_E k_{11}^e \frac{\partial w_j}{\partial y_i}(y) \, dy + k_{11}^e \frac{|E|}{|Y|} \delta_{ij} =$$

$$= \frac{k_{11}^e}{|Y|} \int\limits_E \left(\delta_{ij} + \frac{\partial w_j}{\partial y_i}(y) \right) \, dy \tag{5.87}$$

We obtain the following homogenized equations:

$$\frac{|E|}{|Y|} \frac{\partial c_0^e}{\partial t} - \nabla_x \cdot (\mathbf{K_{11}} \nabla_x c_0^e + \mathbf{K_{12}} \nabla_x \phi_0^e) = \frac{1}{\varepsilon |Y|} \int\limits_\Gamma \mathcal{N}(c_0^e, c_0^s, \phi_0^e, \phi_0^s) \, ds \tag{5.88}$$

$$-\nabla_x \cdot (\mathbf{K_{21}} \nabla_x c_0^e + \mathbf{K_{22}} \nabla_x \phi_0^e) = \frac{1}{\varepsilon |Y|} \int\limits_\Gamma \mathcal{J}(c_0^e, c_0^s, \phi_0^e, \phi_0^s) \, ds \tag{5.89}$$

where Γ is the interface boundary between the electrolyte and the solid in a single representative periodicity cell $Y = E \cup S$ and the matrices $\mathbf{K_{11}}$, $\mathbf{K_{12}}$, $\mathbf{K_{21}}$ and $\mathbf{K_{22}}$ are

given by:

$$(\mathbf{K_{11}})_{ij} = \frac{k^e_{11}(c^e_0)}{|Y|}\int\limits_E \left(\delta_{ij} + \frac{\partial w_j}{\partial y_i}(y)\right) dy, \quad (\mathbf{K_{12}})_{ij} = \frac{k^e_{12}}{|Y|}\int\limits_E \left(\delta_{ij} + \frac{\partial w_j}{\partial y_i}(y)\right) dy$$

$$(\mathbf{K_{21}})_{ij} = \frac{k^e_{21}(c^e_0)}{|Y|}\int\limits_E \left(\delta_{ij} + \frac{\partial w_j}{\partial y_i}(y)\right) dy, \quad (\mathbf{K_{22}})_{ij} = \frac{k^e_{22}}{|Y|}\int\limits_E \left(\delta_{ij} + \frac{\partial w_j}{\partial y_i}(y)\right) dy$$

5.6 Homogenization of the Solid Phase PDEs

We will homogenize only the governing equation for the potential $\phi^s_\varepsilon(x)$.
From $\mathbf{J}^\mathbf{s}_\varepsilon \cdot \mathbf{n_s} = \mathcal{J}_\varepsilon$ for the interface conditions we obtain:

$$\varepsilon^{-2}: \quad 0 = \kappa(y)\nabla_y \phi^s_0 \cdot \mathbf{n_s} \tag{5.90a}$$

$$\varepsilon^{-1}: \quad 0 = \kappa(y)\left(\nabla_x \phi^s_0 + \nabla_y \phi^s_1\right) \cdot \mathbf{n_s} \tag{5.90b}$$

$$\varepsilon^{0}: \quad \frac{1}{\varepsilon}\mathcal{J}\left(c^e_0, c^s, \phi^e_0, \phi^s_0\right) = \tag{5.90c}$$

$$= -\left(\kappa(y)\nabla_x \phi^s_1 + \kappa(y)\nabla_y \phi^s_2\right) \cdot \mathbf{n_s} \tag{5.90d}$$

5.6.1 Homogenization of the PDEs: Order ε^{-2}

We have the equation

$$\nabla_y \cdot \left(\kappa(y)\nabla_y \phi^s_0(x,y,t)\right) = 0, \quad y \in Y \tag{5.91}$$

which is equivalent to

$$\nabla_y \cdot \left(\kappa^s \nabla_y \phi^s_0(x,y,t)\right) = 0, \quad y \in S \tag{5.92}$$

with the following interface conditions:

$$\kappa^s \nabla_y \phi^s_0 \cdot \mathbf{n_s} = 0, \quad y \in \Gamma \equiv \partial S \tag{5.93}$$

From here (and taking into account the boundary conditions), we obtain that

$$\phi^s_0 = \phi^s_0(x,t) \tag{5.94}$$

which coincides with the assumption we made that ϕ^s_0 is a function of x only.

5.6.2 Homogenization of the PDEs: Order ε^{-1}

We have the following equation for $y \in Y$:

$$\nabla_x \cdot \left(\kappa(y)\nabla_y \phi^s_0(x,t)\right) + \nabla_y \cdot \left(\kappa(y)\nabla_x \phi^s_0(x,t) + \kappa(y)\nabla_y \phi^s_1(x,y,t)\right) = 0 \tag{5.95}$$

with periodic boundary conditions on ∂Y for the Y-periodic functions $c^s_1(x,y,t)$ and $\phi^s_1(x,y,t)$, and the following interface conditions on $\Gamma \equiv \partial S$:

$$\left(\kappa(y)\nabla_x \phi^s_0 + \kappa(y)\nabla_y \phi^s_1\right) \cdot \mathbf{n_s} = 0, \quad y \in \Gamma \tag{5.96}$$

Since $\nabla_y \phi_0^s = 0$ because $\phi_0^s = \phi_0^s(x,t)$, the latter equation becomes

$$\nabla_y \cdot (\kappa(y)\nabla_x \phi_0^s(x,t) + \kappa(y)\nabla_y \phi_1^s(x,y,t)) = 0, \quad y \in Y \tag{5.97}$$

We look for the solution ϕ_1^s of equation (5.97) (provided that we consider the function ϕ_0^s given) in the following form

$$\phi_1^s(x,y,t) = \sum_{i=1}^{3} \varphi_i^s(y) \frac{\partial \phi_0^s}{\partial x_i}(x,t) \tag{5.98}$$

where the Y-periodic function $\varphi_l^s(y)$ for $l = 1,2,3$ in $3D$ is the solution of the following auxiliary cell problem for $l = 1,2,3$:

- **"Solid" Cell Problem for $l = 1,2,3$:**

  –

$$\nabla \cdot (\nabla_y \varphi_l^s) = 0, \quad y \in S \tag{5.99a}$$
$$\nabla_y \varphi_l^s \cdot \mathbf{n_s} = -\mathbf{e}_l \cdot \mathbf{n_s}, \quad y \in \Gamma \tag{5.99b}$$

  – Periodic boundary conditions on $\partial S \backslash \Gamma$, i.e. on the boundary of the particles where the particles are connected

  – $\int_S \varphi_l^s(y)\, dy = 0, \quad l = 1,2,3$ in order to fix the solution

5.6.3 Homogenization of the PDEs: Order ε^0

He have the following equation for $y \in Y$:

$$\nabla_x \cdot (\kappa(y)\nabla_x \phi_0^s + \kappa(y)\nabla_y \phi_1^s) + \nabla_y \cdot (\kappa(y)\nabla_x \phi_1^s + \kappa(y)\nabla_y \phi_2^s) = 0 \tag{5.100}$$

with periodic boundary conditions on ∂Y and the following interface conditions on $\Gamma \equiv \partial S$:

$$-(\kappa(y)\nabla_x \phi_1^s + \kappa(y)\nabla_y \phi_2^s) \cdot \mathbf{n_s} = \frac{1}{\varepsilon} \mathcal{J}(c_0^e, c_0^s, \phi_0^e, \phi_0^s), \quad y \in \Gamma = \partial S \tag{5.101}$$

After we integrate the equation over Y and after we substitute $\phi_1^s(x,y,t)$ with its equal expression from (5.98), we obtain the homogenized equation:

$$-\nabla_x \cdot (\Lambda^s \nabla_x \phi_0^s) = -\frac{1}{\varepsilon |Y|} \int_\Gamma \mathcal{J}(c_0^e, c_0^s, \phi_0^e, \phi_0^s)\, ds \tag{5.102}$$

where

$$(\Lambda^s)_{ij} = \frac{1}{|Y|} \int_S \kappa^s \left(\delta_{ij} + \frac{\partial \varphi_j^s}{\partial y_i} \right) dy \tag{5.103}$$

5.7 Homogenized Problem Without Boundary Conditions

Macroscale equations:

$$\frac{|E|}{|Y|}\frac{\partial c_0^e}{\partial t} - \nabla_x \cdot (\mathbf{K_{11}}\nabla_x c_0^e + \mathbf{K_{12}}\nabla_x \phi_0^e) = \frac{1}{\varepsilon\,|Y|}\int_\Gamma \mathcal{N}(c_0^e, c^s, \phi_0^e, \phi_0^s)\,ds, \quad x \in \Omega \tag{5.104a}$$

$$-\nabla_x \cdot (\mathbf{K_{21}}\nabla_x c_0^e + \mathbf{K_{22}}\nabla_x \phi_0^e) = \frac{1}{\varepsilon\,|Y|}\int_\Gamma \mathcal{J}(c_0^e, c^s, \phi_0^e, \phi_0^s)\,ds, \quad x \in \Omega \tag{5.104b}$$

$$-\nabla_x \cdot (\Lambda^s \nabla_x \phi_0^s) = -\frac{1}{\varepsilon\,|Y|}\int_\Gamma \mathcal{J}(c_0^e, c^s, \phi_0^e, \phi_0^s)\,ds, \quad x \in \Omega \tag{5.104c}$$

Microscale equation:

$$\frac{\partial c^s}{\partial t} - \nabla_y \cdot \left(\frac{D^s}{\varepsilon^2}\nabla_y c^s\right) = 0, \quad y \in S \tag{5.105a}$$

$$-\frac{D^s}{\varepsilon^2}\nabla_y c^s \cdot \mathbf{n_s} = \frac{1}{\varepsilon}\mathcal{N}(c_0^e, c^s, \phi_0^e, \phi_0^s), \quad y \in \Gamma \tag{5.105b}$$

6 Homogenization of the Neumann Boundary Conditions

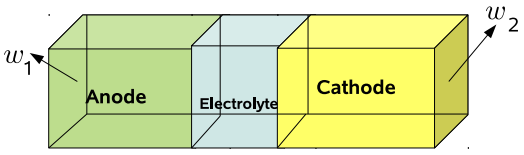

Figure 19: Battery Cell

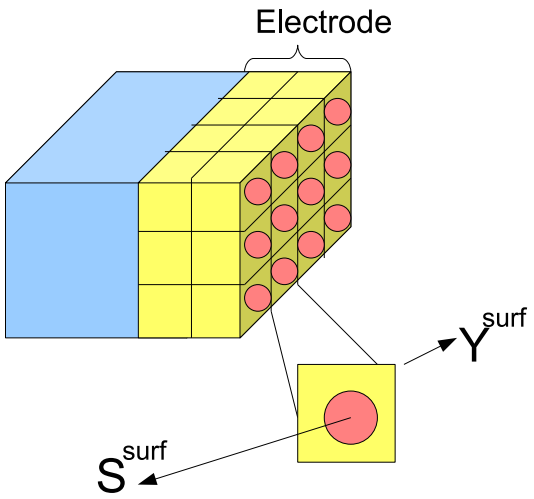

Figure 20: Electrode Outer Boundary

We have the following Neumann boundary condition in the ε-setting of the original microscopic problem:

$$-\kappa_\varepsilon \nabla \phi_\varepsilon^s \cdot \mathbf{n} = E_2^\varepsilon, \quad x \in \omega_2 \tag{6.1}$$

where

- $E_2^\varepsilon = \chi_\varepsilon^s(x) E_2^s = \chi^s\left(\frac{x}{\varepsilon}\right) E_2^s = \chi^s(y) E_2^s$
- $\kappa_\varepsilon(x) = \kappa\left(\frac{x}{\varepsilon}\right) = \chi^s\left(\frac{x}{\varepsilon}\right)\kappa^s = \chi^s(y)\kappa^s$
- $\nabla = \nabla_x + \frac{1}{\varepsilon}\nabla_y$
- $\phi_\varepsilon^s(x) = \phi_0^s(x) + \varepsilon\phi_1^s(x,y) + \varepsilon^2\phi_2^s(x,y)$ and therefore
- $\nabla\phi_\varepsilon^s = \nabla_x\phi_0^s + \nabla_y\phi_1^s + O(\varepsilon) \xrightarrow[\varepsilon\to 0]{} \nabla_x\phi_0^s + \nabla_y\phi_1^s$
- $\phi_1^s(x,y) = \sum_{i=1}^{3} \varphi_i^s(y)\frac{\partial\phi_0^s}{\partial x_i}(x)$

Let $\mathbf{n} = (n_1, n_2, n_3)$. Now we calculate the flux

$$\begin{aligned}
\kappa_\varepsilon \nabla\phi_\varepsilon^s \cdot \mathbf{n} &= \kappa(y)\left(\nabla_x\phi_0^s + \nabla_y\phi_1^s\right)\cdot\mathbf{n} = \\
&= \kappa(y)\left(\frac{\partial\phi_0^s}{\partial x_1}n_1 + \frac{\partial\phi_1^s}{\partial y_1}n_1 + \frac{\partial\phi_0^s}{\partial x_2}n_2 + \frac{\partial\phi_1^s}{\partial y_2}n_2\right) = \\
&= \kappa(y)\left(\frac{\partial\phi_0^s}{\partial x_1}n_1 + \frac{\partial\varphi_1^s}{\partial y_1}\frac{\partial\phi_0^s}{\partial x_1}n_1 + \frac{\partial\varphi_2^s}{\partial y_1}\frac{\partial\phi_0^s}{\partial x_2}n_1 + \right. \\
&\qquad \left. + \frac{\partial\phi_0^s}{\partial x_2}n_2 + \frac{\partial\varphi_1^s}{\partial y_2}\frac{\partial\phi_0^s}{\partial x_1}n_2 + \frac{\partial\varphi_2^s}{\partial y_2}\frac{\partial\phi_0^s}{\partial x_2}n_2\right) = \\
&= \frac{\partial\phi_0^s}{\partial x_1}\left(\kappa(y)\left(1 + \frac{\partial\varphi_1^s}{\partial y_1}\right)\right)n_1 + \kappa(y)\frac{\partial\phi_0^s}{\partial x_2}\frac{\partial\varphi_2^s}{\partial y_1}n_1 + \\
&+ \frac{\partial\phi_0^s}{\partial x_2}\left(\kappa(y)\left(1 + \frac{\partial\varphi_2^s}{\partial y_2}\right)\right)n_2 + \kappa(y)\frac{\partial\phi_0^s}{\partial x_1}\frac{\partial\varphi_1^s}{\partial y_2}n_2 = \\
&= \frac{\partial\phi_0^s}{\partial x_1}A_{11}n_1 + \frac{\partial\phi_0^s}{\partial x_2}A_{12}n_1 + \frac{\partial\phi_0^s}{\partial x_2}A_{22}n_2 + \frac{\partial\phi_0^s}{\partial x_1}A_{21}n_2 = \\
&= \begin{pmatrix} A_{11} & A_{12} \\ A_{21} & A_{22} \end{pmatrix}\begin{pmatrix} \dfrac{\partial\phi_0^s}{\partial x_1} \\ \\ \dfrac{\partial\phi_0^s}{\partial x_2} \end{pmatrix}\cdot\mathbf{n} = \left(A\nabla_x\phi_0^s\right)\cdot\mathbf{n}
\end{aligned} \tag{6.2}$$

where we denote $A_{ij} = \kappa(y)\left(\delta_{ij} + \frac{\partial\varphi_j^s}{\partial y_i}\right) = \chi^s(y)\kappa^s\left(\delta_{ij} + \frac{\partial\varphi_j^s}{\partial y_i}(y)\right)$. Therefore we obtain

$$-\left(A\nabla_x\phi_0^s\right)\cdot\mathbf{n} = \chi^s(y)E_2^s, \quad x \in \omega_2 \quad (y \in Y^{surf}) \tag{6.3}$$

Now we integrate over S (in order to obtain the coefficients Λ^s and respectively the flux $\Lambda^s\nabla\phi_0^s$, see Figure 20) both sides of equality (6.3) and we obtain

$$-\frac{1}{|Y^{surf}|}\int\limits_{S^{surf}}\left(A\nabla_x\phi_0^s\right)\cdot\mathbf{n}\,dS = \frac{1}{|Y^{surf}|}\int\limits_{S^{surf}}\chi^s(y)E_2^s\,dS, \quad x \in \omega_2 \tag{6.4}$$

which is equivalent to

$$
\begin{aligned}
-\left(\Lambda^s \nabla_x \phi_0^s\right) \cdot \mathbf{n} &= \frac{1}{\left|Y^{surf}\right|} \int\limits_{S^{surf}} 1 E_2^s \, dS, \quad x \in \omega_2 \Longleftrightarrow \\
-\left(\Lambda^s \nabla_x \phi_0^s\right) \cdot \mathbf{n} &= \frac{E_2^s}{\left|Y^{surf}\right|} \int\limits_{S^{surf}} 1 \, dS, \quad x \in \omega_2 \Longleftrightarrow \\
-\left(\Lambda^s \nabla_x \phi_0^s\right) \cdot \mathbf{n} &= \frac{\left|S^{surf}\right|}{\left|Y^{surf}\right|} E_2^s, \quad x \in \omega_2
\end{aligned} \tag{6.5}
$$

Upscaled Neumann BC: Verification
We denote the flux

$$
-\Lambda^s \nabla \phi_0^s \cdot \mathbf{n} = C = const \tag{6.6}
$$

Let us also denote with $p = p(\varepsilon)$ the number of all periodicity cells which have an outer boundary on the external cathode (electrode) boundary ω_2 (for simplicity we fix ω_2 to be the external cathode boundary, i.e. ω_2 consists of both solid particles and electrolyte, whereas with $\partial\Omega_c$ we denote only the cathode solid particles outer boundary). Since the total flux across ω_2 should be preserved, i.e. it must be the same in both the upscaled problem and the initial microscopic one, we want to ensure that the following surface integrals are equal

$$
\int\limits_{\omega_2 \cap \partial\Omega_c} -\kappa_\varepsilon(x) \nabla \phi_\varepsilon^s \cdot \mathbf{n} \, dS = \int\limits_{\omega_2} -\Lambda^s \nabla \phi_0^s \cdot \mathbf{n} \, dS
$$

which is equivalent to

$$
\begin{aligned}
\int\limits_{\omega_2 \cap \partial\Omega_c} E_2^\varepsilon \, dS &= \int\limits_{\omega_2} C \, dS \quad \Longleftrightarrow \\
\int\limits_{\omega_2 \cap \partial\Omega_c} \chi_\varepsilon^s(x) E_2^s \, dS &= \int\limits_{\omega_2} C \, dS \quad \Longleftrightarrow \\
\int\limits_{\omega_2 \cap \partial\Omega_c} E_2^s \, dS &= \int\limits_{\omega_2} C \, dS \quad \Longleftrightarrow \\
E_2^s \int\limits_{\omega_2 \cap \partial\Omega_c} 1 \, dS &= C \int\limits_{\omega_2} 1 \, dS \quad \Longleftrightarrow
\end{aligned}
$$

$$
E_2^s \left|\omega_2 \cap \partial\Omega_c\right| = C \left|\omega_2\right| \quad \Longleftrightarrow
$$

$$
E_2^s p(\varepsilon) \left|S^{surf}\right| = C p(\varepsilon) \left|Y^{surf}\right| \Longleftrightarrow
$$

$$
p(\varepsilon) \left(E_2^s \left|S^{surf}\right| - C \left|Y^{surf}\right|\right) = 0 \Longleftrightarrow
$$

$$
E_2^s \left|S^{surf}\right| - C \left|Y^{surf}\right| = 0 \quad (p(\varepsilon) \neq 0) \Longleftrightarrow
$$

$$
C = \frac{\left|S^{surf}\right|}{\left|Y^{surf}\right|} E_2^s
$$

which is true (we obtained the same result via the homogenization method).

7 Homogenized Problem

7.1 Macroscale Problem

We obtain the following homogenized equations for the concentration c^e of ions in the electrolyte, the potential ϕ^e in the electrolyte and for the potential ϕ^s in the solid

$$\frac{|E|}{|Y|}\frac{\partial c_0^e}{\partial t} - \nabla_x \cdot (\mathbf{K_{11}}\nabla_x c_0^e + \mathbf{K_{12}}\nabla_x \phi_0^e) = \frac{1}{\varepsilon\,|Y|}\int\limits_\Gamma \mathcal{N}(c_0^e, c^s, \phi_0^e, \phi_0^s)\,ds, \quad x \in \Omega \tag{7.1a}$$

$$-\nabla_x \cdot (\mathbf{K_{21}}\nabla_x c_0^e + \mathbf{K_{22}}\nabla_x \phi_0^e) = \frac{1}{\varepsilon\,|Y|}\int\limits_\Gamma \mathcal{J}(c_0^e, c^s, \phi_0^e, \phi_0^s)\,ds, \quad x \in \Omega \tag{7.1b}$$

$$-\nabla_x \cdot (\Lambda^s \nabla_x \phi_0^s) = -\frac{1}{\varepsilon\,|Y|}\int\limits_\Gamma \mathcal{J}(c_0^e, c^s, \phi_0^e, \phi_0^s)\,ds, \quad x \in \Omega \tag{7.1c}$$

with the following boundary conditions

$$\phi_0^s = E_1^s, \quad x \in \omega_1 \tag{7.2a}$$

$$(\Lambda^s \nabla_x \phi_0^s) \cdot \mathbf{n} = \frac{\left|S^{surf}\right|}{\left|Y^{surf}\right|} E_2^s, \quad x \in \omega_2 \tag{7.2b}$$

$$\mathbf{N_e^h} \cdot \mathbf{n} = \mathbf{N_s^h} \cdot \mathbf{n} = 0, \quad x \in \partial\Omega \tag{7.2c}$$

$$\mathbf{J_e^h} \cdot \mathbf{n} = \mathbf{J_s^h} \cdot \mathbf{n} = 0, \quad x \in \partial\Omega \tag{7.2d}$$

and homogenized coefficients (which are tensors)

$$(\mathbf{K_{11}})_{ij} = \frac{k_{11}^e(c_0^e)}{|Y|}\int\limits_E \left(\delta_{ij} + \frac{\partial w_j}{\partial y_i}(y)\right) dy, \quad (\mathbf{K_{12}})_{ij} = \frac{k_{12}^e}{|Y|}\int\limits_E \left(\delta_{ij} + \frac{\partial w_j}{\partial y_i}(y)\right) dy$$

$$(\mathbf{K_{21}})_{ij} = \frac{k_{21}^e(c_0^e)}{|Y|}\int\limits_E \left(\delta_{ij} + \frac{\partial w_j}{\partial y_i}(y)\right) dy, \quad (\mathbf{K_{22}})_{ij} = \frac{k_{22}^e}{|Y|}\int\limits_E \left(\delta_{ij} + \frac{\partial w_j}{\partial y_i}(y)\right) dy \tag{7.3}$$

$$(\Lambda^s)_{ij} = \frac{1}{|Y|}\int\limits_S \kappa^s \left(\delta_{ij} + \frac{\partial \varphi_j^s}{\partial y_i}\right) dy$$

with $w_j(y)$ and $\varphi_j^s(y)$ $(j = 1, 2, 3)$ being the solutions of the auxiliary cell problems (5.80a)-(5.80b) and (5.99a)-(5.99b), respectively.

7.2 Microscale Problem

We have to solve the following microscale problem for the concentration of ions in the active particles

$$\frac{\partial c^s}{\partial t} - \nabla_y \cdot \left(\frac{D^s}{\varepsilon^2}\nabla_y c^s\right) = 0, \quad y \in S \tag{7.4a}$$

$$-\frac{D^s}{\varepsilon^2}\nabla_y c^s \cdot \mathbf{n_s} = \frac{1}{\varepsilon}\mathcal{N}(c_0^e, c^s, \phi_0^e, \phi_0^s), \quad y \in \Gamma \tag{7.4b}$$

We impose periodic boundary conditions on $\partial S \backslash \Gamma$, i.e. on the boundary of the solid particle where the particles are connected to each other.

8 Numerical Methods

Since the processes in the homogenized equations are essentially one-dimensional, we can solve them in 1D but we leave the microscale problem for c^s in 3D. For the space discretization we use the Finite Element Method with linear Lagrange elements. For the time discretization we apply the Backward Euler Method and for the linearization of the resulting system of algebraic equations we use the Newton Method.
For each node in the space discretization of the 1D problem we assume to have one active particle. Therefore we solve as many microscale problems as there are nodes in the discretization of equations (7.1).
We use the following time-stepping scheme. First we solve the homogenized equations (7.1) using Backward Euler Method and using the values of c^s from the previous time step. Then we use the obtained values c^e, ϕ^e and ϕ^s to solve the microscale problem for c^s.

9 Numerical Results

In all the numerical experiments we consider a battery cell which consists of two electrodes-anode and cathode, each of them being a cube with length of the side 100 μm (see Figure 21). Between the two electrodes there is a layer of pure electrolyte with thickness of 10 μm. In each of the experiments we run simulations varying the size of the active particles. We begin with particles having a characteristic size of 20 μm and we decrease this size up to 2.5 μm in the last experiment. In Table 1 we give the values of all the parameters which we use for our computations.

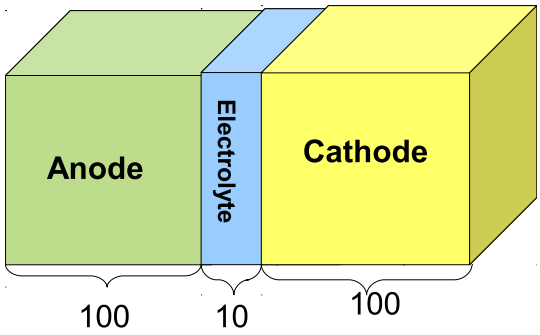

Figure 21: Battery Cell Dimensions

Table 1: Values of the parameters used for the simulations

	D	t_+	κ	c_{max}	$c_{initial}$	k-reaction rate
Electrolyte	7.5×10^{-7}	0.363	0.002	-	0.001	-
Cathode	1.0×10^{-9}	0	0.038	0.023671	0.9*c_{max}	0.2
Anode	3.9×10^{-10}	0	1.0	0.024681	0.1*c_{max}	0.002

For the open circuit potential U_0 we have

$$U_0(c^s) = -0.132 + 1.41e^{-3.52soc}, \quad x \in \Omega_a \tag{9.1a}$$

$$U_0(c^s) = 4.06279 + 0.0677504\tanh(-21.8502soc + 12.8268) - 0.045e^{-71.69soc^8} - 0.105734\left(\frac{1}{(1.00167 - soc)^{0.379571}} - 1.576\right) + 0.01e^{-200(soc-0.19)}, \quad x \in \Omega_c \tag{9.1b}$$

where

$$soc = \frac{c^s}{c^s_{max}} \tag{9.2}$$

The applied current on the cathode is:

$$(\Lambda^s \nabla_x \phi^s_0) \cdot \mathbf{n} = \frac{|S^{surf}|}{|Y^{surf}|} E^s_2, \quad x \in \omega_2, \tag{9.3}$$

$$E^s_2 = 0.01 \tag{9.4}$$

For the potential ϕ^s on the anode outer boundary we impose the following values:

$$\phi^s_0 = E^s_1 = U_0(c^s_{initial}) = 0.8596, \quad x \in \omega_1 \tag{9.5}$$

We run all the simulations with time step of 2s and with t we denote the number of time steps.

9.1 Experiment 1

We run simulations for 5 active particles in each direction, which means that we have a total number of 125 particles in each electrode. The characteristic size of the particles in this case is $l = 20$ μm, whereas the size of the whole electrode is $L = 100$ μm. Consequently $\varepsilon = \dfrac{l}{L} = 0.2$ in this simulation. In Figure 22 and Figure 23 we compare the results from the full microscopic simulation and the homogenized problem. In all the subsequent numerical experiments we show the results for the potential ϕ^s only in the cathode, since throughout the simulation the values of the potential in the anode are virtually constant. The potential ϕ^e in the electrolyte after 40 time steps is shown in Figure 22. In Figure 23 we show the concentration c^s in the second layer anode active particle in both the homogenized model and the microscale model. As we can see from the picture, the values of the concentration in both models are pretty close.

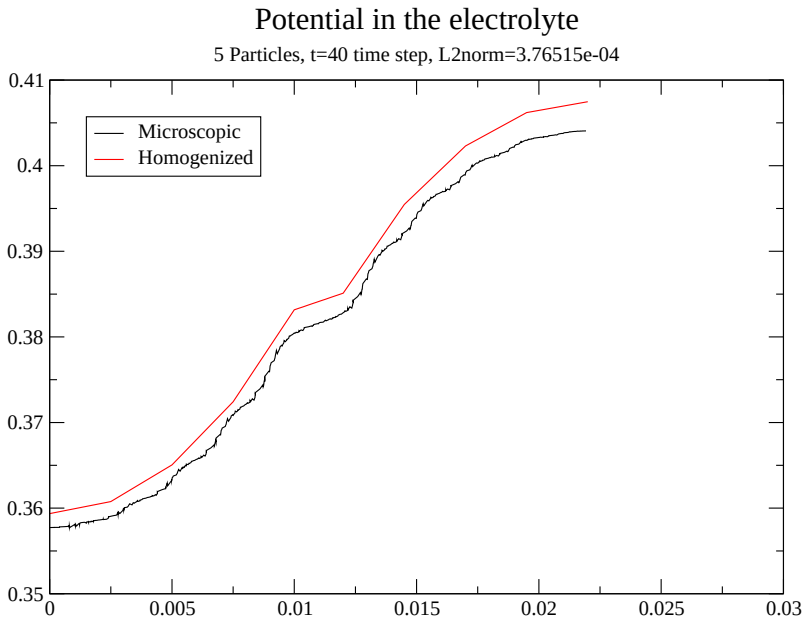

Figure 22: Comparison between the homogenized and the microscopic solution: potential in the electrolyte for $5 \times 5 \times 5$ particles in each electrode

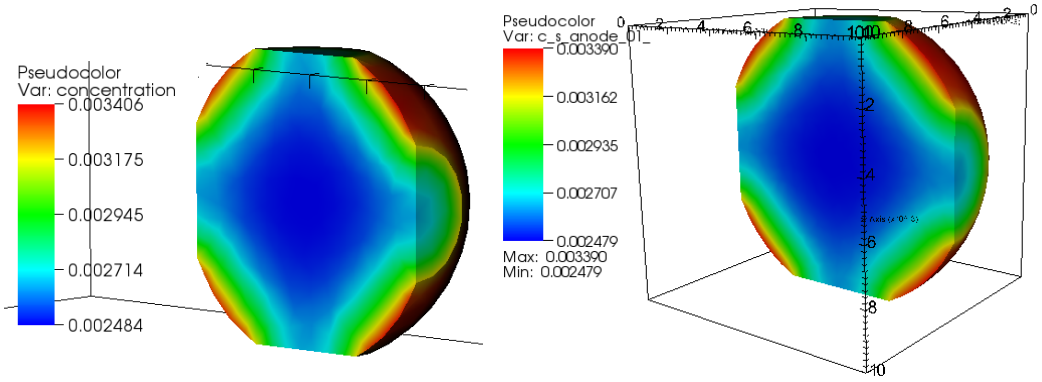

(a) Exact Solution (b) Homogenized Solution

Figure 23: Concentration in the Anode after 80 time steps for 125 particles in each electrode

9.2 Experiment 2

We run simulations for 10 active particles in each direction, which means that we have a total number of 1000 particles in each electrode. Therefore the characteristic size of each particle is 10 μm and $\varepsilon = 0.1$. The results from the full microscopic simulation and from the homogenized problem are shown in Figure 24, 25, 26 and 27.

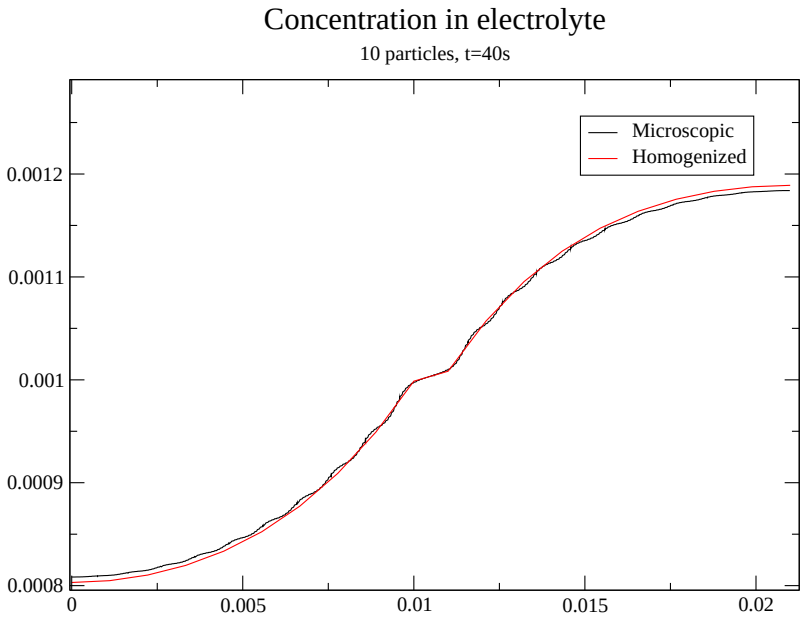

Figure 24: Comparison between the homogenized and the microscopic solution: concentration of Li+ in the electrolyte for $10 \times 10 \times 10$ particles in each electrode

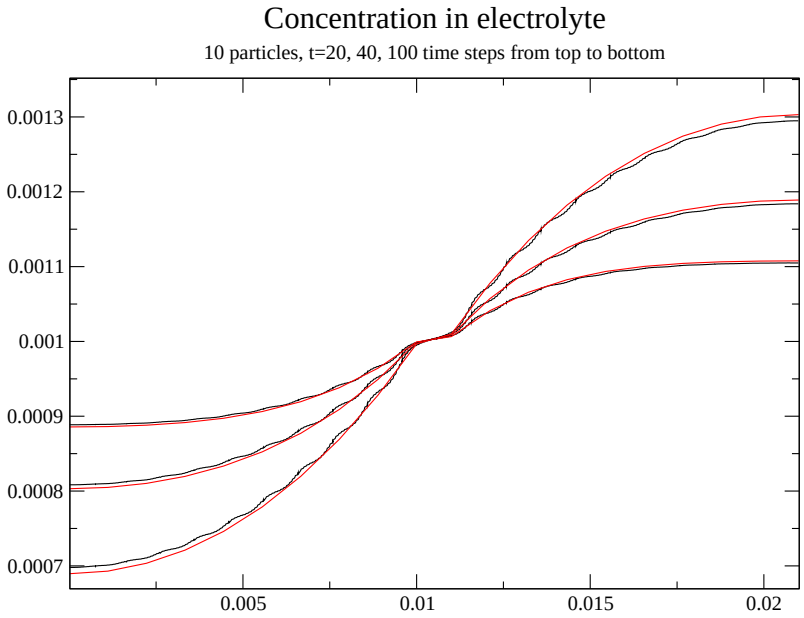

Figure 25: Comparison between the homogenized and the microscopic solution: concentration of Li+ in the electrolyte for $10 \times 10 \times 10$ particles in each electrode for different time steps

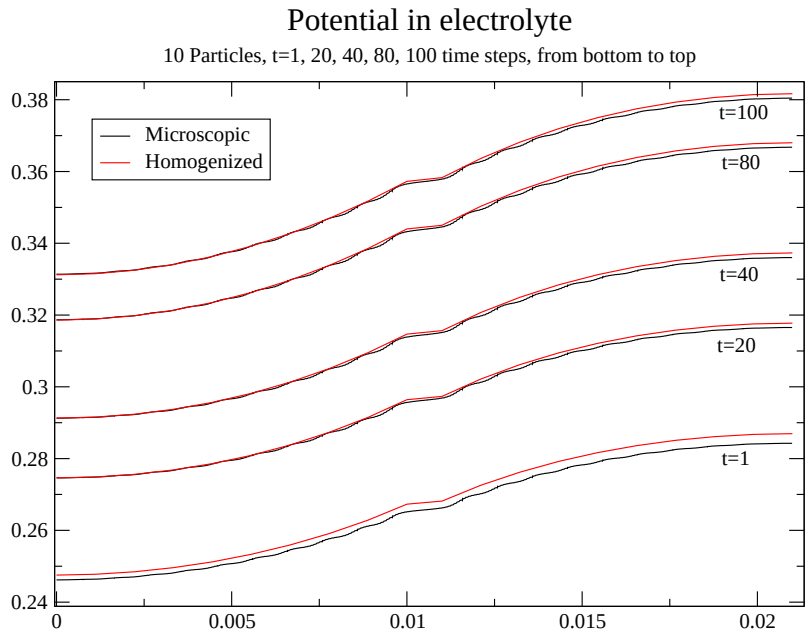

Figure 26: Comparison between the homogenized and the microscopic solution: potential in the electrolyte for $10 \times 10 \times 10$ particles in each electrode for different time steps

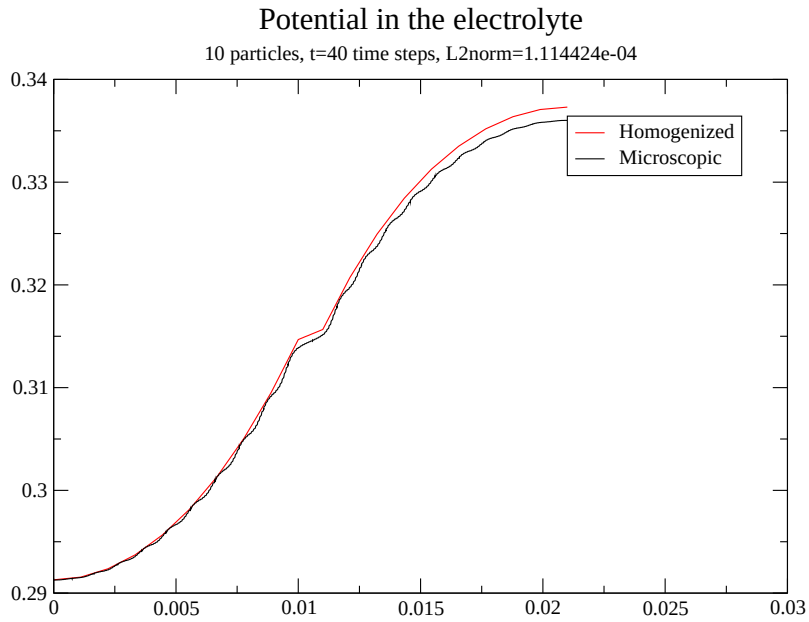

Figure 27: Comparison between the homogenized and the microscopic solution: potential in the electrolyte for $10 \times 10 \times 10$ particles in each electrode

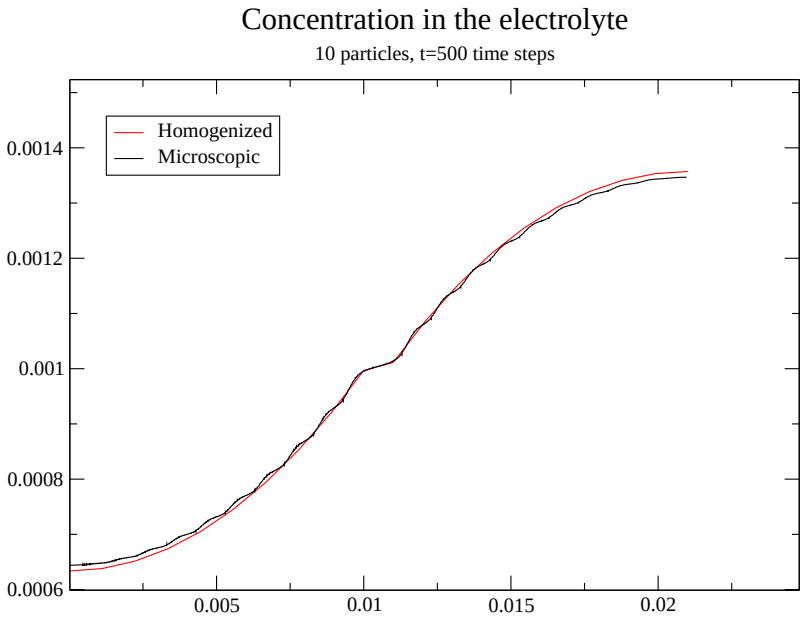

Figure 28: Concentration in the electrolyte for $10 \times 10 \times 10$ particles in each electrode after 500 time steps, L_2 norm=1.05651e-06

9.3 Experiment 3

In this experiment we run simulations for 20 active particles in each direction, which means that we have a total number of 8000 particles in each electrode. The characteristic size of the particles is 5μm and the small parameter is $\varepsilon = 0.05$. The results from the full microscopic simulation and from the homogenized problem are given in Figure 29, 30, 31 and 32. In Figure 33 we show the concentration of Lithium ions in the anode after 80 time steps.

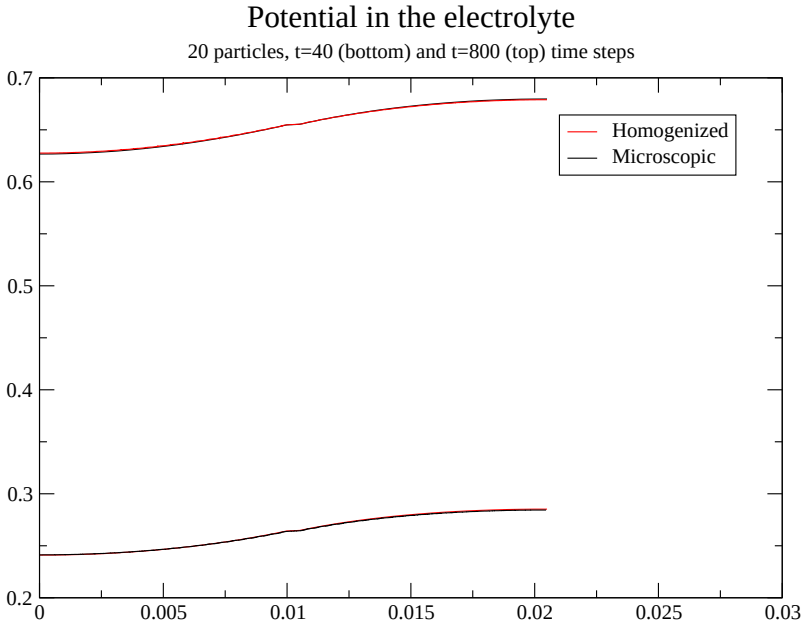

Figure 29: Comparison between the homogenized and the microscopic solution: potential in the electrolyte for $20 \times 20 \times 20$ particles in each electrode for different time steps

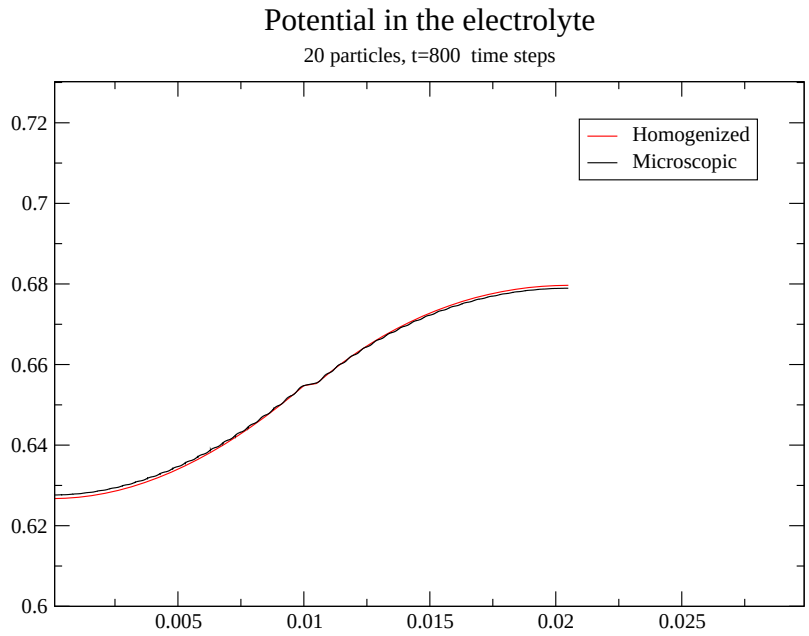

Figure 30: Comparison between the homogenized and the microscopic solution: potential in the electrolyte for $20 \times 20 \times 20$ particles in each electrode for different time steps

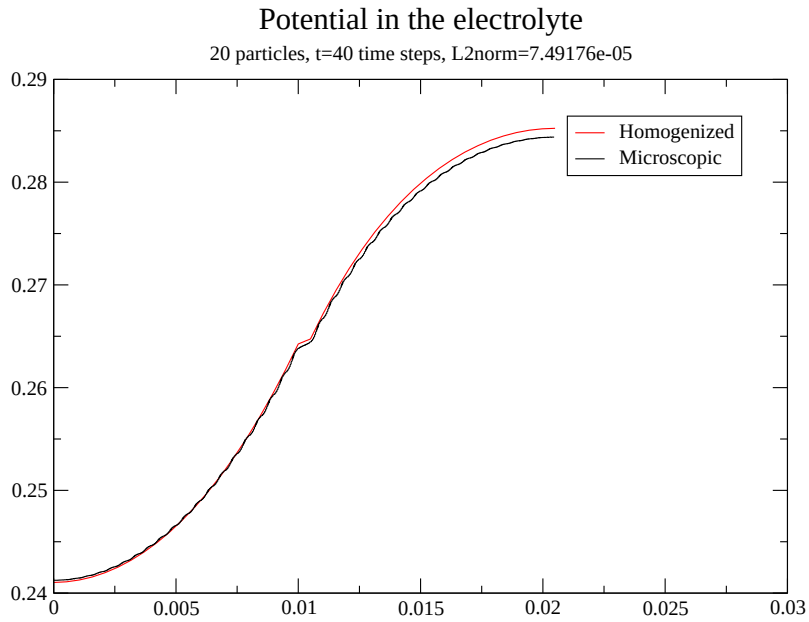

Figure 31: Comparison between the homogenized and the microscopic solution: potential in the electrolyte for $20 \times 20 \times 20$ particles in each electrode

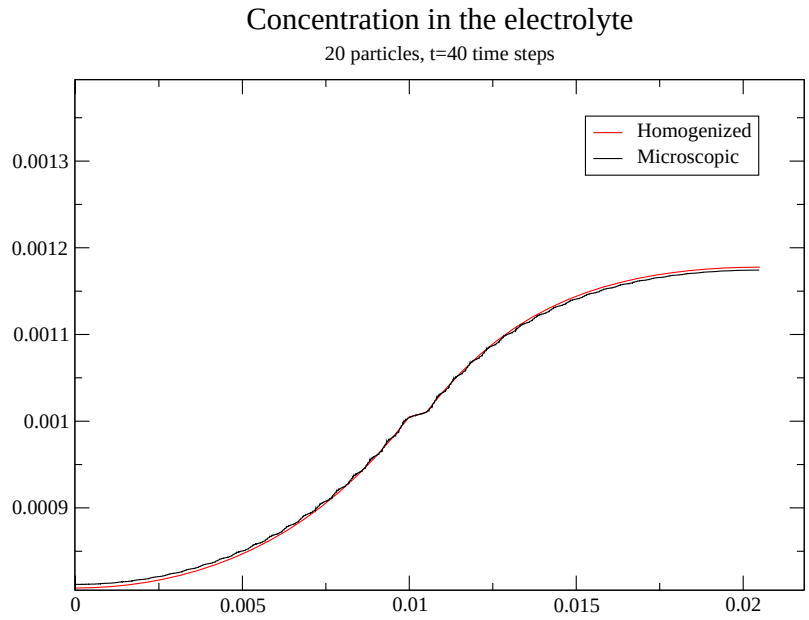

Figure 32: Comparison between the homogenized and the microscopic solution: concentration in the electrolyte for $20 \times 20 \times 20$ particles in each electrode

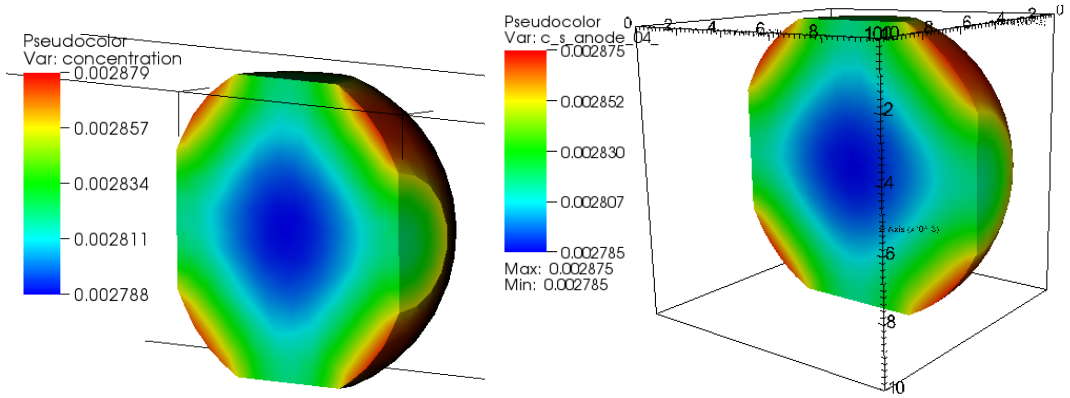

(a) Exact Solution (b) Homogenized Solution

Figure 33: Concentration in the Anode after 80 time steps for 8000 particles in each electrode

9.4 Experiment 4

In this experiment we run simulations for 40 active particles in each direction, which means that we have a total number of 64000 particles with typical size of 2.5μm in each electrode. Consequently we have that $\varepsilon = 0.025$. The results from the full microscopic simulation and from the homogenized problem are given in Figure 34 and 35.

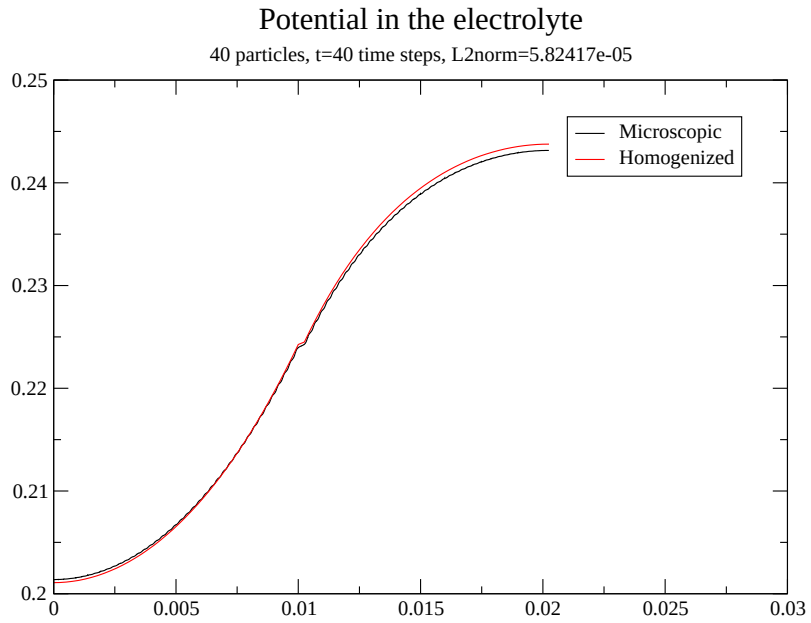

Figure 34: Comparison between the homogenized and the microscopic solution: potential in the electrolyte for $40 \times 40 \times 40$ particles in each electrode

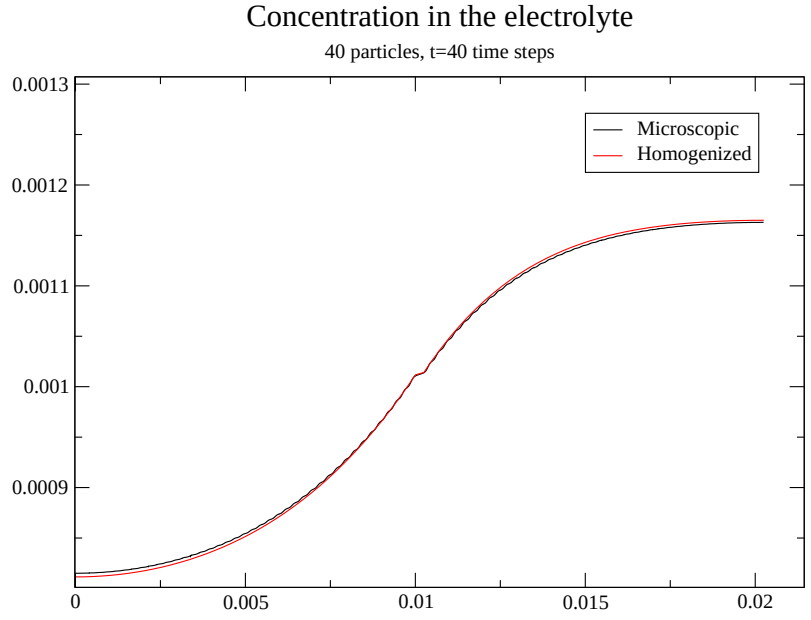

Figure 35: Comparison between the homogenized and the microscopic solution: concentration in the electrolyte for $40 \times 40 \times 40$ particles in each electrode

10 Conlcusion

The theoretical error estimate for linear elliptic problems is

$$\|u_\varepsilon - u_0 - \varepsilon u_1\|_{H^1(\Omega)} \leq C\sqrt{\varepsilon} \tag{10.1}$$

where u_ε is the microscopic solution, u_0 is the solution of the homogenized problem and u_1 is the first order corrector (see [4]). As we can see from Table 2 the L_2 norm of the difference between the homogenized and the microscopic solution decreases when we decrease ε.

Table 2: L_2 norm at time step 40

Particles	ε	$\|\phi_0^e - \phi^e\|_{L_2}$	$\|c_0^e - c^e\|_{L_2}$	$\|\phi_0^s - \phi^s\|_{L_2}$
				Cathode
5	0.2	3.76515e-04	8.73508e-07	0.000393077
10	0.1	1.114424e-04	5.60168e-07	0.000139498
20	0.05	7.49176e-05	4.41375e-07	7.30204e-05
40	0.025	5.82417e-05	3.66711e-07	3.5623e-05

We have successfully derived a coupled micro-macroscale model for the isothermal Li-ion battery model [8]. We rigorously proved the order of the current density which is crucial for the correct homogenization of the microscopic model. We also derived properly upscaled Neumann boundary conditions. Finally we ran a series of numerical simulations for uniformly decreasing ε against FEM solver for the microscopic model. The results of the simulations show good agreement between the homogenized and the microscale solutions. We should also note that the proposed solution algorithm allows for a trivial parallelization for solving the microscale problem for c^s.

References

[1] T. Arbogast, J. Douglas Jr., and U. Hornung. Derivation of the double porosity model of single phase flow via homogenization theory. *SIAM Journal of Mathematical Analysis*, 21(4):823–836, 1990.

[2] T. Arbogast, J. Douglas Jr., and U. Hornung. Modeling of naturally fractured reservoirs by formal homogenization techniques. *Frontiers in Pure and Applied Mathematics*, pages 1–19, 1991.

[3] A. Bensoussan, J. L. Lions, and G. Papanicolaou. *Asymptotic Analysis for Periodic Structures*. North-Holland Publishing Company, 1978.

[4] D. Cioranescu and P. Donato. *An Introduction to Homogenization*. Oxford University Press, 1999.

[5] T.F. Fuller, M. Doyle, and J. Newman. Modeling of galvanostatic charge and discharge of the lithium/polymer/insertion cell. *J. Electrochem. Soc.*, 140(6):1526–1533, 1993.

[6] W. Lai and F. Ciucci. Derivation of micro/macro lithium battery models from homogenization. *Transport in Porous Media*, 88:249–270, 2011.

[7] Wei Lai and Francesco Ciucci. Mathematical modeling of porous battery electrodes revisit of newman's model. *Electrochimica Acta*, 56(11):4369–4377, April 2011.

[8] Arnulf Latz, Jochen Zausch, and Oleg Iliev. Modeling of species and charge transport in li-ion batteries based on non-equilibrium thermodynamics. In *Proceedings of the 7th international conference on Numerical methods and applications*, NMA'10, pages 329–337, Berlin, Heidelberg, 2011. Springer-Verlag.

[9] G. Richardson, G. Denuault, and C.P. Please. Multiscale modelling and analysis of lithium-ion battery charge and discharge. *Journal of Engineering Mathematics*, 72:41–72, 2012.

[10] E. Sanchez-Palencia. *Non-Homogeneous Media and Vibration Theory*. Springer-Verlag, 1980.

[11] M. Taralov and O. Iliev. Three dimensional finite element simulations of electrochemical processes in li-ion batteries. ITWM Technical Report, 2012.

[12] M. Taralov, V. Taralova, P. Popov, and J. Zausch O. Iliev, A. Latz. Report on finite elements simulations of electrochemical processes in li-ion batteries with thermic effects. *Berichte des Fraunhofer ITWM*, 2012.

Published reports of the Fraunhofer ITWM

The PDF-files of the following reports are available under:
www.itwm.fraunhofer.de/presse-und-publikationen/

1. D. Hietel, K. Steiner, J. Struckmeier
A Finite - Volume Particle Method for Compressible Flows
(19 pages, 1998)

2. M. Feldmann, S. Seibold
Damage Diagnosis of Rotors: Application of Hilbert Transform and Multi-Hypothesis Testing
Keywords: Hilbert transform, damage diagnosis, Kalman filtering, non-linear dynamics
(23 pages, 1998)

3. Y. Ben-Haim, S. Seibold
Robust Reliability of Diagnostic Multi-Hypothesis Algorithms: Application to Rotating Machinery
Keywords: Robust reliability, convex models, Kalman filtering, multi-hypothesis diagnosis, rotating machinery, crack diagnosis
(24 pages, 1998)

4. F.-Th. Lentes, N. Siedow
Three-dimensional Radiative Heat Transfer in Glass Cooling Processes
(23 pages, 1998)

5. A. Klar, R. Wegener
A hierarchy of models for multilane vehicular traffic
Part I: Modeling
(23 pages, 1998)

Part II: Numerical and stochastic investigations
(17 pages, 1998)

6. A. Klar, N. Siedow
Boundary Layers and Domain Decomposition for Radiative Heat Transfer and Diffusion Equations: Applications to Glass Manufacturing Processes
(24 pages, 1998)

7. I. Choquet
Heterogeneous catalysis modelling and numerical simulation in rarified gas flows Part I: Coverage locally at equilibrium
(24 pages, 1998)

8. J. Ohser, B. Steinbach, C. Lang
Efficient Texture Analysis of Binary Images
(17 pages, 1998)

9. J. Orlik
Homogenization for viscoelasticity of the integral type with aging and shrinkage
(20 pages, 1998)

10. J. Mohring
Helmholtz Resonators with Large Aperture
(21 pages, 1998)

11. H. W. Hamacher, A. Schöbel
On Center Cycles in Grid Graphs
(15 pages, 1998)

12. H. W. Hamacher, K.-H. Küfer
Inverse radiation therapy planning - a multiple objective optimisation approach
(14 pages, 1999)

13. C. Lang, J. Ohser, R. Hilfer
On the Analysis of Spatial Binary Images
(20 pages, 1999)

14. M. Junk
On the Construction of Discrete Equilibrium Distributions for Kinetic Schemes
(24 pages, 1999)

15. M. Junk, S. V. Raghurame Rao
A new discrete velocity method for Navier-Stokes equations
(20 pages, 1999)

16. H. Neunzert
Mathematics as a Key to Key Technologies
(39 pages, 1999)

17. J. Ohser, K. Sandau
Considerations about the Estimation of the Size Distribution in Wicksell's Corpuscle Problem
(18 pages, 1999)

18. E. Carrizosa, H. W. Hamacher, R. Klein, S. Nickel
Solving nonconvex planar location problems by finite dominating sets
Keywords: Continuous Location, Polyhedral Gauges, Finite Dominating Sets, Approximation, Sandwich Algorithm, Greedy Algorithm
(19 pages, 2000)

19. A. Becker
A Review on Image Distortion Measures
Keywords: Distortion measure, human visual system
(26 pages, 2000)

20. H. W. Hamacher, M. Labbé, S. Nickel, T. Sonneborn
Polyhedral Properties of the Uncapacitated Multiple Allocation Hub Location Problem
Keywords: integer programming, hub location, facility location, valid inequalities, facets, branch and cut
(21 pages, 2000)

21. H. W. Hamacher, A. Schöbel
Design of Zone Tariff Systems in Public Transportation
(30 pages, 2001)

22. D. Hietel, M. Junk, R. Keck, D. Teleaga
The Finite-Volume-Particle Method for Conservation Laws
(16 pages, 2001)

23. T. Bender, H. Hennes, J. Kalcsics, M. T. Melo, S. Nickel
Location Software and Interface with GIS and Supply Chain Management
Keywords: facility location, software development, geographical information systems, supply chain management
(48 pages, 2001)

24. H. W. Hamacher, S. A. Tjandra
Mathematical Modelling of Evacuation Problems: A State of Art
(44 pages, 2001)

25. J. Kuhnert, S. Tiwari
Grid free method for solving the Poisson equation
Keywords: Poisson equation, Least squares method, Grid free method
(19 pages, 2001)

26. T. Götz, H. Rave, D. Reinel-Bitzer, K. Steiner, H. Tiemeier
Simulation of the fiber spinning process
Keywords: Melt spinning, fiber model, Lattice Boltzmann, CFD
(19 pages, 2001)

27. A. Zemitis
On interaction of a liquid film with an obstacle
Keywords: impinging jets, liquid film, models, numerical solution, shape
(22 pages, 2001)

28. I. Ginzburg, K. Steiner
Free surface lattice-Boltzmann method to model the filling of expanding cavities by Bingham Fluids
Keywords: Generalized LBE, free-surface phenomena, interface boundary conditions, filling processes, Bingham viscoplastic model, regularized models
(22 pages, 2001)

29. H. Neunzert
»Denn nichts ist für den Menschen als Menschen etwas wert, was er nicht mit Leidenschaft tun kann«
Vortrag anlässlich der Verleihung des Akademiepreises des Landes Rheinland-Pfalz am 21.11.2001
Keywords: Lehre, Forschung, angewandte Mathematik, Mehrskalenanalyse, Strömungsmechanik
(18 pages, 2001)

30. J. Kuhnert, S. Tiwari
Finite pointset method based on the projection method for simulations of the incompressible Navier-Stokes equations
Keywords: Incompressible Navier-Stokes equations, Meshfree method, Projection method, Particle scheme, Least squares approximation
AMS subject classification: 76D05, 76M28
(25 pages, 2001)

31. R. Korn, M. Krekel
Optimal Portfolios with Fixed Consumption or Income Streams
Keywords: Portfolio optimisation, stochastic control, HJB equation, discretisation of control problems
(23 pages, 2002)

32. M. Krekel
Optimal portfolios with a loan dependent credit spread
Keywords: Portfolio optimisation, stochastic control, HJB equation, credit spread, log utility, power utility, non-linear wealth dynamics
(25 pages, 2002)

33. J. Ohser, W. Nagel, K. Schladitz
The Euler number of discretized sets – on the choice of adjacency in homogeneous lattices
Keywords: image analysis, Euler number, neighborhod relationships, cuboidal lattice
(32 pages, 2002)

34. I. Ginzburg, K. Steiner
Lattice Boltzmann Model for Free-Surface flow and Its Application to Filling Process in Casting
Keywords: Lattice Boltzmann models; free-surface phenomena; interface boundary conditions; filling processes; injection molding; volume of fluid method; interface boundary conditions; advection-schemes; upwind-schemes
(54 pages, 2002)

35. M. Günther, A. Klar, T. Materne, R. Wegener
Multivalued fundamental diagrams and stop and go waves for continuum traffic equations
Keywords: traffic flow, macroscopic equations, kinetic derivation, multivalued fundamental diagram, stop and go waves, phase transitions
(25 pages, 2002)

36. S. Feldmann, P. Lang, D. Prätzel-Wolters
Parameter influence on the zeros of network determinants
Keywords: Networks, Equicofactor matrix polynomials, Realization theory, Matrix perturbation theory
(30 pages, 2002)

37. K. Koch, J. Ohser, K. Schladitz
Spectral theory for random closed sets and estimating the covariance via frequency space
Keywords: Random set, Bartlett spectrum, fast Fourier transform, power spectrum
(28 pages, 2002)

38. D. d'Humières, I. Ginzburg
Multi-reflection boundary conditions for lattice Boltzmann models
Keywords: lattice Boltzmann equation, boudary condistions, bounce-back rule, Navier-Stokes equation
(72 pages, 2002)

39. R. Korn
Elementare Finanzmathematik
Keywords: Finanzmathematik, Aktien, Optionen, Portfolio-Optimierung, Börse, Lehrerweiterbildung, Mathematikunterricht
(98 pages, 2002)

40. J. Kallrath, M. C. Müller, S. Nickel
Batch Presorting Problems: Models and Complexity Results
Keywords: Complexity theory, Integer programming, Assigment, Logistics
(19 pages, 2002)

41. J. Linn
On the frame-invariant description of the phase space of the Folgar-Tucker equation
Key words: fiber orientation, Folgar-Tucker equation, injection molding
(5 pages, 2003)

42. T. Hanne, S. Nickel
A Multi-Objective Evolutionary Algorithm for Scheduling and Inspection Planning in Software Development Projects
Key words: multiple objective programming, project management and scheduling, software development, evolutionary algorithms, efficient set
(29 pages, 2003)

43. T. Bortfeld , K.-H. Küfer, M. Monz, A. Scherrer, C. Thieke, H. Trinkaus
Intensity-Modulated Radiotherapy - A Large Scale Multi-Criteria Programming Problem
Keywords: multiple criteria optimization, representative systems of Pareto solutions, adaptive triangulation, clustering and disaggregation techniques, visualization of Pareto solutions, medical physics, external beam radiotherapy planning, intensity modulated radiotherapy
(31 pages, 2003)

44. T. Halfmann, T. Wichmann
Overview of Symbolic Methods in Industrial Analog Circuit Design
Keywords: CAD, automated analog circuit design, symbolic analysis, computer algebra, behavioral modeling, system simulation, circuit sizing, macro modeling, differential-algebraic equations, index
(17 pages, 2003)

45. S. E. Mikhailov, J. Orlik
Asymptotic Homogenisation in Strength and Fatigue Durability Analysis of Composites
Keywords: multiscale structures, asymptotic homogenization, strength, fatigue, singularity, non-local conditions
(14 pages, 2003)

46. P. Domínguez-Marín, P. Hansen, N. Mladenovic , S. Nickel
Heuristic Procedures for Solving the Discrete Ordered Median Problem
Keywords: genetic algorithms, variable neighborhood search, discrete facility location
(31 pages, 2003)

47. N. Boland, P. Domínguez-Marín, S. Nickel, J. Puerto
Exact Procedures for Solving the Discrete Ordered Median Problem
Keywords: discrete location, Integer programming
(41 pages, 2003)

48. S. Feldmann, P. Lang
Padé-like reduction of stable discrete linear systems preserving their stability
Keywords: Discrete linear systems, model reduction, stability, Hankel matrix, Stein equation
(16 pages, 2003)

49. J. Kallrath, S. Nickel
A Polynomial Case of the Batch Presorting Problem
Keywords: batch presorting problem, online optimization, competetive analysis, polynomial algorithms, logistics
(17 pages, 2003)

50. T. Hanne, H. L. Trinkaus
knowCube for MCDM – Visual and Interactive Support for Multicriteria Decision Making
Key words: Multicriteria decision making, knowledge management, decision support systems, visual interfaces, interactive navigation, real-life applications.
(26 pages, 2003)

51. O. Iliev, V. Laptev
On Numerical Simulation of Flow Through Oil Filters
Keywords: oil filters, coupled flow in plain and porous media, Navier-Stokes, Brinkman, numerical simulation
(8 pages, 2003)

52. W. Dörfler, O. Iliev, D. Stoyanov, D. Vassileva
On a Multigrid Adaptive Refinement Solver for Saturated Non-Newtonian Flow in Porous Media
Keywords: Nonlinear multigrid, adaptive refinement, non-Newtonian flow in porous media
(17 pages, 2003)

53. S. Kruse
On the Pricing of Forward Starting Options under Stochastic Volatility
Keywords: Option pricing, forward starting options, Heston model, stochastic volatility, cliquet options
(11 pages, 2003)

54. O. Iliev, D. Stoyanov
Multigrid – adaptive local refinement solver for incompressible flows
Keywords: Navier-Stokes equations, incompressible flow, projection-type splitting, SIMPLE, multigrid methods, adaptive local refinement, lid-driven flow in a cavity
(37 pages, 2003)

55. V. Starikovicius
The multiphase flow and heat transfer in porous media
Keywords: Two-phase flow in porous media, various formulations, global pressure, multiphase mixture model, numerical simulation
(30 pages, 2003)

56. P. Lang, A. Sarishvili, A. Wirsen
Blocked neural networks for knowledge extraction in the software development process
Keywords: Blocked Neural Networks, Nonlinear Regression, Knowledge Extraction, Code Inspection
(21 pages, 2003)

57. H. Knaf, P. Lang, S. Zeiser
Diagnosis aiding in Regulation Thermography using Fuzzy Logic
Keywords: fuzzy logic,knowledge representation, expert system
(22 pages, 2003)

58. M. T. Melo, S. Nickel, F. Saldanha da Gama
Largescale models for dynamic multicommodity capacitated facility location
Keywords: supply chain management, strategic planning, dynamic location, modeling
(40 pages, 2003)

59. J. Orlik
Homogenization for contact problems with periodically rough surfaces
Keywords: asymptotic homogenization, contact problems
(28 pages, 2004)

60. A. Scherrer, K.-H. Küfer, M. Monz, F. Alonso, T. Bortfeld
IMRT planning on adaptive volume structures – a significant advance of computational complexity
Keywords: Intensity-modulated radiation therapy (IMRT), inverse treatment planning, adaptive volume structures, hierarchical clustering, local refinement, adaptive clustering, convex programming, mesh generation, multi-grid methods
(24 pages, 2004)

61. D. Kehrwald
Parallel lattice Boltzmann simulation of complex flows
Keywords: Lattice Boltzmann methods, parallel computing, microstructure simulation, virtual material design, pseudo-plastic fluids, liquid composite moulding
(12 pages, 2004)

62. O. Iliev, J. Linn, M. Moog, D. Niedziela, V. Starikovicius
On the Performance of Certain Iterative Solvers for Coupled Systems Arising in Dis-

cretization of Non-Newtonian Flow Equations
Keywords: Performance of iterative solvers, Preconditioners, Non-Newtonian flow
(17 pages, 2004)

63. R. Ciegis, O. Iliev, S. Rief, K. Steiner
On Modelling and Simulation of Different Regimes for Liquid Polymer Moulding
Keywords: Liquid Polymer Moulding, Modelling, Simulation, Infiltration, Front Propagation, non-Newtonian flow in porous media
(43 pages, 2004)

64. T. Hanne, H. Neu
Simulating Human Resources in Software Development Processes
Keywords: Human resource modeling, software process, productivity, human factors, learning curve
(14 pages, 2004)

65. O. Iliev, A. Mikelic, P. Popov
Fluid structure interaction problems in deformable porous media: Toward permeability of deformable porous media
Keywords: fluid-structure interaction, deformable porous media, upscaling, linear elasticity, stokes, finite elements
(28 pages, 2004)

66. F. Gaspar, O. Iliev, F. Lisbona, A. Naumovich, P. Vabishchevich
On numerical solution of 1-D poroelasticity equations in a multilayered domain
Keywords: poroelasticity, multilayered material, finite volume discretization, MAC type grid
(41 pages, 2004)

67. J. Ohser, K. Schladitz, K. Koch, M. Nöthe
Diffraction by image processing and its application in materials science
Keywords: porous microstructure, image analysis, random set, fast Fourier transform, power spectrum, Bartlett spectrum
(13 pages, 2004)

68. H. Neunzert
Mathematics as a Technology: Challenges for the next 10 Years
Keywords: applied mathematics, technology, modelling, simulation, visualization, optimization, glass processing, spinning processes, fiber-fluid interaction, trubulence effects, topological optimization, multicriteria optimization, Uncertainty and Risk, financial mathematics, Malliavin calculus, Monte-Carlo methods, virtual material design, filtration, bio-informatics, system biology
(29 pages, 2004)

69. R. Ewing, O. Iliev, R. Lazarov, A. Naumovich
On convergence of certain finite difference discretizations for 1D poroelasticity interface problems
Keywords: poroelasticity, multilayered material, finite volume discretizations, MAC type grid, error estimates
(26 pages,2004)

70. W. Dörfler, O. Iliev, D. Stoyanov, D. Vassileva
On Efficient Simulation of Non-Newtonian Flow in Saturated Porous Media with a Multigrid Adaptive Refinement Solver
Keywords: Nonlinear multigrid, adaptive renement, non-Newtonian in porous media
(25 pages, 2004)

71. J. Kalcsics, S. Nickel, M. Schröder
Towards a Unified Territory Design Approach – Applications, Algorithms and GIS Integration
Keywords: territory desgin, political districting, sales territory alignment, optimization algorithms, Geographical Information Systems
(40 pages, 2005)

72. K. Schladitz, S. Peters, D. Reinel-Bitzer, A. Wiegmann, J. Ohser
Design of acoustic trim based on geometric modeling and flow simulation for non-woven
Keywords: random system of fibers, Poisson line process, flow resistivity, acoustic absorption, Lattice-Boltzmann method, non-woven
(21 pages, 2005)

73. V. Rutka, A. Wiegmann
Explicit Jump Immersed Interface Method for virtual material design of the effective elastic moduli of composite materials
Keywords: virtual material design, explicit jump immersed interface method, effective elastic moduli, composite materials
(22 pages, 2005)

74. T. Hanne
Eine Übersicht zum Scheduling von Baustellen
Keywords: Projektplanung, Scheduling, Bauplanung, Bauindustrie
(32 pages, 2005)

75. J. Linn
The Folgar-Tucker Model as a Differetial Algebraic System for Fiber Orientation Calculation
Keywords: fiber orientation, Folgar–Tucker model, invariants, algebraic constraints, phase space, trace stability
(15 pages, 2005)

76. M. Speckert, K. Dreßler, H. Mauch, A. Lion, G. J. Wierda
Simulation eines neuartigen Prüfsystems für Achserprobungen durch MKS-Modellierung einschließlich Regelung
Keywords: virtual test rig, suspension testing, multibody simulation, modeling hexapod test rig, optimization of test rig configuration
(20 pages, 2005)

77. K.-H. Küfer, M. Monz, A. Scherrer, P. Süss, F. Alonso, A. S. A. Sultan, Th. Bortfeld, D. Craft, Chr. Thieke
Multicriteria optimization in intensity modulated radiotherapy planning
Keywords: multicriteria optimization, extreme solutions, real-time decision making, adaptive approximation schemes, clustering methods, IMRT planning, reverse engineering
(51 pages, 2005)

78. S. Amstutz, H. Andrä
A new algorithm for topology optimization using a level-set method
Keywords: shape optimization, topology optimization, topological sensitivity, level-set
(22 pages, 2005)

79. N. Ettrich
Generation of surface elevation models for urban drainage simulation
Keywords: Flooding, simulation, urban elevation models, laser scanning
(22 pages, 2005)

80. H. Andrä, J. Linn, I. Matei, I. Shklyar, K. Steiner, E. Teichmann
OPTCAST – Entwicklung adäquater Strukturoptimierungsverfahren für Gießereien Technischer Bericht (KURZFASSUNG)
Keywords: Topologieoptimierung, Level-Set-Methode, Gießprozesssimulation, Gießtechnische Restriktionen, CAE-Kette zur Strukturoptimierung
(77 pages, 2005)

81. N. Marheineke, R. Wegener
Fiber Dynamics in Turbulent Flows
Part I: General Modeling Framework
Keywords: fiber-fluid interaction; Cosserat rod; turbulence modeling; Kolmogorov's energy spectrum; double-velocity correlations; differentiable Gaussian fields
(20 pages, 2005)

Part II: Specific Taylor Drag
Keywords: flexible fibers; k-ε turbulence model; fiber-turbulence interaction scales; air drag; random Gaussian aerodynamic force; white noise; stochastic differential equations; ARMA process
(18 pages, 2005)

82. C. H. Lampert, O. Wirjadi
An Optimal Non-Orthogonal Separation of the Anisotropic Gaussian Convolution Filter
Keywords: Anisotropic Gaussian filter, linear filtering, orientation space, nD image processing, separable filters
(25 pages, 2005)

83. H. Andrä, D. Stoyanov
Error indicators in the parallel finite element solver for linear elasticity DDFEM
Keywords: linear elasticity, finite element method, hierarchical shape functions, domain decom-position, parallel implementation, a posteriori error estimates
(21 pages, 2006)

84. M. Schröder, I. Solchenbach
Optimization of Transfer Quality in Regional Public Transit
Keywords: public transit, transfer quality, quadratic assignment problem
(16 pages, 2006)

85. A. Naumovich, F. J. Gaspar
On a multigrid solver for the three-dimensional Biot poroelasticity system in multilayered domains
Keywords: poroelasticity, interface problem, multigrid, operator-dependent prolongation
(11 pages, 2006)

86. S. Panda, R. Wegener, N. Marheineke
Slender Body Theory for the Dynamics of Curved Viscous Fibers
Keywords: curved viscous fibers; fluid dynamics; Navier-Stokes equations; free boundary value problem; asymptotic expansions; slender body theory
(14 pages, 2006)

87. E. Ivanov, H. Andrä, A. Kudryavtsev
Domain Decomposition Approach for Automatic Parallel Generation of Tetrahedral Grids
Key words: Grid Generation, Unstructured Grid, Delaunay Triangulation, Parallel Programming, Domain Decomposition, Load Balancing
(18 pages, 2006)

88. S. Tiwari, S. Antonov, D. Hietel, J. Kuhnert, R. Wegener
A Meshfree Method for Simulations of Interactions between Fluids and Flexible Structures
Key words: Meshfree Method, FPM, Fluid Structure Interaction, Sheet of Paper, Dynamical Coupling
(16 pages, 2006)

89. R. Ciegis , O. Iliev, V. Starikovicius, K. Steiner
Numerical Algorithms for Solving Problems of Multiphase Flows in Porous Media

Keywords: nonlinear algorithms, finite-volume method, software tools, porous media, flows
(16 pages, 2006)

90. D. Niedziela, O. Iliev, A. Latz
On 3D Numerical Simulations of Viscoelastic Fluids
Keywords: non-Newtonian fluids, anisotropic viscosity, integral constitutive equation
(18 pages, 2006)

91. A. Winterfeld
Application of general semi-infinite Programming to Lapidary Cutting Problems
Keywords: large scale optimization, nonlinear programming, general semi-infinite optimization, design centering, clustering
(26 pages, 2006)

92. J. Orlik, A. Ostrovska
Space-Time Finite Element Approximation and Numerical Solution of Hereditary Linear Viscoelasticity Problems
Keywords: hereditary viscoelasticity; kern approximation by interpolation; space-time finite element approximation, stability and a priori estimate
(24 pages, 2006)

93. V. Rutka, A. Wiegmann, H. Andrä
EJIIM for Calculation of effective Elastic Moduli in 3D Linear Elasticity
Keywords: Elliptic PDE, linear elasticity, irregular domain, finite differences, fast solvers, effective elastic moduli
(24 pages, 2006)

94. A. Wiegmann, A. Zemitis
EJ-HEAT: A Fast Explicit Jump Harmonic Averaging Solver for the Effective Heat Conductivity of Composite Materials
Keywords: Stationary heat equation, effective thermal conductivity, explicit jump, discontinuous coefficients, virtual material design, microstructure simulation, EJ-HEAT
(21 pages, 2006)

95. A. Naumovich
On a finite volume discretization of the three-dimensional Biot poroelasticity system in multilayered domains
Keywords: Biot poroelasticity system, interface problems, finite volume discretization, finite difference method
(21 pages, 2006)

96. M. Krekel, J. Wenzel
A unified approach to Credit Default Swaption and Constant Maturity Credit Default Swap valuation
Keywords: LIBOR market model, credit risk, Credit Default Swaption, Constant Maturity Credit Default Swap-method
(43 pages, 2006)

97. A. Dreyer
Interval Methods for Analog Circiuts
Keywords: interval arithmetic, analog circuits, tolerance analysis, parametric linear systems, frequency response, symbolic analysis, CAD, computer algebra
(36 pages, 2006)

98. N. Weigel, S. Weihe, G. Bitsch, K. Dreßler
Usage of Simulation for Design and Optimization of Testing
Keywords: Vehicle test rigs, MBS, control, hydraulics, testing philosophy
(14 pages, 2006)

99. H. Lang, G. Bitsch, K. Dreßler, M. Speckert
Comparison of the solutions of the elastic and elastoplastic boundary value problems
Keywords: Elastic BVP, elastoplastic BVP, variational inequalities, rate-independency, hysteresis, linear kinematic hardening, stop- and play-operator
(21 pages, 2006)

100. M. Speckert, K. Dreßler, H. Mauch
MBS Simulation of a hexapod based suspension test rig
Keywords: Test rig, MBS simulation, suspension, hydraulics, controlling, design optimization
(12 pages, 2006)

101. S. Azizi Sultan, K.-H. Küfer
A dynamic algorithm for beam orientations in multicriteria IMRT planning
Keywords: radiotherapy planning, beam orientation optimization, dynamic approach, evolutionary algorithm, global optimization
(14 pages, 2006)

102. T. Götz, A. Klar, N. Marheineke, R. Wegener
A Stochastic Model for the Fiber Lay-down Process in the Nonwoven Production
Keywords: fiber dynamics, stochastic Hamiltonian system, stochastic averaging
(17 pages, 2006)

103. Ph. Süss, K.-H. Küfer
Balancing control and simplicity: a variable aggregation method in intensity modulated radiation therapy planning
Keywords: IMRT planning, variable aggregation, clustering methods
(22 pages, 2006)

104. A. Beaudry, G. Laporte, T. Melo, S. Nickel
Dynamic transportation of patients in hospitals
Keywords: in-house hospital transportation, dial-a-ride, dynamic mode, tabu search
(37 pages, 2006)

105. Th. Hanne
Applying multiobjective evolutionary algorithms in industrial projects
Keywords: multiobjective evolutionary algorithms, discrete optimization, continuous optimization, electronic circuit design, semi-infinite programming, scheduling
(18 pages, 2006)

106. J. Franke, S. Halim
Wild bootstrap tests for comparing signals and images
Keywords: wild bootstrap test, texture classification, textile quality control, defect detection, kernel estimate, nonparametric regression
(13 pages, 2007)

107. Z. Drezner, S. Nickel
Solving the ordered one-median problem in the plane
Keywords: planar location, global optimization, ordered median, big triangle small triangle method, bounds, numerical experiments
(21 pages, 2007)

108. Th. Götz, A. Klar, A. Unterreiter, R. Wegener
Numerical evidance for the non-existing of solutions of the equations desribing rotational fiber spinning
Keywords: rotational fiber spinning, viscous fibers, boundary value problem, existence of solutions
(11 pages, 2007)

109. Ph. Süss, K.-H. Küfer
Smooth intensity maps and the Bortfeld-Boyer sequencer
Keywords: probabilistic analysis, intensity modulated radiotherapy treatment (IMRT), IMRT plan application, step-and-shoot sequencing
(8 pages, 2007)

110. E. Ivanov, O. Gluchshenko, H. Andrä, A. Kudryavtsev
Parallel software tool for decomposing and meshing of 3d structures
Keywords: a-priori domain decomposition, unstructured grid, Delaunay mesh generation
(14 pages, 2007)

111. O. Iliev, R. Lazarov, J. Willems
Numerical study of two-grid preconditioners for 1d elliptic problems with highly oscillating discontinuous coefficients
Keywords: two-grid algorithm, oscillating coefficients, preconditioner
(20 pages, 2007)

112. L. Bonilla, T. Götz, A. Klar, N. Marheineke, R. Wegener
Hydrodynamic limit of the Fokker-Planck-equation describing fiber lay-down processes
Keywords: stochastic dierential equations, Fokker-Planck equation, asymptotic expansion, Ornstein-Uhlenbeck process
(17 pages, 2007)

113. S. Rief
Modeling and simulation of the pressing section of a paper machine
Keywords: paper machine, computational fluid dynamics, porous media
(41 pages, 2007)

114. R. Ciegis, O. Iliev, Z. Lakdawala
On parallel numerical algorithms for simulating industrial filtration problems
Keywords: Navier-Stokes-Brinkmann equations, finite volume discretization method, SIMPLE, parallel computing, data decomposition method
(24 pages, 2007)

115. N. Marheineke, R. Wegener
Dynamics of curved viscous fibers with surface tension
Keywords: Slender body theory, curved viscous bers with surface tension, free boundary value problem
(25 pages, 2007)

116. S. Feth, J. Franke, M. Speckert
Resampling-Methoden zur mse-Korrektur und Anwendungen in der Betriebsfestigkeit
Keywords: Weibull, Bootstrap, Maximum-Likelihood, Betriebsfestigkeit
(16 pages, 2007)

117. H. Knaf
Kernel Fisher discriminant functions – a concise and rigorous introduction
Keywords: wild bootstrap test, texture classification, textile quality control, defect detection, kernel estimate, nonparametric regression
(30 pages, 2007)

118. O. Iliev, I. Rybak
On numerical upscaling for flows in heterogeneous porous media
Keywords: numerical upscaling, heterogeneous porous media, single phase flow, Darcy's law, multiscale problem, effective permeability, multipoint flux approximation, anisotropy
(17 pages, 2007)

119. O. Iliev, I. Rybak
On approximation property of multipoint flux approximation method
Keywords: Multipoint flux approximation, finite volume method, elliptic equation, discontinuous tensor coefficients, anisotropy
(15 pages, 2007)

120. O. Iliev, I. Rybak, J. Willems
On upscaling heat conductivity for a class of industrial problems
Keywords: Multiscale problems, effective heat conductivity, numerical upscaling, domain decomposition
(21 pages, 2007)

121. R. Ewing, O. Iliev, R. Lazarov, I. Rybak
On two-level preconditioners for flow in porous media
Keywords: Multiscale problem, Darcy's law, single phase flow, anisotropic heterogeneous porous media, numerical upscaling, multigrid, domain decomposition, efficient preconditioner
(18 pages, 2007)

122. M. Brickenstein, A. Dreyer
POLYBORI: A Gröbner basis framework for Boolean polynomials
Keywords: Gröbner basis, formal verification, Boolean polynomials, algebraic cryptoanalysis, satisfiability
(23 pages, 2007)

123. O. Wirjadi
Survey of 3d image segmentation methods
Keywords: image processing, 3d, image segmentation, binarization
(20 pages, 2007)

124. S. Zeytun, A. Gupta
A Comparative Study of the Vasicek and the CIR Model of the Short Rate
Keywords: interest rates, Vasicek model, CIR-model, calibration, parameter estimation
(17 pages, 2007)

125. G. Hanselmann, A. Sarishvili
Heterogeneous redundancy in software quality prediction using a hybrid Bayesian approach
Keywords: reliability prediction, fault prediction, non-homogeneous poisson process, Bayesian model averaging
(17 pages, 2007)

126. V. Maag, M. Berger, A. Winterfeld, K.-H. Küfer
A novel non-linear approach to minimal area rectangular packing
Keywords: rectangular packing, non-overlapping constraints, non-linear optimization, regularization, relaxation
(18 pages, 2007)

127. M. Monz, K.-H. Küfer, T. Bortfeld, C. Thieke
Pareto navigation – systematic multi-criteria-based IMRT treatment plan determination
Keywords: convex, interactive multi-objective optimization, intensity modulated radiotherapy planning
(15 pages, 2007)

128. M. Krause, A. Scherrer
On the role of modeling parameters in IMRT plan optimization
Keywords: intensity-modulated radiotherapy (IMRT), inverse IMRT planning, convex optimization, sensitivity analysis, elasticity, modeling parameters, equivalent uniform dose (EUD)
(18 pages, 2007)

129. A. Wiegmann
Computation of the permeability of porous materials from their microstructure by FFF-Stokes
Keywords: permeability, numerical homogenization, fast Stokes solver
(24 pages, 2007)

130. T. Melo, S. Nickel, F. Saldanha da Gama
Facility Location and Supply Chain Management – A comprehensive review
Keywords: facility location, supply chain management, network design
(54 pages, 2007)

131. T. Hanne, T. Melo, S. Nickel
Bringing robustness to patient flow management through optimized patient transports in hospitals
Keywords: Dial-a-Ride problem, online problem, case study, tabu search, hospital logistics
(23 pages, 2007)

132. R. Ewing, O. Iliev, R. Lazarov, I. Rybak, J. Willems
An efficient approach for upscaling properties of composite materials with high contrast of coefficients
Keywords: effective heat conductivity, permeability of fractured porous media, numerical upscaling, fibrous insulation materials, metal foams
(16 pages, 2008)

133. S. Gelareh, S. Nickel
New approaches to hub location problems in public transport planning
Keywords: integer programming, hub location, transportation, decomposition, heuristic
(25 pages, 2008)

134. G. Thömmes, J. Becker, M. Junk, A. K. Vaikuntam, D. Kehrwald, A. Klar, K. Steiner, A. Wiegmann
A Lattice Boltzmann Method for immiscible multiphase flow simulations using the Level Set Method
Keywords: Lattice Boltzmann method, Level Set method, free surface, multiphase flow
(28 pages, 2008)

135. J. Orlik
Homogenization in elasto-plasticity
Keywords: multiscale structures, asymptotic homogenization, nonlinear energy
(40 pages, 2008)

136. J. Almquist, H. Schmidt, P. Lang, J. Deitmer, M. Jirstrand, D. Prätzel-Wolters, H. Becker
Determination of interaction between MCT1 and CAII via a mathematical and physiological approach
Keywords: mathematical modeling; model reduction; electrophysiology; pH-sensitive microelectrodes; proton antenna
(20 pages, 2008)

137. E. Savenkov, H. Andrä, O. Iliev
An analysis of one regularization approach for solution of pure Neumann problem
Keywords: pure Neumann problem, elasticity, regularization, finite element method, condition number
(27 pages, 2008)

138. O. Berman, J. Kalcsics, D. Krass, S. Nickel
The ordered gradual covering location problem on a network
Keywords: gradual covering, ordered median function, network location
(32 pages, 2008)

139. S. Gelareh, S. Nickel
Multi-period public transport design: A novel model and solution approaches
Keywords: Integer programming, hub location, public transport, multi-period planning, heuristics
(31 pages, 2008)

140. T. Melo, S. Nickel, F. Saldanha-da-Gama
Network design decisions in supply chain planning
Keywords: supply chain design, integer programming models, location models, heuristics
(20 pages, 2008)

141. C. Lautensack, A. Särkkä, J. Freitag, K. Schladitz
Anisotropy analysis of pressed point processes
Keywords: estimation of compression, isotropy test, nearest neighbour distance, orientation analysis, polar ice, Ripley's K function
(35 pages, 2008)

142. O. Iliev, R. Lazarov, J. Willems
A Graph-Laplacian approach for calculating the effective thermal conductivity of complicated fiber geometries
Keywords: graph laplacian, effective heat conductivity, numerical upscaling, fibrous materials
(14 pages, 2008)

143. J. Linn, T. Stephan, J. Carlsson, R. Bohlin
Fast simulation of quasistatic rod deformations for VR applications
Keywords: quasistatic deformations, geometrically exact rod models, variational formulation, energy minimization, finite differences, nonlinear conjugate gradients
(7 pages, 2008)

144. J. Linn, T. Stephan
Simulation of quasistatic deformations using discrete rod models
Keywords: quasistatic deformations, geometrically exact rod models, variational formulation, energy minimization, finite differences, nonlinear conjugate gradients
(9 pages, 2008)

145. J. Marburger, N. Marheineke, R. Pinnau
Adjoint based optimal control using mesh-less discretizations
Keywords: Mesh-less methods, particle methods, Eulerian-Lagrangian formulation, optimization strategies, adjoint method, hyperbolic equations
(14 pages, 2008

146. S. Desmettre, J. Gould, A. Szimayer
Own-company stockholding and work effort preferences of an unconstrained executive
Keywords: optimal portfolio choice, executive compensation
(33 pages, 2008)

147. M. Berger, M. Schröder, K.-H. Küfer
A constraint programming approach for the two-dimensional rectangular packing problem with orthogonal orientations
Keywords: rectangular packing, orthogonal orientations non-overlapping constraints, constraint propagation
(13 pages, 2008)

148. K. Schladitz, C. Redenbach, T. Sych, M. Godehardt
Microstructural characterisation of open foams using 3d images
Keywords: virtual material design, image analysis, open foams
(30 pages, 2008)

149. E. Fernández, J. Kalcsics, S. Nickel, R. Ríos-Mercado
A novel territory design model arising in the implementation of the WEEE-Directive
Keywords: heuristics, optimization, logistics, recycling
(28 pages, 2008)

150. H. Lang, J. Linn
Lagrangian field theory in space-time for geometrically exact Cosserat rods
Keywords: Cosserat rods, geometrically exact rods, small strain, large deformation, deformable bodies, Lagrangian field theory, variational calculus
(19 pages, 2009)

151. K. Dreßler, M. Speckert, R. Müller, Ch. Weber
Customer loads correlation in truck engineering
Keywords: Customer distribution, safety critical components, quantile estimation, Monte-Carlo methods
(11 pages, 2009)

152. H. Lang, K. Dreßler
An improved multiaxial stress-strain correction model for elastic FE postprocessing
Keywords: Jiang's model of elastoplasticity, stress-strain correction, parameter identification, automatic differentiation, least-squares optimization, Coleman-Li algorithm
(6 pages, 2009)

153. J. Kalcsics, S. Nickel, M. Schröder
A generic geometric approach to territory design and districting
Keywords: Territory design, districting, combinatorial optimization, heuristics, computational geometry
(32 pages, 2009)

154. Th. Fütterer, A. Klar, R. Wegener
An energy conserving numerical scheme for the dynamics of hyperelastic rods
Keywords: Cosserat rod, hyperealstic, energy conservation, finite differences
(16 pages, 2009)

155. A. Wiegmann, L. Cheng, E. Glatt, O. Iliev, S. Rief
Design of pleated filters by computer simulations
Keywords: Solid-gas separation, solid-liquid separation, pleated filter, design, simulation
(21 pages, 2009)

156. A. Klar, N. Marheineke, R. Wegener
Hierarchy of mathematical models for production processes of technical textiles
Keywords: Fiber-fluid interaction, slender-body theory, turbulence modeling, model reduction, stochastic differential equations, Fokker-Planck equation, asymptotic expansions, parameter identification
(21 pages, 2009)

157. E. Glatt, S. Rief, A. Wiegmann, M. Knefel, E. Wegenke
Structure and pressure drop of real and virtual metal wire meshes
Keywords: metal wire mesh, structure simulation, model calibration, CFD simulation, pressure loss
(7 pages, 2009)

158. S. Kruse, M. Müller
Pricing American call options under the assumption of stochastic dividends – An application of the Korn-Rogers model
Keywords: option pricing, American options, dividends, dividend discount model, Black-Scholes model
(22 pages, 2009)

159. H. Lang, J. Linn, M. Arnold
Multibody dynamics simulation of geometrically exact Cosserat rods
Keywords: flexible multibody dynamics, large deformations, finite rotations, constrained mechanical systems, structural dynamics
(20 pages, 2009)

160. P. Jung, S. Leyendecker, J. Linn, M. Ortiz
Discrete Lagrangian mechanics and geometrically exact Cosserat rods
Keywords: special Cosserat rods, Lagrangian mechanics, Noether's theorem, discrete mechanics, frame-indifference, holonomic constraints
(14 pages, 2009)

161. M. Burger, K. Dreßler, A. Marquardt, M. Speckert
Calculating invariant loads for system simulation in vehicle engineering
Keywords: iterative learning control, optimal control theory, differential algebraic equations (DAEs)
(18 pages, 2009)

162. M. Speckert, N. Ruf, K. Dreßler
Undesired drift of multibody models excited by measured accelerations or forces
Keywords: multibody simulation, full vehicle model, force-based simulation, drift due to noise
(19 pages, 2009)

163. A. Streit, K. Dreßler, M. Speckert, J. Lichter, T. Zenner, P. Bach
Anwendung statistischer Methoden zur Erstellung von Nutzungsprofilen für die Auslegung von Mobilbaggern
Keywords: Nutzungsvielfalt, Kundenbeanspruchung, Bemessungsgrundlagen
(13 pages, 2009)

164. I. Correia, S. Nickel, F. Saldanha-da-Gama
The capacitated single-allocation hub location problem revisited: A note on a classical formulation
Keywords: Capacitated Hub Location, MIP formulations
(10 pages, 2009)

165. F. Yaneva, T. Grebe, A. Scherrer
An alternative view on global radiotherapy optimization problems
Keywords: radiotherapy planning, path-connected sublevelsets, modified gradient projection method, improving and feasible directions
(14 pages, 2009)

166. J. I. Serna, M. Monz, K.-H. Küfer, C. Thieke
Trade-off bounds and their effect in multi-criteria IMRT planning
Keywords: trade-off bounds, multi-criteria optimization, IMRT, Pareto surface
(15 pages, 2009)

167. W. Arne, N. Marheineke, A. Meister, R. Wegener
Numerical analysis of Cosserat rod and string models for viscous jets in rotational spinning processes
Keywords: Rotational spinning process, curved viscous fibers, asymptotic Cosserat models, boundary value problem, existence of numerical solutions
(18 pages, 2009)

168. T. Melo, S. Nickel, F. Saldanha-da-Gama
An LP-rounding heuristic to solve a multi-period facility relocation problem
Keywords: supply chain design, heuristic, linear programming, rounding
(37 pages, 2009)

169. I. Correia, S. Nickel, F. Saldanha-da-Gama
Single-allocation hub location problems with capacity choices
Keywords: hub location, capacity decisions, MILP formulations
(27 pages, 2009)

170. S. Acar, K. Natcheva-Acar
A guide on the implementation of the Heath-Jarrow-Morton Two-Factor Gaussian Short Rate Model (HJM-G2++)
Keywords: short rate model, two factor Gaussian, G2++, option pricing, calibration
(30 pages, 2009)

171. A. Szimayer, G. Dimitroff, S. Lorenz
A parsimonious multi-asset Heston model: calibration and derivative pricing
Keywords: Heston model, multi-asset, option pricing, calibration, correlation
(28 pages, 2009)

172. N. Marheineke, R. Wegener
Modeling and validation of a stochastic drag for fibers in turbulent flows
Keywords: fiber-fluid interactions, long slender fibers, turbulence modelling, aerodynamic drag, dimensional analysis, data interpolation, stochastic partial differential algebraic equation, numerical simulations, experimental validations
(19 pages, 2009)

173. S. Nickel, M. Schröder, J. Steeg
Planning for home health care services
Keywords: home health care, route planning, metaheuristics, constraint programming
(23 pages, 2009)

174. G. Dimitroff, A. Szimayer, A. Wagner
Quanto option pricing in the parsimonious Heston model
Keywords: Heston model, multi asset, quanto options, option pricing
(14 pages, 2009) 174. G. Dimitroff, A. Szimayer, A. Wagner

175. S. Herkt, K. Dreßler, R. Pinnau
Model reduction of nonlinear problems in structural mechanics
Keywords: flexible bodies, FEM, nonlinear model reduction, POD
(13 pages, 2009)

176. M. K. Ahmad, S. Didas, J. Iqbal
Using the Sharp Operator for edge detection and nonlinear diffusion
Keywords: maximal function, sharp function,image processing, edge detection, nonlinear diffusion
(17 pages, 2009)

177. M. Speckert, N. Ruf, K. Dreßler, R. Müller, C. Weber, S. Weihe
Ein neuer Ansatz zur Ermittlung von Erprobungslasten für sicherheitsrelevante Bauteile
Keywords: sicherheitsrelevante Bauteile, Kundenbeanspruchung, Festigkeitsverteilung, Ausfallwahrscheinlichkeit, Konfidenz, statistische Unsicherheit, Sicherheitsfaktoren
(16 pages, 2009)

178. J. Jegorovs
Wave based method: new applicability areas
Keywords: Elliptic boundary value problems, inhomogeneous Helmholtz type differential equations in bounded domains, numerical methods, wave based method, uniform B-splines
(10 pages, 2009)

179. H. Lang, M. Arnold
Numerical aspects in the dynamic simulation of geometrically exact rods
Keywords: Kirchhoff and Cosserat rods, geometrically exact rods, deformable bodies, multibody dynamics,artial differential algebraic equations, method of lines, time integration
(21 pages, 2009)

180. H. Lang
Comparison of quaternionic and rotation-free null space formalisms for multibody dynamics
Keywords: Parametrisation of rotations, differential-algebraic equations, multibody dynamics, constrained mechanical systems, Lagrangian mechanics
(40 pages, 2010)

181. S. Nickel, F. Saldanha-da-Gama, H.-P. Ziegler
Stochastic programming approaches for risk aware supply chain network design problems
Keywords: Supply Chain Management, multi-stage stochastic programming, financial decisions, risk
(37 pages, 2010)

182. P. Ruckdeschel, N. Horbenko
Robustness properties of estimators in generalized Pareto Models
Keywords: global robustness, local robustness, finite sample breakdown point, generalized Pareto distribution
(58 pages, 2010)

183. P. Jung, S. Leyendecker, J. Linn, M. Ortiz
A discrete mechanics approach to Cosserat rod theory – Part 1: static equilibria
Keywords: Special Cosserat rods; Lagrangian mechanics; Noether's theorem; discrete mechanics; frame-indifference; holonomic constraints; variational formulation
(35 pages, 2010)

184. R. Eymard, G. Printsypar
A proof of convergence of a finite volume scheme for modified steady Richards' equation describing transport processes in the pressing section of a paper machine
Keywords: flow in porous media, steady Richards' equation, finite volume methods, convergence of approximate solution
(14 pages, 2010)

185. P. Ruckdeschel
Optimally Robust Kalman Filtering
Keywords: robustness, Kalman Filter, innovation outlier, additive outlier
(42 pages, 2010)

186. S. Repke, N. Marheineke, R. Pinnau
On adjoint-based optimization of a free surface Stokes flow
Keywords: film casting process, thin films, free surface Stokes flow, optimal control, Lagrange formalism
(13 pages, 2010)

187. O. Iliev, R. Lazarov, J. Willems
Variational multiscale Finite Element Method for flows in highly porous media
Keywords: numerical upscaling, flow in heterogeneous porous media, Brinkman equations, Darcy's law, subgrid approximation, discontinuous Galerkin mixed FEM
(21 pages, 2010)

188. S. Desmettre, A. Szimayer
Work effort, consumption, and portfolio selection: When the occupational choice matters
Keywords: portfolio choice, work effort, consumption, occupational choice
(34 pages, 2010)

189. O. Iliev, Z. Lakdawala, V. Starikovicius
On a numerical subgrid upscaling algorithm for Stokes-Brinkman equations
Keywords: Stokes-Brinkman equations, subgrid approach, multiscale problems, numerical upscaling
(27 pages, 2010)

190. A. Latz, J. Zausch, O. Iliev
Modeling of species and charge transport in Li-Ion Batteries based on non-equilibrium thermodynamics
Keywords: lithium-ion battery, battery modeling, electrochemical simulation, concentrated electrolyte, ion transport
(8 pages, 2010)

191. P. Popov, Y. Vutov, S. Margenov, O. Iliev
Finite volume discretization of equations describing nonlinear diffusion in Li-Ion batteries
Keywords: nonlinear diffusion, finite volume discretization, Newton method, Li-Ion batteries
(9 pages, 2010)

192. W. Arne, N. Marheineke, R. Wegener
Asymptotic transition from Cosserat rod to string models for curved viscous inertial jets
Keywords: rotational spinning processes; inertial and viscous-inertial fiber regimes; asymptotic limits; slender-body theory; boundary value problems
(23 pages, 2010)

193. L. Engelhardt, M. Burger, G. Bitsch
Real-time simulation of multibody-systems for on-board applications
Keywords: multibody system simulation, real-time simulation, on-board simulation, Rosenbrock methods
(10 pages, 2010)

194. M. Burger, M. Speckert, K. Dreßler
Optimal control methods for the calculation of invariant excitation signals for multibody systems
Keywords: optimal control, optimization, mbs simulation, invariant excitation
(9 pages, 2010)

195. A. Latz, J. Zausch
Thermodynamic consistent transport theory of Li-Ion batteries
Keywords: Li-Ion batteries, nonequilibrium thermodynamics, thermal transport, modeling
(18 pages, 2010)

196. S. Desmettre
Optimal investment for executive stockholders with exponential utility
Keywords: portfolio choice, executive stockholder, work effort, exponential utility
(24 pages, 2010)

197. W. Arne, N. Marheineke, J. Schnebele, R. Wegener
Fluid-fiber-interactions in rotational spinning process of glass wool production
Keywords: Rotational spinning process, viscous thermal jets, fluid-fiber-interactions, two-way coupling, slender-body theory, Cosserat rods, drag models, boundary value problem, continuation method
(20 pages, 2010)

198. A. Klar, J. Maringer, R. Wegener
A 3d model for fiber lay-down in nonwoven production processes
Keywords: fiber dynamics, Fokker-Planck equations, diffusion limits
(15 pages, 2010)

199. Ch. Erlwein, M. Müller
A regime-switching regression model for hedge funds
Keywords: switching regression model, Hedge funds, optimal parameter estimation, filtering
(26 pages, 2011)

200. M. Dalheimer
Power to the people – Das Stromnetz der Zukunft
Keywords: Smart Grid, Stromnetz, Erneuerbare Energien, Demand-Side Management
(27 pages, 2011)

201. D. Stahl, J. Hauth
PF-MPC: Particle Filter-Model Predictive Control
Keywords: Model Predictive Control, Particle Filter, CSTR, Inverted Pendulum, Nonlinear Systems, Sequential Monte Carlo
(40 pages, 2011)

202. G. Dimitroff, J. de Kock
Calibrating and completing the volatility cube in the SABR Model
Keywords: stochastic volatility, SABR, volatility cube, swaption
(12 pages, 2011)

203. J.-P. Kreiss, T. Zangmeister
Quantification of the effectiveness of a safety function in passenger vehicles on the basis of real-world accident data
Keywords: logistic regression, safety function, real-world accident data, statistical modeling
(23 pages, 2011)

204. P. Ruckdeschel, T. Sayer, A. Szimayer
Pricing American options in the Heston model: a close look on incorporating correlation
Keywords: Heston model, American options, moment matching, correlation, tree method
(30 pages, 2011)

205. H. Ackermann, H. Ewe, K.-H. Küfer, M. Schröder
Modeling profit sharing in combinatorial exchanges by network flows
Keywords: Algorithmic game theory, profit sharing, combinatorial exchange, network flows, budget balance, core
(17 pages, 2011)

206. O. Iliev, G. Printsypar, S. Rief
A one-dimensional model of the pressing section of a paper machine including dynamic capillary effects
Keywords: steady modified Richards' equation, finite volume method, dynamic capillary pressure, pressing section of a paper machine
(29 pages, 2011)

207. I. Vecchio, K. Schladitz, M. Godehardt, M. J. Heneka
Geometric characterization of particles in 3d with an application to technical cleanliness
Keywords: intrinsic volumes, isoperimetric shape factors, bounding box, elongation, geodesic distance, technical cleanliness
(21 pages, 2011)

208. M. Burger, K. Dreßler, M. Speckert
Invariant input loads for full vehicle multibody system simulation
Keywords: multibody systems, full-vehicle simulation, optimal control
(8 pages, 2011)

209. H. Lang, J. Linn, M. Arnold
Multibody dynamics simulation of geometrically exact Cosserat rods
Keywords: flexible multibody dynamics, large deformations, finite rotations, constrained mechanical systems, structural dynamics
(28 pages, 2011)

210. G. Printsypar, R. Ciegis
On convergence of a discrete problem describing transport processes in the pressing section of a paper machine including dynamic capillary effects: one-dimensional case
Keywords: saturated and unsaturated fluid flow in porous media, Richards' approach, dynamic capillary pressure, finite volume methods, convergence of approximate solution
(24 pages, 2011)

211. O. Iliev, G. Printsypar, S. Rief
A two-cimensional model of the pressing section of a paper machine including dynamic capillary effects
Keywords: two-phase flow in porous media, steady modified Richards' equation, finite volume method, dynamic capillary pressure, pressing section of a paper machine, multipoint flux approximation
(44 pages, 2012)

212. M. Buck, O. Iliev, H. Andrä
Multiscale finite element coarse spaces for the analysis of linear elastic composites
Keywords: linear elasticity, domain decomposition, multiscale finite elements, robust coarse spaces, rigid body modes, discontinuous coefficients
(31 pages, 2012)

213. A. Wagner
Residual demand modeling and application to electricity pricing
Keywords: residual demand modeling, renewable infeed, wind infeed, solar infeed, electricity demand, German power market, merit-order effect
(28 pages, 2012)

214. O. Iliev, A. Latz, J. Zausch, S. Zhang
An overview on the usage of some model reduction approaches for simulations of Li-ion transport in batteries
Keywords: Li-ion batteries, porous electrode model, model reduction
(21 pages, 2012)

215. C. Zémerli, A. Latz, H. Andrä
Constitutive models for static granular systems and focus to the Jiang-Liu hyperelastic law
Keywords: granular elasticity, constitutive modelling, non-linear finite element method
(33 pages, 2012)

216. T. Gornak, J. L. Guermond, O. Iliev, P. D. Minev
A direction splitting approach for incompressible Brinkmann flow
Keywords: unsteady Navier-Stokes-Brinkman equations, direction splitting algorithms, nuclear reactors safety simulations
(16 pages, 2012)

217. Y. Efendiev, O. Iliev, C. Kronsbein
Multilevel Monte Carlo methods using ensemble level mixed MsFEM for two-phase flow and transport simulations
Keywords: two phase flow in porous media, uncertainty quantification, multilevel Monte Carlo
(28 pages, 2012)

218. J. Linn, H. Lang, A. Tuganov
Geometrically exact Cosserat rods with Kelvin-Voigt type viscous damping
Keywords: geometrically exact rods, viscous damping, Kelvin-Voigt model, material damping parameters
(10 pages, 2012)

219. M. Schulze, S. Dietz, J. Linn, H. Lang, A. Tuganov
Integration of nonlinear models of flexible body deformation in Multibody System Dynamics
Keywords: multibody system dynamics, flexible structures, discrete Cosserat rods, wind turbine rotor blades
(10 pages, 2012)

220. C. Weischedel, A. Tuganov, T. Hermansson, J. Linn, M. Wardetzky
Construction of discrete shell models by geometric finite differences
Keywords: geometrically exact shells, discrete differential geometry, rotation-free Kirchhoff model, triangular meshes
(10 pages, 2012)

221. M. Taralov, V. Taralova, P. Popov, O. Iliev, A. Latz, J. Zausch
Report on Finite Element Simulations of Electrochemical Processes in Li-ion Batteries with Thermic Effects
Keywords: Li-ion battery, FEM for nonlinear problems, FEM for discontinuous solutions, Nonlinear diffusion, Nonlinear interface conditions
(40 pages, 2012)

222. A. Scherrer, T. Grebe, F. Yaneva, K.-H. Küfer
Interactive DVH-based planning of intensity-modulated radiation therapy (IMRT)
Keywords: intensity-modulated radiation therapy (IMRT), cumulative dose-volume histogram (DVH), interactive IMRT planning, DVH-based planning criteria
(22 pages, 2012)

223. S. Frei, H. Andrä, R. Pinnau, O. Tse
An adjoint-based gradient-type algorithm for optimal fiber orientation in fiber-reinforced materials
Keywords: pde constrained optimization, fiber-reinforced materials, fiber orientation, linear elasticity, upscaling, adjoint-based optimization, microstructural optimization
(17 pages, 2012)

224. M. Kabel, H. Andrä
Fast numerical computation of precise bounds of effective elastic moduli
Keywords: composite materials, numerical homogenization, effective elasticity coefficients, Hashin-Shtrikman bounds, Lippmann-Schwinger equation, FFT
(16 pages, 2013)

225. J. Linn, H. Lang, A. Tuganov
Derivation of a viscoelastic constitutive model of Kelvin-Voigt type for Cosserat rods
Keywords: geometrically exact rods, viscoelasticity, Kelvin-Voigt model, nonlinear structural dynamics
(42 pages, 2013)

226. H. Knaf
Distanzen zwischen Partitionen – zur Anwendung und Theorie
Keywords: Metrik, Partitionenverband, Clusteranalyse, Ergebnisbewertung
(35 pages, 2013)

227. S. Desmettre, R. Korn, F. Th. Seifried
Worst-case consumption-portfolio optimization
Keywords: worst-case, crash, consumption, verification
(30 pages, 2013)

228. M. Obermayr, Ch. Vrettos, J. Kleinert, P. Eberhard
A Discrete Element Method for assessing reaction forces in excavation tools
Keywords: discrete element method, rolling resistance, cohesionless soil, draft force
(17 pages, 2013)

229. S. Schmidt, L. Kreußer, S. Zhang
POD-DEIM based model order reduction for a three-dimensional microscopic Li-Ion battery model
Keywords: Model order reduction, nonlinear PDE, POD-DEIM, Li-Ion battery simulation
(33 pages, 2013)

230. Y. Efendiev, O. Iliev, V. Taralova
Upscaling of an isothermal Li-ion battery model via the Homogenization Theory
Keywords: Li-Ion batteries, homogenization
(66 pages, 2013)

Status quo: June 2013